

**UNCLASSIFIED**

---

---

**AD 268 503**

---

*Reproduced  
by the*

**ARMED SERVICES TECHNICAL INFORMATION AGENCY  
ARLINGTON HALL STATION  
ARLINGTON 12, VIRGINIA**



---

---

**UNCLASSIFIED**

**NOTICE:** When government or other drawings, specifications or other data are used for any purpose other than in connection with a definitely related government procurement operation, the U. S. Government thereby incurs no responsibility, nor any obligation whatsoever; and the fact that the Government may have formulated, furnished, or in any way supplied the said drawings, specifications, or other data is not to be regarded by implication or otherwise as in any manner licensing the holder or any other person or corporation, or conveying any rights or permission to manufacture, use or sell any patented invention that may in any way be related thereto.

268-503

AFOSR-1603

STANFORD RADIO ASTRONOMY INSTITUTE PUBLICATION NO. 18A

# A Study of Radio-Astronomy Receivers

by  
R. S. Colvin

Scientific Report No. 18  
31 October 1961

XEROX

62-1-5

Prepared under  
Air Force Contract AF 18 (603) -53

268 503

**RADIOSCIENCE LABORATORY**

**STANFORD ELECTRONICS LABORATORIES**

**STANFORD UNIVERSITY • STANFORD, CALIFORNIA**



**A STUDY OF RADIO-ASTRONOMY RECEIVERS**

by

**R. S. Colvin**

**Scientific Report No. 18  
31 October 1961**

**Prepared under  
Air Force Contract AF18(603)-53**

**Reproduction in whole or in part  
is permitted for any purpose of  
the United States Government.**

**Radioscience Laboratory  
Stanford Electronics Laboratories  
Stanford University          Stanford, California**

## ABSTRACT

The major objective of this study of radio-astronomy receivers is to furnish a consistent basis for predicting and comparing the performance of different systems. This basis is provided by clearly defining the important factors, particularly the integrating time  $\tau$  and the bandwidth  $\Delta f$ , and by analyzing a variety of receivers and comparing their performance with a total-power receiver.

The minimum-detectable average input-level increment  $\Delta T$  (defined to equal the rms value of the noise fluctuation about the mean level) is used as the basic performance measure. In the general expression derived,

$$\Delta T = T_{es} M / \sqrt{\tau \Delta f},$$

where  $T_{es}$  (the system effective-input-noise temperature) is used in preference to a noise-figure relationship,

$M$  is a factor depending on the type of receiver considered,

$\tau$  is the reciprocal of the equivalent width of the smoothing-filter power-transfer characteristic, and

$\Delta f$  is one-half of the equivalent width of the self-convolution of the reception-filter power-transfer characteristic.

Tables of  $\tau$  and  $\Delta f$  values for common types of filters have been calculated. Previously, because  $\tau$  and  $\Delta f$  had not been adequately defined, the comparison of results was difficult, since the factor here defined as  $M$  frequently included bandwidth and smoothing-filter characteristics. By means of the definitions above,  $M$  values free from filter specifications have been determined and tabulated. This approach has made it possible to reconcile apparently contradictory results from the earlier literature.

The important intrinsic capabilities of several stabilized systems to reduce the effect of instabilities due to non-ideal components and environments have been compared. For example, two cases of Dicke-receiver operation are frequently of interest: (1) using square-wave modulation and demodulation for which  $M = 2$ ; and (2) using square-wave modulation with a narrow video filter at the switching frequency for which  $M = \pi/\sqrt{2}$ . In the latter case,  $M$  is independent of the demodulation waveform.

For the Selove d-c comparison and correlation receivers,  $M = \sqrt{2}$ ; however, dual channels are required for both receivers. Comparison on a total-bandwidth basis increases  $M$  to 2.

A comprehensive study of Ryle and Vonberg's null-balancing receiver, which is generally insensitive to instabilities, has shown that its  $\Delta T$  value is equal to that of a Dicke receiver, provided the integrating time for the null-balancing receiver includes an over-all value considering the effect of the servo loop. The analysis also showed that a particular sensitivity to loop-gain stability exists in the following sense. Signals passing through the receiver suffer time delays that must be allowed for in data reduction. The fractional error in delay correction is directly related to the fractional error in loop gain and is independent of the servo-transfer function of the receiver.

A study of the automatic-gain-control (AGC) system for a total-power receiver and a modulated pilot-signal receiver showed that, when applied to a total-power receiver, AGC is useful only when d-c output levels are not needed.

The modulated pilot-signal system is shown to be theoretically capable of achieving M values at least equal to 2 when large integrating times are used in the AGC loop. In contrast to the Dicke receiver, stabilization against gain changes is independent of the signal level for the modulated pilot-signal receiver.

The concepts developed in this study have been used to analyze and evaluate the performance of the Stanford microwave spectroheliograph receiver, which is described in detail, and to establish the relationship of the instrument to its antenna and its observational requirements.

## CONTENTS

	Page
I. Introduction . . . . .	1
II. Basic Receiver Considerations . . . . .	4
A. General Receiver Requirements . . . . .	4
B. The Basic Measurement -- Power Level . . . . .	5
C. Minimum Detectable Signal . . . . .	5
1. Definition . . . . .	5
2. Ideal vs. Practical Evaluation . . . . .	6
D. An Elemental Receiver . . . . .	6
1. Description . . . . .	6
2. Analysis . . . . .	9
3. Definitions of Fundamental Parameters . . . . .	11
4. Parameter Values for Typical Filters . . . . .	12
E. Noise Temperature Concept . . . . .	15
F. Effective Input-Noise Temperature . . . . .	17
G. Detector Considerations . . . . .	19
H. Stability Discussion . . . . .	19
III. Total-Power Receivers and Stabilization . . . . .	24
A. Characteristics of Total Power Receivers . . . . .	24
1. Minimum Detectable Signal . . . . .	24
2. Practical Limitations . . . . .	24
B. Calibration Procedures . . . . .	24
1. Astronomical Sources . . . . .	25
2. Temperature-Controlled Sources . . . . .	25
3. Gas-Discharge Noise Generators . . . . .	25
4. Diode Noise Generators . . . . .	26
5. Recalibration . . . . .	26
C. Extreme Gain Stability Requirements . . . . .	26
D. Types of Stabilization . . . . .	27
1. Zero-Point Stabilization . . . . .	28
2. Two-Point Stabilization . . . . .	31
IV. More-Complex Receivers . . . . .	39
A. Stabilized Receivers with Unmodulated Signal . . . . .	39
1. Selove-Type Receivers . . . . .	39
2. Correlation-Type Receivers . . . . .	42
B. Stabilized Receivers with Modulated Signals . . . . .	51
1. Introduction . . . . .	51
2. Dicke Type Receivers . . . . .	51
C. Receivers with Servo Stabilization . . . . .	58
1. Introduction . . . . .	58
2. Automatic Gain Control Theory . . . . .	59
3. Pilot Signal Receivers . . . . .	61
4. Other AGC Systems . . . . .	71

CONTENTS (Cont'd)

	Page
V. Ryle and Vonberg Type Receivers . . . . .	73
A. General Description . . . . .	73
1. Controllable Reference Sources . . . . .	73
2. Error Voltage Amplifiers . . . . .	75
3. Comparison Devices . . . . .	76
B. Noise Analysis . . . . .	76
C. Dynamic Behavior . . . . .	78
D. Limitations . . . . .	81
E. Supplementary Smoothing Filters . . . . .	85
VI. Stanford Microwave Spectroheliograph Receiver . . . . .	86
A. General Requirements . . . . .	86
1. Bandwidth and Beamwidth Relationship . . . . .	86
2. The Temporal Response of the Receiver . . . . .	89
3. Accuracy . . . . .	89
B. Description of the Receiver . . . . .	92
1. General . . . . .	92
2. Input Circuitry . . . . .	94
3. R-F and I-F Sections . . . . .	96
4. Detector and Low-Frequency Section . . . . .	100
5. Demodulation and Output Sections . . . . .	101
6. Auxiliary Apparatus . . . . .	105
C. Characteristics and Performance . . . . .	106
1. Critical Features . . . . .	106
2. Minimum Detectable Signal . . . . .	108
D. Sample Records . . . . .	108
1. Fan-Beam Solar Record . . . . .	108
2. Pencil Beam Solar Record . . . . .	109
3. Weak Source Record . . . . .	109
VII. Conclusions . . . . .	111
A. Summary . . . . .	111
B. Comparative Results . . . . .	113
C. Suggested Further Study . . . . .	116
Appendix A. Useful Relationships . . . . .	118
Appendix B. Analysis of a Correlation Receiver . . . . .	120
Appendix C. Detailed Analysis of the Modulated Receiver . . . . .	124
Appendix D. Proof of Theorem on Time Displacements Due to smoothing . . . . .	132
Appendix E. Details of the Varactor Diode Shorting Section . . . . .	134

TABLES

Table		Page
2.1	A Variety of Smoothing Filters and Their $\tau$ Values . . . . .	14
2.2	A Variety of Reception Filter Power Transfer Characteristics . . . . .	16
4.1	Values of the Modifying Factor M in the Formula for $\Delta T$ for the Case of no Video Filter [ $J(f) = 1$ ] . . . . .	56
4.2	Values of the Modifying Factor M in the Formula for $\Delta T$ for a Narrow-Band Video Filter Which Passes Only the Fundamental Component of the Modulation Waveform $\mu(t)$ . . . . .	57
7.1	Relative Merits of Several Receivers With Equal $U_L$ 's . . .	112

ILLUSTRATIONS

Figure		Page
2.1	Block Diagram of Elemental Receiver . . . . .	7
2.2	The Effect of Changes of $\tau$ and $\Delta f$ on $C(f)$ . . . . .	13
2.3	A Favorable Location for the Modulation Frequency $f_m$ . . .	22
3.1	A Typical Calibration Curve for a Total Power Receiver . .	27
3.2	Gated AGC, Gated Total-Power Receiver with Zero Signal Point Stabilization . . . . .	29
3.3	Dicke Type Receiver with Zero Point Stabilization . . . . .	30
3.4	A Gated AGC Dicke Receiver with Zero Point Stabilization .	32
3.5	Dual-Reference Modulated Receiver with one Servo Gain Control . . . . .	33
3.6	Dual-Reference Modulated Receiver with two Servo Gain Controls . . . . .	34
3.7	Modulated Pilot-Signal Total-Power Receiver . . . . .	35
3.8	Receiver Giving Two Point Stabilization Using a Ratio Indicator for the Output . . . . .	36
3.9	Null-Balancing Receiver . . . . .	38
4.1	A Block Diagram of a Selove Type "D-C Comparison" Receiver	40
4.2	Conditions of Relative Bandwidth and Instability Factors When a Total-Power Receiver is Superior to a D-C Comparison Receiver . . . . .	41
4.3	Correlation Receiver Using Circulators . . . . .	44
4.4	Correlation Receivers Using a Magic Tee at the Input . . .	49
4.5	A Block Diagram of the Modulated Receiver . . . . .	54
4.6	A Coherent Demodulator . . . . .	56
4.7	The Effect of Instabilities in the Receiver Components Between the Detector and Demodulator on the Power Spectrum $B_{y_1}(f)$ . . . . .	59

ILLUSTRATIONS (Cont'd)

Figure		Page
4.8	Block Diagram of an AGC Loop in a Total Power Receiver . . .	60
4.9	Assymptotic-Frequency-Response Curves for the Receiver With AGC . . . . .	62
4.10	Requirements on Filter Break Frequencies . . . . .	63
4.11	Block Diagram for a Modulated Pilot-Signal-Stabilized Receiver . . . . .	64
4.12	Representation of the AGC Loop in the Modulated Pilot- Signal Receiver . . . . .	66
4.13	Ratio of Pilot-Signal to Signal Integrating Times as a Function of M Factor for a Pilot-Signal AGC Receiver . . .	69
4.14	Normalized Asymptotic Response to Instabilities of a Modulated Pilot Signal Receiver . . . . .	70
5.1	Simplified Block Diagram for a Ryle and Vonberg Type Noise-Balancing Receiver . . . . .	74
5.2	Simple Servo-System Block Diagram . . . . .	80
5.3	Spectra and Time Functions Showing the two Smoothing Operations Occurring During the Observation of a Discrete Source . . . . .	83
6.1	The Relative Beam Broadening . . . . .	88
6.2	Half-Power Beam Width for a Single Array vs. Order of Interference . . . . .	90
6.3	Half-Power Beam Widths for the Cross Antenna vs. Order of Interference . . . . .	91
6.4	Block Diagram of the Cross Receiver . . . . .	93
6.5	Diagram of the Phase Switch for Cross Operation . . . . .	95
6.6	Variable Phase Length Shorts for the Phase Switch . . . . .	97
6.7	Addition to the Phase Switch Which Produces a Double-Throw Microwave Switch . . . . .	98
6.8	Block Diagram of the R-F and I-F Sections of the Receiver . . . . .	99
6.9	Power Response Curve for the Complete Receiver . . . . .	100
6.10	Block Diagram of the Receiver from I-F Attenuator Through the Coherent Demodulator . . . . .	102
6.11	Coherent Demodulator . . . . .	103
6.12	Smoothing Filter Switching and Integrating Times . . . . .	104
6.13	Cathode Follower Output Circuit . . . . .	105
6.14	Sample Solar Record Showing Fan-Beam Scans . . . . .	109
6.15	A Sample Solar Record Showing Pencil-Beam Scans . . . . .	110
6.16	A Sample Record Showing a Fan Beam Scan of the Moon . . . . .	110

## SYMBOLS

c	output voltage of a servo system; velocity of light
e	error voltage of a servo system
f	frequency
h	impulse response
k	Boltzman's constant
l	junction load voltage
m	order of interference
n	noise voltage
p	strength
q	angle measured from a plane perpendicular to an antenna array
r	input voltage of a servo system
s	complex frequency
t	time
v	voltage
w	equivalent width
x	detector-input voltage
y	detector-output voltage
z	meter deflection at output of receiver
A, B, C, D	power spectral densities (PSD)
F	noise figure
G, H	power-transfer characteristics of reception filter, smoothing filter
I	fractional rms variation of the output due to instabilities
J	power-transfer characteristic of video filter
K	coefficients
L	reference level
M	factor to account for mode of receiver operation
N	noise power at receiver output
P	antenna response (field)
R	resistance
S	signal power
T	temperature ( $^{\circ}$ K)
U	uncertainty figure
Y	voltage transform of detector output $\langle y \rangle$
m	voltage from the equivalent modulator
s	spatial frequency
t	time-displacement variable

SYMBOLS (Cont'd)

$w$	width between half-power points
$C$	transform of the output signal in a servo system
$D$	voltage-transfer characteristic of the AGC amplifier
$E$	transform of the error signal in a servo system
$F$	Fourier transform
$G$	transfer function of a servo system
$I$	unit impulse function
$J$	portion of $G(s)$ after loop-gain factor is removed
$N$	no. of elements in an antenna array
$R$	transform of input signal in a servo system
$S$	sensitivity
$T$	time interval, time constant
$W$	ratio of half-power width to $\phi_c$
$\alpha$	ratio
$\beta$	fraction
$\gamma$	instability factor
$\delta$	(small variation, unit impulse function)
$\epsilon$	ratio
$\zeta$	instability-reduction factor
$\eta$	effective transfer characteristic for the modulated element
$\theta$	transfer function
$\mu$	zero-mean time-varying function
$\nu$	waveform whose square = $\eta(t)$
$\xi$	demodulation waveform
$\rho$	autocorrelation
$\sigma$	standard deviation
$\tau$	integrating time
$\phi_c$	peculiar interval
$\Gamma$	a-c open-loop gain
$\Delta$	increment
$\Omega$	scanning rate (rad/sec)
$\lambda$	wavelength
$\psi$	phase shift error angle

SYMBOLS (Cont'd)

Subscripts

a	AGC loop
b	break
c	continuous
d	noise diode
e	effective input
f	ferrite attenuator
g	loop gain of servo
h	impulse response
i, j	indices
l	low-frequency cut off
m	modulation
n	number
o	center frequency of receiver response
p	pilot
q	angle measured from a plane perpendicular to an antenna array
r	receiver
s	system
u	unwanted source
v	voltage
w	wanted source
x	before detection
y	after detection
A	acceleration
C	circulator
D	demodulator
F	video filter
G, H	power-transfer characteristics of reception filter, smoothing filter
I	instability
J	hybrid-tee junction
L	level
M	motor
P	position
S	signal power
T	total
V	velocity

SYMBOLS (Cont'd)

Subscripts

a	amplifier
c	comparison
h	highest
p	pilot
s	signal
t	tuned filter
$\eta$	modulated
$\kappa$	index no.
$\mu$	modulated waveform
$\nu$	index for error coefficient
$\xi$	demodulated waveform
$\phi$	feedback

### ACKNOWLEDGMENT

I wish to express my gratitude to Professor R. N. Bracewell for his guidance and supervision and to Professor G. Swarup for many helpful comments. Mr. C. L. Seeger deserves special thanks for his inspiration, encouragement and support. Thanks also go to Mr. D. D. Cudaback to whom I am indebted for many valuable discussions as well as assistance during the development of the receiver. The associations with colleagues and the staff of the Radioscience Laboratory have been of great value.

I wish to express to my wife, Mary Mae, my never-ending appreciation for her encouragement and understanding, which carried me through to the completion of this work.

## I. INTRODUCTION

A radio-astronomy receiver produces at its output an indication of the total effective noise power applied to its input. This indication changes when a signal is present. Whenever a measurement is made, the signal induced change is compared with changes made by substituted sources of known noise power. Assuming a perfectly stable receiver we can readily determine the theoretical accuracy of such a measurement.

It is convenient, in practice, to measure the signal powers in units of degrees Kelvin by the use and extension of Nyquist's theorem, which linearly relates an equivalent temperature with a noise power whenever a definite frequency band is involved. In this way Dicke [Ref. 1] first derived the expression,

$$\Delta T = (\text{Constant}) T_{e_s} / \sqrt{\tau \Delta f}$$

which relates the rms variation of the receiver output  $\Delta T$  to certain characteristics of the measurement procedure. Here,  $T_{e_s}$  is the effective system input-noise temperature in degrees Kelvin;  $\Delta f$  is the pre-detection, or high-frequency, bandwidth of the receiving system; and  $\tau$  is the post-detection integrating, or averaging, time.

Although the above parameters are generally included in some form in all receiver discussions, the diversity of arrangements arising because of individual requirements has led to certain difficulties when comparing performance. That is, the parameters are often modified for special cases and so are not easily generalized. Also, further complexity is introduced because of special designs that are employed to minimize practical limitations set by particular component characteristics, especially in relation to their stability.

In this study explicit, general definitions for the parameters of bandwidth and integration time are given. They are derived from the analysis of an elemental receiver, then modified and expanded to include a wide range of complex receivers

With the advent of masers and parametric amplifiers, our knowledge of the fundamental causes of system noise has increased rapidly until, now, we believe the theory is fairly complete. As a result, the new low-noise devices approach ever closer to predictable, natural limits [Ref. 2], and the belief is that the existence of these limits is well established, so

that future developments in amplifying devices will not yield large percentage improvements in their effective noise temperature. As a consequence, receiver stability assumes an ever more serious character, since it is then becoming the major limitation to receiver performance. Instability increases  $\Delta T$  in practice just as effectively as does a large increase in system-noise temperature, so that either intrinsic stability must be improved or the effects of instability must be reduced by the adoption of special observing procedures. Stabilities of one part in  $10^3$  are normal good practice, while  $10^4$  is unusual.

Because of imperfections in existing equipment, correlation receivers and various forms of switched-input receivers have been developed or proposed. Comparisons of the theoretical capabilities of many of these receivers differ by factors on the order of 2, root 2 and pi, which, although small, have considerable economic significance. In this study we provide useful theoretical comparisons, derived in a consistent manner, which should be applicable to all radio-astronomy receivers. In a number of cases, numerical calculations are presented to illustrate a practical range of situations

The "minimum detectable mean-input-level increment" is used as the performance criterion in this work. Although the phrase "minimum detectable signal" suffices at times, the longer and more exact statement always should be understood. The basis for this criterion is a simple level measurement

Techniques of stabilization may be divided into three categories, depending on methods of treating the signal in the receiver. The signal may be

- 1 unmodulated,
- 2 modulated, or
- 3 a null balanced or error signal.

The analysis of correlation and Dicke-type receivers in Chapter IV uses examples from categories 1 and 2. The null-balancing receiver is discussed in Chapter V. Whereas the material in Chapter IV is mainly an extension and codification of previous work, but in a much more general form, the analysis of the null balancing receiver is believed to be a new contribution to the field. The application of servo control or automatic gain control (AGC) to radio-astronomy receivers is treated in detail, and many interesting aspects are presented for which there has been no prior discussion

A specialized receiver developed for use with the Stanford Microwave Spectroheliograph is described in Chapter VI. The concepts developed in earlier chapters are used in the discussion of the specifications and the performance of this receiver. Also the effects of restrictions placed on receiver design because of the antenna system and the anticipated observing programs are considered.

Finally, it is pointed out that the successful development of a high-performance receiver for sensitive radio-astronomical investigations is an art, as much as it appears to be a matter of straightforward engineering.

## II. BASIC RECEIVER CONSIDERATIONS

### A. GENERAL RECEIVER REQUIREMENTS

In radio astronomy, receivers are often designed to operate with a particular antenna to form a radiotelescope, which is frequently designed for, or is inherently capable of performing, only a limited variety of measurements in a satisfactory manner. Because of these facts, it is necessary to compare receivers with care, concentrating on those characteristics which are basic to all systems.

Here we consider the radiotelescope as a transducer acting between incident electromagnetic energy and a record of one or more of the characteristics of this radiation. We can list a general set of requirements for this transducer as follows:

1. It must sense a region of space or sky with a particular antenna pattern
2. It must use a particular portion of the radio-frequency (r-f) spectrum.
3. The time-varying aspects of the observation must be handled satisfactorily
4. The record produced should be, as much as possible, only a measure of the desired characteristic.
5. The record should have the requisite range and accuracy

In general, and as a practical matter, these items are interrelated. For instance, items 1 and 2 must be considered together since the antenna pattern is a function of frequency although the receiver chiefly determines the frequency reception band.

Now we can assume that the over-all design provides for the measurement of the desired characteristics and we can then list some general receiver specifications as follows:

1. Spectral response, i. e., operating frequency, bandshape, and bandwidth
2. Temporal response, i. e., ability to follow expected changes of the input with time
3. Range and accuracy, i. e., least to greatest value of the measured variables with specified limits of error

The effect of design parameters on item 3, particularly as regards the least values of the desired measures, is of great interest.

Receivers in use up to this time have exhibited wide ranges in these specifications. Nearly the whole spectrum made available through current radio technology has been used. The values of signal strength, in terms of temperature, range from a few hundredths of a degree to more than  $10^6$  °K. Bandwidths vary from a few kilocycles to hundreds of megacycles. Measurements made include, for example, the detection of weak sources with measurements of their strengths and positions, source-brightness distributions, spectral variations and temporal variations of sources, and so forth. The objectives of radio astronomy cover a wide field.

## B. THE BASIC MEASUREMENT POWER LEVEL

Underlying the majority of measurements with radiotelescopes is a requirement for the determination of relative power at low levels. In the detection of sources, the problem often is to determine that minimum change in power level, as indicated by the receiver, which can be correctly ascribed to a source, and not to "faults" in the receiver. By thoroughly discussing just this simple measurement--the determination of the power level or strength of a constant source--we are well prepared to understand more complex measurements. The capabilities of a receiver with regard to this simple measurement of power level will be discussed below and a general expression will be given which specifies a performance figure, or figure of merit.

## C. MINIMUM DETECTABLE SIGNAL

The detection of a simple change in input power level depends, in practice, on more than just the properties of the radiotelescope or the receiver alone. However, for our purposes, considerations other than those relating to the receiver alone are not included, since we wish to establish only the properties of the receiver.

### 1. Definition

In order to be removed from any characteristics of the operator, we establish a criterion of detectability on the basis of a convenient mathematical definition. This criterion may be stated as follows: when at the output meter the mean deflection increment corresponding to a signal increase equals the standard deviation of the fluctuations about the mean deflection, this mean deflection increment is said to be detectable \*

---

\* In practice, of course, experience often wisely dictates the use of a several-times larger increment

## 2. Ideal vs. Practical Evaluation

The idealized design of the receiver sets forth the necessary details from which a performance figure for detectability can be calculated. The practical receiver will have instabilities of gain, bandwidth, and effective-input-noise temperature which will degrade the ideal performance by some factor.

### D. AN ELEMENTAL RECEIVER

The quantity to be measured by the receiver is the strength of a source of energy having an essentially uniform power-spectral density (PSD) over the observing range of frequencies. Furthermore, as is frequently the case, the source is assumed to produce an ideal fluctuating voltage, i e., one with a stationary gaussian amplitude distribution about a zero mean value. Within the receiver, the energy from a particular source undergoes alterations and ultimately produces a deflection on the output meter. In general the meter deflection consists of unwanted components, such as receiver noise and zero offset, in addition to the component due to signal from the source to be measured. If the receiver is calibrated\* to yield a unit mean deflection for a unit mean-input-level increment, deflection and incremental input level can be equated. This stratagem allows us, for an idealized, stable receiver, to dispense with discussing receiver gain, which, although of practical importance, does not affect intrinsically the power-level-detection performance.

The ratio of the detectable mean-deflection increment to the mean meter deflection may be considered constant for a given elemental-receiver design, as will be shown, so that this ratio is a measure of performance. The minimum detectable input-level increment will therefore depend on the unwanted source strengths, referred to the receiver input, which for the elemental receiver determine the mean output-meter deflection at zero signal.

#### 1. Description

The elemental receiver analyzed below is shown in block diagram form in Fig 2.1. The receiver responds both to the signal and to an

---

\* Calibration is assumed possible with an accuracy much greater than the accuracy of the measurements to be made. This assumption keeps practical details such as needle width, dead zone, ink-line width, and scale reading in general from contributing to the detectability criterion.

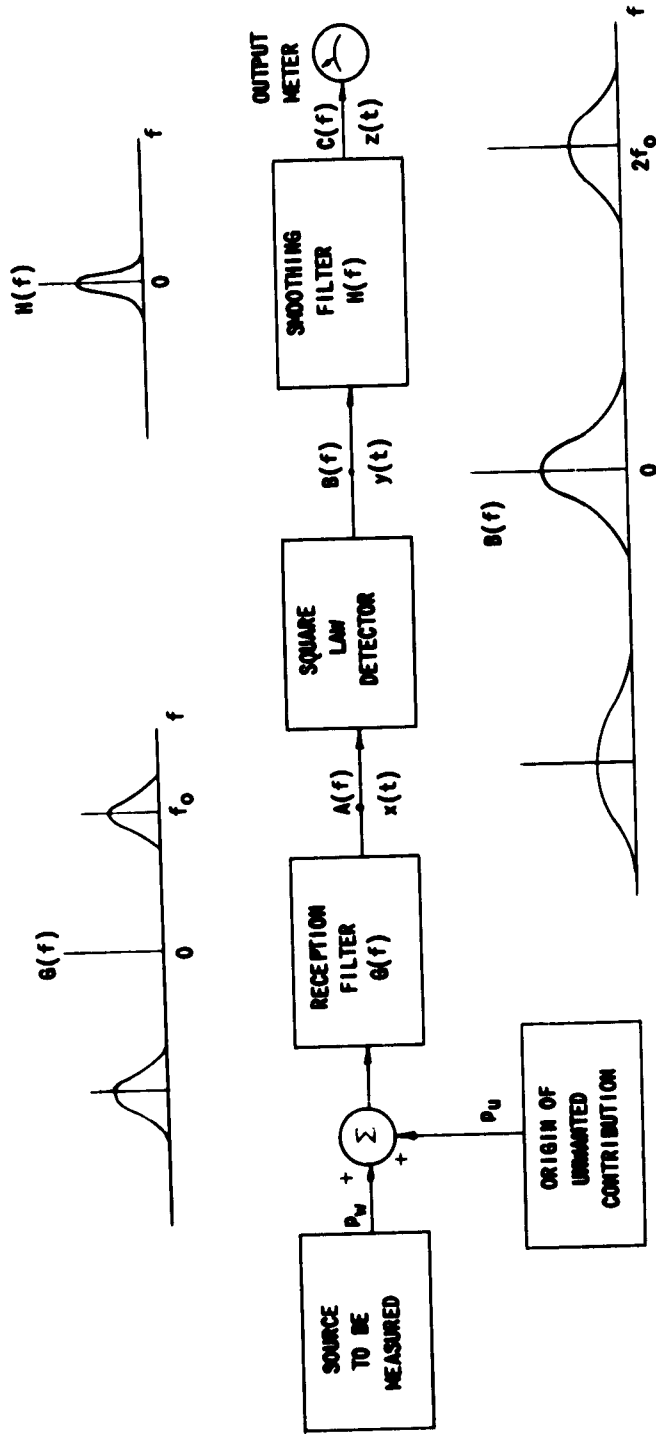


FIG. 2.1. BLOCK DIAGRAM OF ELEMENTAL RECEIVER.

unwanted source of energy at its input. The latter input is equivalent, with regard to meter deflection, to all actual unwanted contributions distributed throughout the receiver, such as those associated with transmission loss, amplifier noise, and frequency-conversion loss. We shall consider only inputs having uniform power per unit frequency interval. All elements except the final detector are assumed to be linear.

The reception filter is equivalent to the combined effect of all the frequency-sensitive elements in the system, such as the antennas, transmission lines, r-f and i-f amplifiers, mixers, and any selective filters that may be used. Thus the portion of the spectrum from which energy can be received is defined by a power-transfer characteristic  $G(f)$ , which is the ratio of the output to input PSD's of the reception filter at all points in the spectrum. Since we are dealing here only with inputs having uniform PSD's, the PSD of the reception-filter output, and of the detector input, will be

$$A(f) = (p_w + p_u) G(f)$$

where  $p_w$  is the strength of the source to be measured and  $p_u$  is the strength of the unwanted source at the input measured in units of  $w/cps$ . The spread of  $A(f)$  is assumed to be small compared with the mean frequency.

The voltage  $x(t)$  at the detector input has a gaussian amplitude distribution with zero mean and PSD  $A(f)$ . The exact voltage as a function of time  $x(t)$  is actually not known, of course, but its statistical properties are, and they are used in the detector analysis and after. Similar statements hold for other quantities such as  $y(t)$  and  $z(t)$ , used later.

For the elemental receiver, an ideal square-law detector circuit is employed with one ohm impedance levels so that

$$y(t) = x^2(t)$$

and the mean output voltage  $\langle y \rangle$  equals the power at the detector input thus

$$\langle y \rangle = \langle x^2 \rangle$$

The sharp brackets indicate the following averaging operation,

$$\langle y \rangle = \lim_{T \rightarrow \infty} \frac{1}{2T} \int_{-T}^T y(t) dt.$$

Fluctuations of  $y(t)$  about the mean are governed by the continuous portion of the detector output PSD  $B(f)$ .

After detection, the fluctuations about the mean are reduced by a smoothing filter with power-transfer characteristic  $H(f)$ . A typical smoothing filter might be a single-section, lowpass RC circuit. The smoothed output voltage is then displayed as a meter deflection. For generality we include any selective effects (usually further smoothing) of the meter in  $H(f)$  by taking  $z(t)$  to be the true meter deflection.

## 2. Analysis

As stated above, the PSD  $A(f)$  of the detector input voltage  $x(t)$  is

$$A(f) = (p_w + p_u) G(f).$$

The total power at the detector input is, using Eq. (A.4)\*

$$\int_{-\infty}^{\infty} A(f) df = \rho_x(0) = \langle x^2 \rangle$$

where  $\rho_x(0)$  is the central ordinate of the autocorrelation function of the detector input voltage. Now, using the relationship of Eq. (A.8) for the PSD of the detector output voltage  $y(t)$ ,

$$\begin{aligned} B(f) &= 2 \int_{-\infty}^{\infty} \rho_x^2 \exp(-j2\pi f\tau) d\tau + \rho_x^2(0) \delta(f) \\ &= 2[A(f) * A(f)] + \rho_x^2(0) \delta(f) \end{aligned}$$

---

\* Appendix A, Eq. (A.4).

At the output of the receiver, the PSD of the meter deflection  $z(t)$  is

$$\begin{aligned} C(f) &= H(f) B(f) \\ &= 2H(f) [A(f) * A(f)] + H(f) \rho_x^2(0) \delta(f). \end{aligned}$$

Since  $z(t)$  and  $y(t)$  are related by the voltage response of the smoothing filter, it follows that

$$\langle z \rangle = \sqrt{H(0)} \langle y \rangle = \sqrt{H(0)} \rho_x(0).$$

We can now form an expression for the detectable mean-deflection increment  $\Delta z$ , which we defined earlier to be equal to the rms variation about the mean of the meter deflection  $z(t)$ .

$$\begin{aligned} \Delta z &= \sqrt{\langle z^2 \rangle - \langle z \rangle^2} \\ &= \sqrt{\int_{-\infty}^{\infty} C(f) df - H(0) \rho_x^2(0)} \end{aligned}$$

This becomes

$$\Delta z = \sqrt{2 \int_{-\infty}^{\infty} H(f) [A(f) * A(f)] df}$$

Generally, the smoothing-filter power-transfer characteristic will be only a few cycles per second wide while the PSD  $B(f)$  will have widths on the order of megacycles per second. When this is true  $[A * A]$  can be assumed constant over the total effective width of  $H(f)$  so that

$$\int_{-\infty}^{\infty} H(f) [A * A] df \approx [A * A] \int_{-\infty}^{\infty} H(f) df. \quad (1)$$

With this assumption, the expression for the ratio of detectable mean deflection increment to the mean deflection will be

$$\Delta z / \langle z \rangle = \sqrt{2[A^*A] \Big|_0 \int_{-\infty}^{\infty} H(f) df / \rho_x^2(0) H(0)}$$

Using the equivalent width  $w_H^*$  and expressing  $\rho_x^2(0)$  in terms of  $A(f)$ , the equation above becomes

$$\Delta z / \langle z \rangle = \sqrt{2[A^*A] \Big|_0 w_H / \left[ \int_{-\infty}^{\infty} A(f) df \right]^2} \quad (2)$$

Using Eqs. (A.4) and (A.5),

$$\left[ \int_{-\infty}^{\infty} A(f) df \right]^2 = \rho_x^2(0) = \int_{-\infty}^{\infty} [A^*A] df.$$

When  $A(f)$  is replaced in (2) with  $(p_w + p_u) G(f)$ , terms in  $(p_w + p_u)$  vanish, and when equivalent width  $w_{G^*G}$  is used it is now evident that

$$\Delta z / \langle z \rangle = \sqrt{2w_H / w_{G^*G}}$$

### 3. Definitions of Fundamental Parameters

If we define an integrating time  $\tau$  and a bandwidth  $\Delta f$  as follows,

$$\tau = 1/w_H = H(0) / \int_{-\infty}^{\infty} H(f) df \quad (3)$$

$$\Delta f = w_{G^*G} / 2 = \int_{-\infty}^{\infty} [G^*G] df / 2[G^*G] \Big|_0 \quad (4)$$

we can express the ratio

$$\Delta z / \langle z \rangle = 1 / \sqrt{\tau \Delta f} \hat{=} U_L \quad (5)$$

\* See Appendix A, Eq (A.6)

Henceforth this ratio will be called the *level-uncertainty* figure. For the elemental receiver,  $U_L$  equals the minimum-detectable increment of mean meter deflection divided by the mean meter deflection. For generality,  $U_L$ , expressed in terms of the input, equals the fractional uncertainty of measurement of input level, or the ratio of minimum-detectable mean input-level increment to the mean input level. As will be discussed below, many receivers operate with a suppression of the zero-signal mean meter deflection. Then the mean input level is no longer directly related to the mean meter deflection, so that  $U_L$  has meaning in terms of input levels only.

The form  $U_L$  describes the instrument's capabilities with respect to indicating changes in input level. In order to evaluate  $U_L$  it is necessary to be able to assign values of  $\tau$  and  $\Delta f$  to the receiver. Since these parameters have been explicitly defined in Eqs. (3) and (4) their values and the resulting value for  $U_L$  can be determined.

To understand better the roles of  $\tau$  and  $\Delta f$ , consider the PSD  $C(f)$  at the output meter and note the effect of changes in  $\tau$  and  $\Delta f$ . Figure 2.2(a) shows a typical  $C(f)$ . Note the following points: there is an impulse function at zero frequency, indicated by a vertical arrow, of strength equal to  $\langle z \rangle^2$ ; the central ordinate of the continuous portion of the function is designated  $C_c(0)$ ; and the shading in Fig. 2.2 shows the area under the continuous portion,  $C_c(f)$ . The smoothing filter limits the extent in frequency of  $C_c(f)$ . Since the area under  $C_c(f)$  equals the square of the detectable mean deflection increment, we see that, by narrowing  $H(f)$ , and, hence,  $C_c(f)$ , the detectable mean deflection increment is reduced. Figure 2.2(b) shows the effect of narrowing  $H(f)$ , which is equivalent to increasing  $\tau$ .

#### 4 Parameter Values for Typical Filters

In Table 2.1,  $w_H$  and  $\tau$  are listed for a variety of smoothing filters in terms of filter specifications. Many circuit configurations can yield the same  $\tau$ , so that, for simple measurements of input-level increments, as discussed here, the choice of filter is a matter of convenience, but with the restriction that its response be limited to a region of the spectrum where its input power spectral density can be assumed constant. [See Eq. (1)]

The reception filter determines the amplitude of  $C_c(0)$  in relation to  $\langle z \rangle^2$ . The following relationships show that  $\Delta f$  implicitly contains this information.

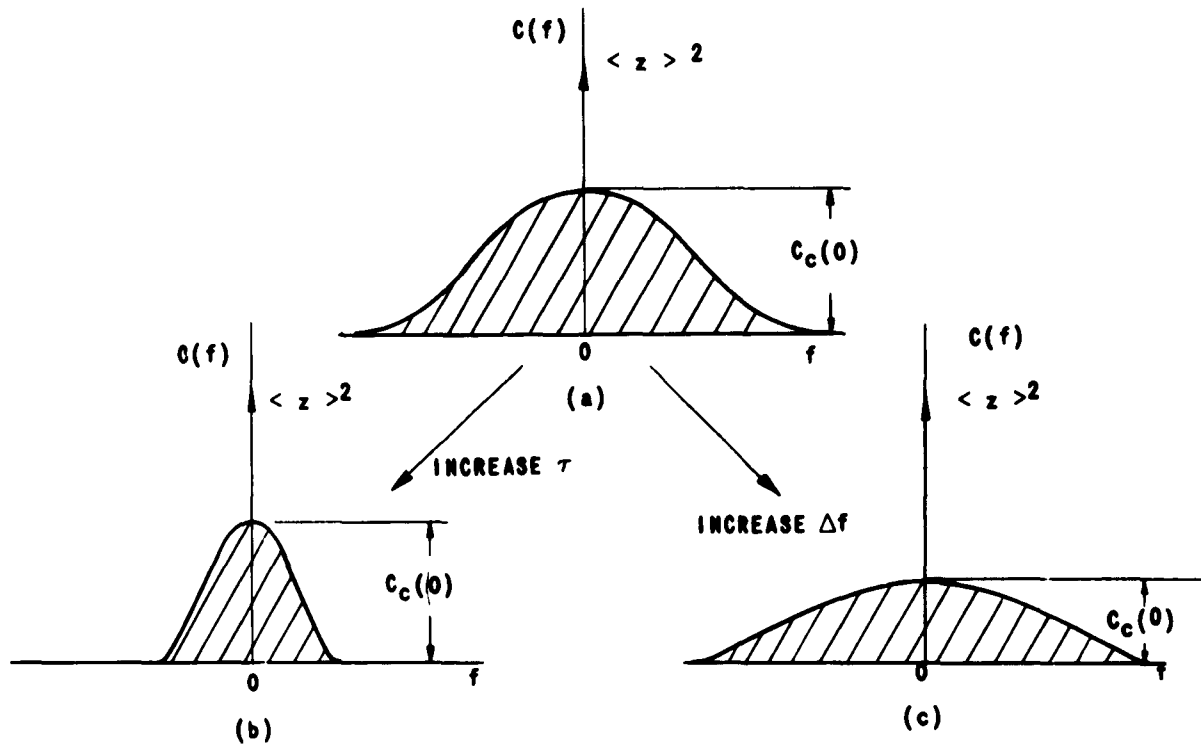
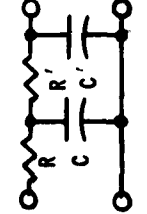


FIG. 2.2 EFFECT OF CHANGES OF  $\tau$  AND  $\Delta f$  ON  $C(f)$ . IN (a) A COMPARISON SITUATION IS SHOWN WITH (b) SHOWING THE EFFECT OF INCREASING  $\tau$  AND (c) SHOWING THE EFFECT OF INCREASING  $\Delta f$ . THE SCALE OF (c) IS NORMALIZED TO HAVE THE SAME AMPLITUDE FOR  $\langle z \rangle^2$  AS IN (a).

TABLE 2.1. A VARIETY OF SMOOTHING FILTERS AND THEIR  $\tau$  VALUES.

SMOOTHING FILTER	$\tau$	$\tau$	CIRCUIT	$\tau$
SINGLE-SECTION RC LOW PASS	$2 RC$	$\frac{1}{2} RC$		$\frac{1}{1 + (2\pi f RC)^2}$
TWO-SECTION IMPEDANCE-TAPED RC LOW PASS * $RC = R'C'$ ; $R \gg R'$	$4 RC$	$\frac{1}{4} RC$		$\frac{1}{[1 + (2\pi f RC)^2]^2}$
CRITICALLY DAMPED $\alpha = R/(2L) = 1/\sqrt{LC}$	$4/\alpha$	$\alpha/4$		$\frac{\alpha^4}{[(2\pi f)^2 + \alpha^2]^2}$
IDEAL LOW PASS	$1/f_0$	$f_0$		
IDEAL RUNNING MEAN OVER TIME T	$T$	$1/T$		$\frac{\sin^2 \pi f T}{(\pi f T)^2}$
GAUSSIAN	$1/f_g$	$f_g = \sqrt{2\pi} \sigma$		$\exp(-\pi f^2 / f_g^2)$ $\exp(-f^2 / 2\sigma^2)$

$$\Delta f = \frac{w_{G \cdot G}}{2} = \frac{\int_{-\infty}^{\infty} [G \cdot G] df}{2[G \cdot G]_0} = \frac{\int_{-\infty}^{\infty} [A \cdot A] df}{2[A \cdot A]_0}$$

$$\Delta f = \frac{\rho_x^2(0)}{2[A \cdot A]_0} \cdot \frac{H(0)}{H(0)}$$

$$= \frac{\langle z \rangle^2}{C_c(0)}$$

Figure 2.2(c) shows the effect of an increased  $\Delta f$  on  $C(f)$  over the condition of Fig. 2.2(a).

The equivalent width, defined above as a self-convolution of the even function  $G(f)$ , is suitable for describing reception-filter responses for which the usual concepts of bandwidth break down or are difficult to apply. It will cover, for instance, bands with notches or peaks in their response and so may not have unequivocal center frequencies or maximum responses. Values of  $\Delta f$  for a few reception-filter responses are listed in Table 2.2.

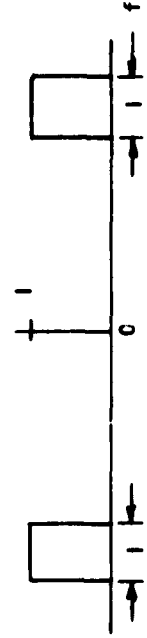
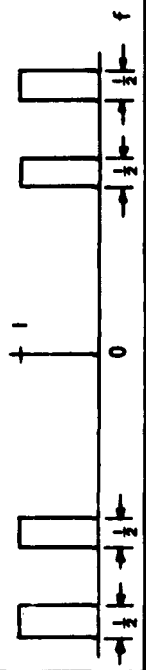
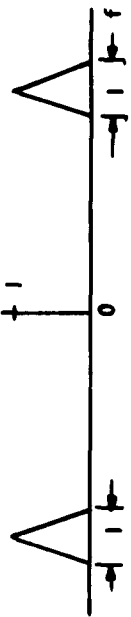
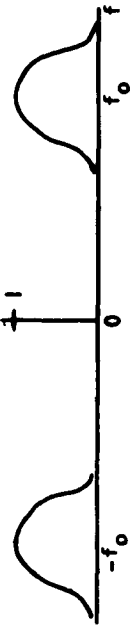
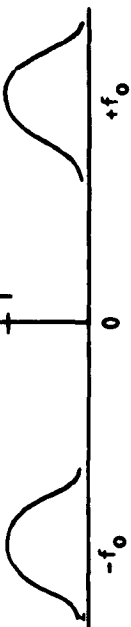
The level-uncertainty figure  $U_L$  was introduced as a parameter to indicate the measuring ability of the combined reception and smoothing filters when fully utilized. Since techniques for improving other characteristics of a receiver sometimes result in reduced utilization of the filters, the uncertainty of measurement for a complete receiver may involve a modifying factor  $M$  applied to  $U_L$ .

Before covering various receiving systems and their associated  $M$  values, a discussion of some of the practical aspects of receivers that affect  $U_L$  will be given in the next sections.

#### E. NOISE-TEMPERATURE CONCEPT

The total power at the detector input can be divided by the power gain of the receiver up to that point in order to refer the power to the receiver input. When this input noise power is equated to the thermal noise power from a matched termination at the input to the receiver, the required temperature of the termination becomes a convenient measure of the effective input noise power.

TABLE 2.2. A VARIETY OF RECEPTION FILTER POWER TRANSFER CHARACTERISTICS  $[G(f)]$  AND THEIR WIDTHS  $(\Delta f)$ .

RECEPTION FILTER CHARACTERISTIC SHAPE	$G(f)$	$\int_{-\infty}^{\infty} G(f) df$	$\Delta f$	$\frac{\Delta f}{(3\text{db BANDWIDTH})}$
RECTANGULAR		2	1	1
RECTANGULAR PAIR		2	1	1
TRIANGULAR		1	0.75	1.5
SINGLE TUNED CIRCUIT		$2\pi$	$2\pi$	$\pi$
T.O. SYNCHRONOUSLY TUNED STAGES		$\pi$	$0.8\pi$	1.953
Gaussian		2	$\sqrt{2}$	1.505

The source strengths  $p_w$  and  $p_u$  can be described by an effective noise temperature by being equated to the strength of a thermal source at some temperature  $T$  by the relation

$$p = kT$$

w/cps when they have constant power per unit frequency interval. This is a common and highly precise assumption. For incoherent sources, the strengths of two or more sources add to give the total strength and likewise their effective noise temperatures add.

Input noise temperature will be used almost exclusively in discussing signals and unwanted sources with their strengths having been referred to the receiver input.

#### F EFFECTIVE INPUT-NOISE TEMPERATURE

An elemental receiver includes unwanted sources of energy that contribute to the mean meter deflection. When the signal source strength is reduced to zero, there remains a mean meter deflection which can be ascribed to an equivalent unwanted source strength  $p_u$  at the receiver input. This equivalent receiver input and the level-uncertainty figure determine the minimum detectable input level increment for the receiver. If we express this increment and the equivalent unwanted source strength in terms of input-noise temperatures, the relation of Eq. (5) becomes

$$\frac{\Delta T}{T_{es}} = U_L$$

where  $\Delta T$  is the minimum detectable input temperature increment and  $T_{es}$  is the effective system input noise temperature. In radio astronomy the measurement of signal strength is limited by the total effective noise power present. Expressed in terms of the receiver input as  $T_{es}$ , it becomes an important parameter which is used to represent the temperature of an equivalent source of noise including receiver noise, transmission-line loss noise and all sources of unwanted noise in the antenna reception pattern. The inclusion of this last unwanted noise results from a broad use of the system concept.

If we were to use an "average noise factor" [Ref 3] to describe the system and determine  $\Delta T$ , we would be limited by the accepted definition

of the term. First,  $\bar{F}$  is defined in terms of a standard temperature for the signal source. Since signal source temperature is what we are trying to measure the introduction of a standard temperature seems inappropriate in order to describe receiver performance. However, if we use the corresponding term "average effective input-noise temperature"  $\bar{T}_e$ , we are free from any standard temperature requirement.  $T_e$  is "the input termination noise temperature which, when the input termination is connected to a noise-free equivalent of the transducer, would result in the same output noise power as that of the actual transducer connected to a noise-free input termination... [and]  $T_e = 290 (F-1)$ " [Ref. 3]. The symbol  $T_{e_s}$ \* is a special use of this concept in that the transducer must be extended to include not only the receiver and antenna but the background radiation upon which the signal is superimposed, and averaged over the reception band. We can then paraphrase the above definition, " $T_{e_s}$  is the average... the actual transducer "connected" to a signal-free region of the sky." (The underlined portions are changed )

A second reason for avoiding  $\bar{F}$  is that radiometer usage of heterodyne systems make the definition of  $\bar{F}$  inappropriate since a different relation between it and  $T_{e_s}$  must be used for each case. For instance, in a tuned r-f receiver

$$T_{e_s} = 290 (\bar{F} - 1)$$

and for the usual heterodyne case when both the image and signal bands contribute equally to signal and unwanted output components

$$T_{e_s} = 290 [(\bar{F}/2) - 1]$$

For minimum-detectable input-temperature increments, given a condition of signal level, which we designate  $\Delta T(T)$  where  $T$  is signal-input temperature, the mean input level will include a contribution from the signal as well as from unwanted sources. Then

---

\*We drop the bar over  $T_{e_s}$  for convenience, but  $T_{e_s}$  is an average.

$$\Delta T(T) = M T'_{e_s} U_L$$

where  $T'_{e_s}$  is the effective input temperature, including effective signal temperature. For the elemental receiver

$$T'_{e_s} = T_{e_s} + T.$$

#### G. DETECTOR CONSIDERATIONS

Although the detection process can be accomplished with different types of detectors, the square-law detector was chosen for the above analysis, a choice which, for small signals, results in no loss of generality. Strum [Ref. 4] points out that  $\Delta T$  must be increased only 1.05 if a linear detector is used and that the behavior of other general-law detectors approaches that of the square-law detector for small signals.

Lampard [Ref. 5] and Kelly, Lyons, and Root [Ref. 6] have shown the optimum detector law to be the square law for a simple change in level measurement.

#### H. STABILITY DISCUSSION

In the analysis of the elemental receiver, complete stability, in the sense of constancy of the receiver characteristics was assumed (although non-ideal operation as far as unwanted noise sources was considered), but, in fact, the fluctuating component of the meter deflection is dependent on the stability of the receiver. All departures from a stable operating condition contribute an addition to the meter deflection power spectrum. In general, the additional spectral components will have these characteristics:

1. No d-c component (by definition)
2. Concentration of spectral density around d-c
3. Rapidly decreasing strength with increase of frequency
4. Possible peaks or line spectra associated with power-source harmonics or microphonics

The result of the output variations due to instability will be to increase  $\Delta T$ . However, depending on the instability spectrum compared to that of the signal, the result can be more or less deleterious since, for signal variations rapid compared to those due to instability, the

detectability of the signal will not be greatly affected. Slow variations in the output due to such things as gain deterioration are generally referred to as drifts. When the period of measurement is short, the drift is quasi-linear and can be removed from the record without serious effect. As the relative period of measurement increases and the drifts take on curvature and inflections, they constitute a serious degradation of signal which is difficult to evaluate. When the variations have taken on the character of fluctuations they are amenable to inclusion in the minimum detectable signal expression as follows. The rms value of fluctuations in the meter deflection referred to the input will be the quadratic sum of components due to sources and to instabilities.

$$\Delta T = T_{es} \sqrt{U_L^2 + I^2},$$

where  $I$  is the fractional rms variation due to instability alone. This expression can be written in the form

$$\Delta T/T_{es} = U_L \sqrt{1 + (I/U_L)^2} = U_L \gamma \quad (6)$$

where  $\gamma$  is the instability factor for the receiver.

Three characteristics of a receiver that can produce instabilities are its gain, equivalent noise temperature, and frequency response. A change of any of the three will produce a change in meter deflection. The noise temperature, however, is essentially different, since it does not directly influence the signal amplitude

One approach to achieving stability is by stabilizing the gain through an automatic-gain control (AGC) system. What is commonly called AGC usually operates to maintain constant output from the receiver over periods long compared to signal observing times and does not operate to produce constant gain. Consequently any gain change controlled by this AGC may in fact be compensating for a change in equivalent noise temperature. This situation results in possible subtle changes in calibration and must be considered when this AGC is used. A true AGC system is discussed in Chapter IV, Section C.3.

The answer to difficulties of this type is a mode of operation which makes the mean meter deflection zero in the absence of signal. Dicke

[Ref. 1] described such a receiver, which used modulation of the signal at the input and a coherent demodulation at the receiver output. In the absence of signal the modulation component in the receiver is ideally zero, so that instabilities do not contribute to the mean output of the coherent demodulator. The PSD of the coherent demodulator output is determined by the input spectrum in a band set by the smoothing filter around the modulation frequency  $f_m$ . By locating the modulation frequency in a region of the instability spectrum  $B_I(f)$ , where the value of  $B_I(f)$  is small, the major effects of instabilities are eliminated. Figure 2.3 shows a typical instability power spectrum and a favorably located modulation frequency

Knowledge of the function  $B_I(f)$  is usually poor, but the general form shown in Fig. 2.3 seems to hold in practice. One would suspect  $B_I(f)$  to be nonstationary and hence difficult to predict from simple and quick measurements, since it originates chiefly from temperature, power supply, and aging variations. Steinberg [Ref. 7] measured the instability spectrum for some receivers and showed the general decrease in intensity with frequency. For the cases he considered, it appeared advantageous to use modulation frequencies in the kilocycle range in order to take advantage of the modulation technique.

Dicke receivers must sometimes be operated with a modulation component present at all times because of practical problems. For this case, Bracewell [Ref. 8] gives a reduction factor to be applied to the gain-instability contribution, which is expressed in terms of the noise temperatures present in both a Dicke system and in an elemental receiver. A tacit requirement that  $B_I(f_m) = 0$  is involved, however. In the analysis of various operation modes to follow, factors of this type will be discussed.

Another approach to the problem of operating with instabilities has been described by Selove [Ref. 9]. This "d-c comparison" receiver reduces the mean meter deflection for zero signal to zero by subtracting an equal mean output component derived from a second receiver channel designed to be as similar as possible to the signal channel and fed from a fixed source. The assumption is that instabilities would affect both channels equally and produce compensating outputs yielding a net zero mean meter deflection. The instability reduction factor for this receiver will depend on the similarity of the two channels.

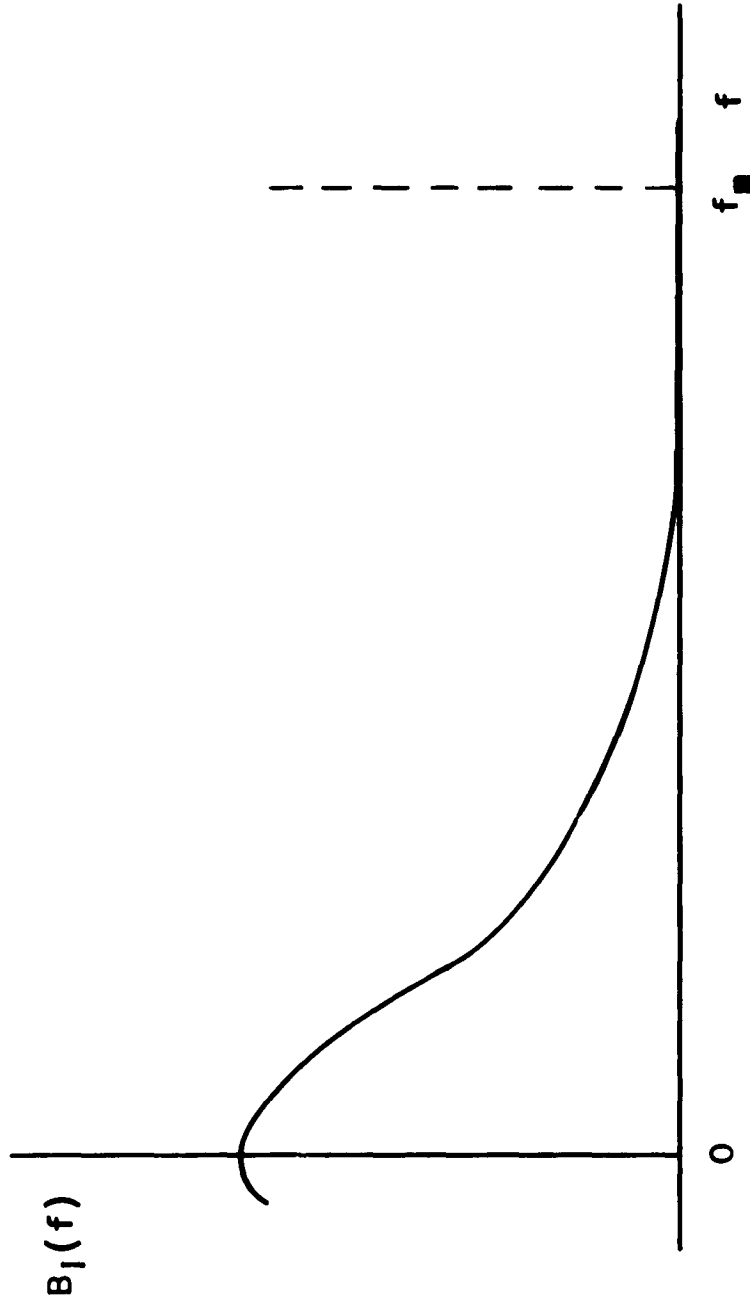


FIG. 2.3. FAVORABLE LOCATION FOR THE MODULATION FREQUENCY  $f_m$  IN RELATION TO THE INSTABILITY POWER SPECTRUM  $B_I(f)$ .

A third approach to the instability problem was analysed by Goldstein [Refs. 10,11]. In this receiver the input signal is impressed on two channels, which have independent equivalent-receiver-noise sources. After amplification the outputs of the two channels are multiplied together. In the absence of signal the output of the multiplier should be zero. Receivers of this type are also discussed in detail in the following chapters.

### III. TOTAL-POWER RECEIVERS AND STABILIZATION

#### A. CHARACTERISTICS OF TOTAL-POWER RECEIVERS

##### 1. Minimum Detectable Signal

The analysis of the elemental receiver is directly applicable to a type of receiver usually called a total-power or d-c receiver. In this receiver we find all the components of the elemental receiver, but with the gain present in r-f and i-f amplifiers before the detector and in d-c amplifiers after the detector. The expression for  $\Delta T$  of the elemental receiver is usable with the addition of the instability factor defined in Eq. (6); thus

$$\Delta T = T_{e.s} U_L \gamma$$

for the total power receiver.

##### 2. Practical Limitations

The mean meter deflection due to  $T_{e.s}$ , at zero signal, is often larger than the deflection due to the signal, so that it is common practice to subtract a fixed d-c level corresponding to the expected mean meter deflection before impressing the output on the meter. (The quantity subtracted is often called the "buck-out" or "back-off".) This practice increases the percentage of full-scale deflection per unit signal but, of course, also increases the percentage deflection for output changes due to instability in the receiver.

Since the only way to stabilize a total-power receiver is to make each part more stable than required of the whole receiver, great, and sometimes impractical, care is required in its design and construction. A useful receiver of this type designed for observations at meter wavelengths, is described by Seeger, Stumpers and van Hurck [Ref. 12].

#### B. CALIBRATION PROCEDURES

For a radio-astronomy receiver, convenient scale units for the output are  $^{\circ}\text{K}$  of effective noise temperature at the input. A calibration curve shows the relationship between input temperature and scale divisions on the output meter

Ideally, an instrument would have a permanent calibration and preferably a linear relationship between the input and output. In practice, the curve will depart from the linear ideal to some extent and will require recalibration from time to time because of changing conditions in the receiver. A particular point of concern is the detector law. Unless a square-law device is used, the average level into the detector will affect the calibration.

The available standards of noise power for calibration purposes are:

- 1 Astronomical sources,
- 2 Temperature-controlled terminations or loads,
- 3 Gas-discharge noise generators, and
4. Diode noise generators.

Each of these can be used in a variety of ways to determine the calibration curve.

### 1. Astronomical Sources

Astronomical sources as standards have the advantage of giving an over-all measure of the performance of the radiotelescope. The antenna, feed system, and receiver all affect the resulting output when a radio source is observed. Much work is being done to establish the strengths of the stronger sources for just such use [Refs. 13 - 16]. Two disadvantages associated with their use are the scarcity of standard sources and the limited range of strengths represented

### 2. Temperature Controlled Terminations

Temperature-controlled terminations are the most accurate standards of power in use at the present time. In conjunction with a precision attenuator, a limited range of strengths can be obtained for use in a detailed determination of receiver calibration. The temperature range is restricted because of practical details involving materials at extreme temperatures, temperature coefficients of resistance affecting impedance match and gradients of temperature in the calibration system.

### 3 Gas-Discharge Noise Generators

Gas-discharge noise generators have maximum noise temperatures of 10,000 to 20,000 °K. Their stability is good, and in the microwave region they provide the most versatile and useful sources at known temperatures. In general, they must be calibrated against thermal sources (2. above)

#### 4. Diode Noise Generators

Diode noise generators have a somewhat lower frequency range, extending down from the lower microwaves. To obtain good accuracy with a diode noise source care must be used in the measurement of diode current and in the provision of a good termination over the frequencies of interest. These noise sources also must be calibrated against thermal-noise sources.

#### 5. Recalibration

The receiver must be calibrated frequently enough to provide the desired accuracy. Sometimes a calibration procedure must be carried out before and after each measurement of a series, while sometimes a partial calibration only at one or two points need be inserted several times in the course of observation. Naturally the quality of the instrument determines how often calibration is necessary.

A typical calibration curve for a total power receiver is shown in Fig. 3.1. Deflection of the output meter is plotted against signal input with the point for zero signal indicated. The curve is shown extrapolated to a zero for total noise input, which is  $T_{es}$  degrees below the signal zero.

### C. EXTREME GAIN-STABILITY REQUIREMENTS

Total-power receivers have been constructed and used with effective input temperatures from a few hundred to several thousands of degrees Kelvin. Typical  $U_L$ 's, as calculated from theoretical receiver parameters, go as low as a few parts in ten thousand. It is evident that, in order that the receiver be fully utilized, it must be stable to a similar extent. In order to achieve stabilities on this order, one must begin with, use power sources that are sufficiently stable and then design the receiver itself to be as free as possible from other sources of instability. Finally, operation in a controlled environment is very important.

As well as providing a receiver as stable as possible, one resorts to calibration checks as frequently as practical in an effort to minimize the effects of the remaining instabilities. Many receiving systems perform part of this calibration function as part of their mode of operation, with the type and amount of stabilization achieved depending on their system design. For instance, the Dicke receiver can be thought of

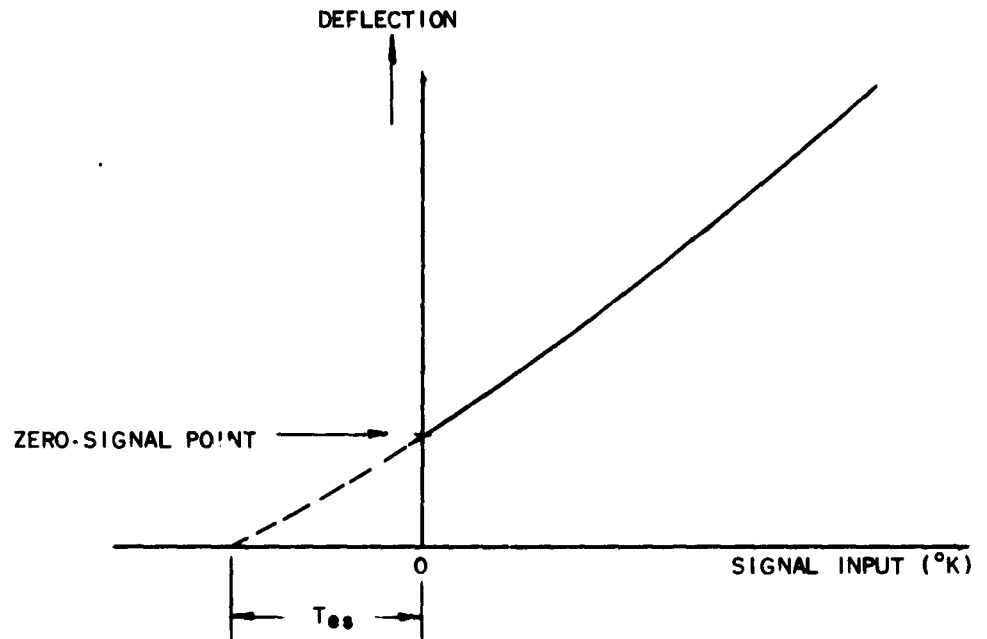


FIG. 3.1 TYPICAL CALIBRATION CURVE FOR A TOTAL-POWER RECEIVER SHOWING THE ZERO-SIGNAL POINT AT AN APPRECIABLE DEFLECTION. THE DOTTED EXTRA-POLATION YIELDS A ZERO FOR TOTAL NOISE INPUT  $T_{es}$  DEGREES BELOW ZERO SIGNAL.

as one which, at the modulation frequency, provides automatic partial calibrations spaced from each other by very short intervals of time.

#### D. TYPES OF STABILIZATION

For a receiver that is ideally linear except for the detector-power response, we can express the calibration curve ( $z$  vs.  $T$ ) for changes in signal temperature  $T$  as

$$z(T) = f(K_1, K_2, T_{es}, T)$$

for a given detector law. Here  $K_1$  is the power gain before the detector,  $K_2$  is the voltage gain after the detector, and  $T_{es}$  is the average effective system noise. The detector output is a function of the total power at its input, represented by  $T_T$ . This output can be expanded in a Taylor

expansion about the  $T_T = T_{e_s}$  level, where signals are then represented by  $T = T_T - T_{e_s}$ , thus

$$y(T) = g(K_1 T_{e_s}) + g'(K_1 T_{e_s}) K_1 T + \frac{g''(K_1 T_{e_s})}{2!} (K_1 T)^2 + \dots$$

With the gain factor  $K_2$  applied,

$$z(T) = K_2 y(T) = g(K_1 T_{e_s}) K_2 + g'(K_1 T_{e_s}) K_2 K_1 T + \frac{g''(K_1 T_{e_s})}{2!} K_2 (K_1 T)^2 + \dots \quad (7)$$

When considering minimum detectable signals with  $T$  zero,

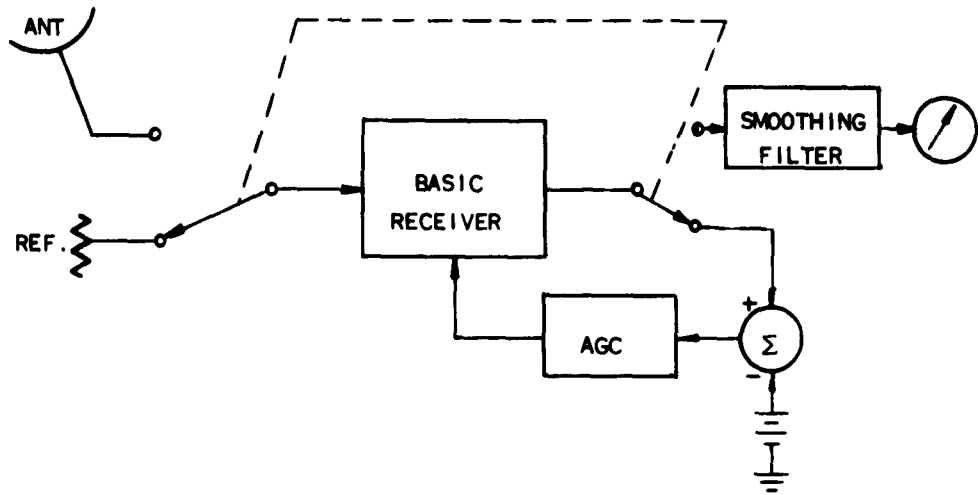
$$z(0) = K_2 g(K_1 T_{e_s}),$$

which has three variables-- $K_2$ ,  $K_1$ , and  $T_{e_s}$ .

### 1. Zero-Point Stabilization

Zero-point stabilization is achieved when  $z(0)$  is independent of gain and system noise. A servo system that compares  $z(0)$  against a standard and operates on the receiver gain to make  $z(0)$  equal to the standard can produce zero-point stabilization. Gain changes will be corrected if the servo operates to change  $K_1$ . Changes in  $T_{e_s}$ , however, will require a compensating change in gain that changes the scale of the calibration curve. The detector operating level will be held constant so that the shape of the calibration curve will change only as a large-signal effect. (The coefficients  $g^i(K_1 T_{e_s})$  in Eq. (7) remain constant but the  $(K_1 T)^i$  factors become significantly changed for large signals.) Figure 3.2 shows a gated AGC system with these characteristics.

Another way of assuring  $z(0)$  equals a constant is by making  $g(K_1 T_{e_s})$  equal to zero. The Dicke receiver does not respond to  $T_{e_s}$  and hence effectively sets  $z(0) = 0$ . In this, then, receiver-gain changes result in changes of calibration-scale factors and  $T_{e_s}$  changes have no effect directly. Since the detector level is not maintained in any way, both gain and  $T_{e_s}$  changes will tend to shift the operating level and thus can change the calibration. Figure 3.3 shows such a Dicke receiver and the resultant calibration curves for changes in gain and  $T_{e_s}$ .



DETECTOR OPERATING POINT CONSTANT BUT CALIBRATION CHANGES

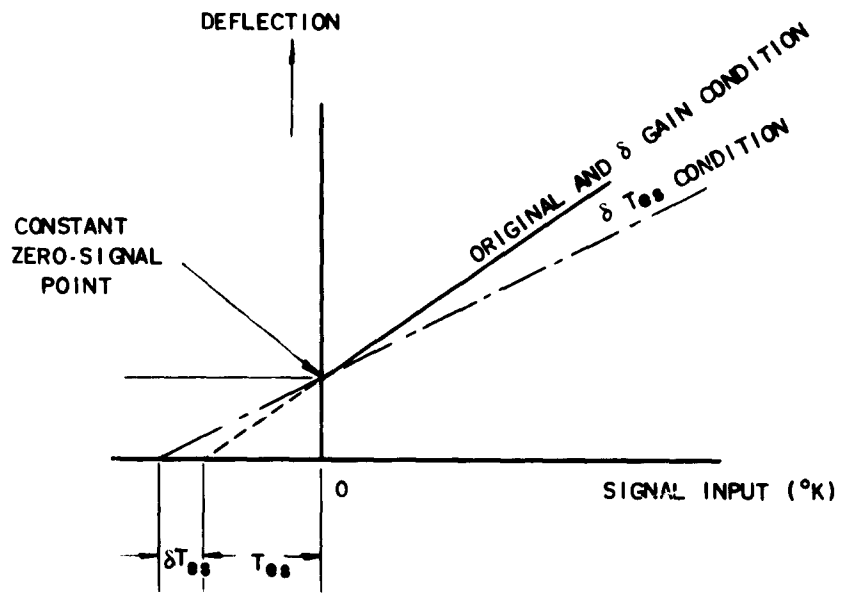
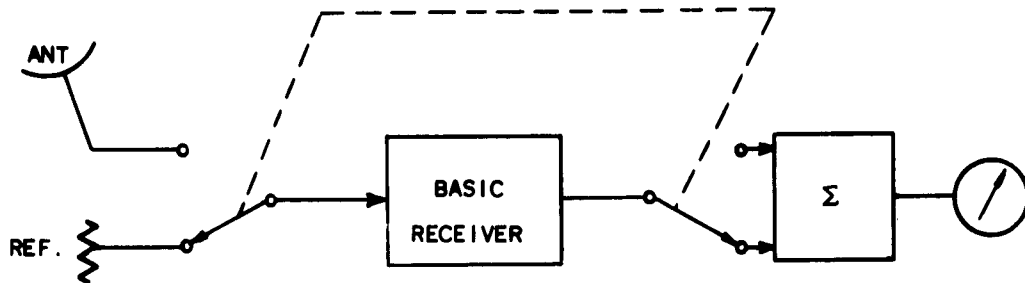


FIG. 3.2 GATED AGC, GATED TOTAL-POWER RECEIVER WITH ZERO-SIGNAL POINT STABILIZATION



NEITHER DETECTOR OPERATING POINT, NOR CALIBRATION CONSTANT

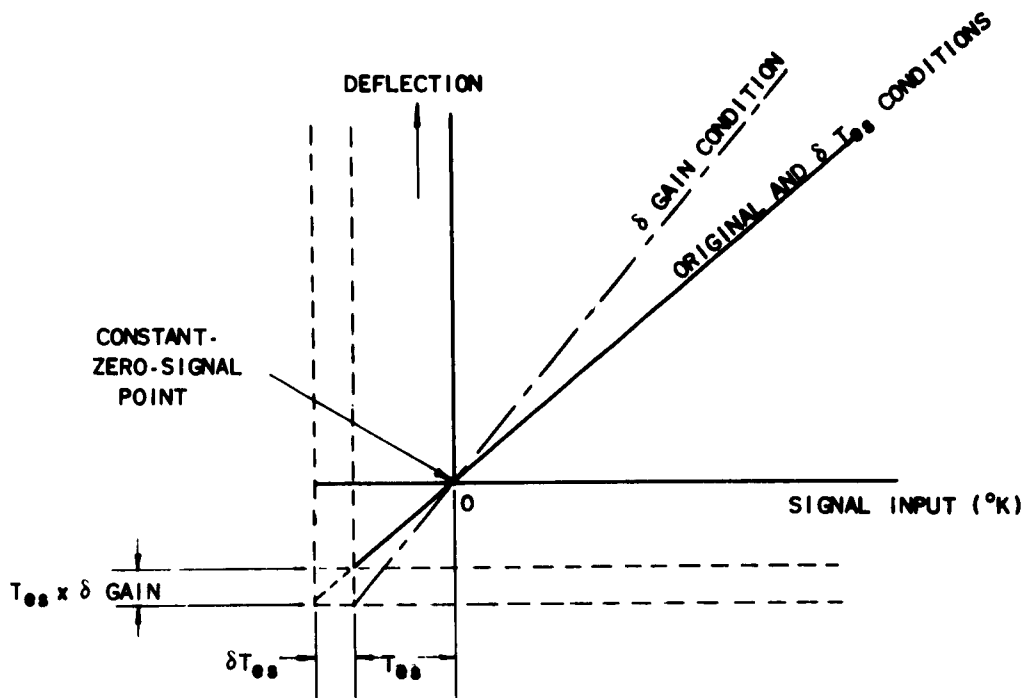


FIG. 3.3 DICKE-TYPE RECEIVER WITH ZERO-SIGNAL POINT STABILIZATION.

Another possible zero-point stabilization method is to use a combination of the two systems above [Ref. 7]. Figure 3.4 shows such a receiver with a Dicke signal output but gated AGC. This receiver maintains constant calibration-scale factors with gain changes but not  $T_{es}$  changes, in contrast to the straight Dicke receiver, in which the opposite is true.

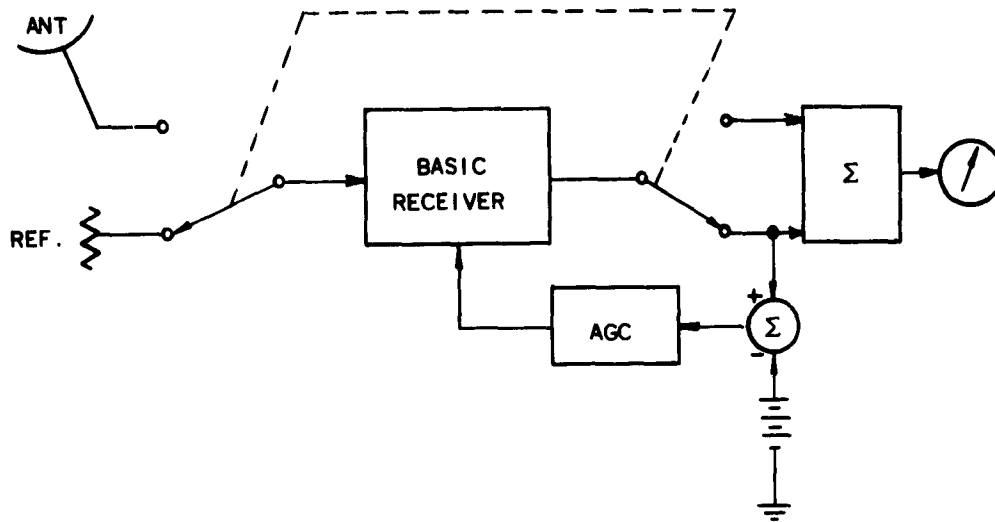
## 2. Two-Point Stabilization

Two-point stabilization is achieved when two fixed inputs result in two fixed outputs. The control of the two gain variables  $K_1$  and  $K_2$  is not sufficient to ensure that the calibration curve will pass through two points, in general, unless we make  $z(0) = 0$  in some way. Then control of only one gain variable can force the calibration curve through a desired point as well as the constant-zero signal point. If we can control both gain variables, then the detector operating level can also be held constant. Figures 3.5 and 3.6 show block diagrams and calibration-curve sketches for two point-stabilized receivers. Information concerning the three input levels must be recoverable at the receiver output through suitable modulation techniques. The receiver shown in Fig. 3.6 has the two servo gain controls and maintains the detector operating level constant.

When the characteristics of the receivers are not known explicitly it is difficult to predict whether two-point stabilization with or without maintaining detector operating level will be more advantageous. The one showing the least departure from the original calibration curve over the range of signals expected would be most desirable. These facts point out the great advantage of a linear power response (such as the ideal square-law detector provides) which eliminates detector-operating-level problems.

The slope of the calibration curve can be stabilized by using the additive modulation scheme shown in Fig. 3.7. A modulated component is added to the total noise input and the receiver gain is adjusted to keep the output constant for this modulated component. This process permits the effective sensing of the slope of the calibration curve and keeps the slope constant for large dynamic ranges. As shown, however, the zero signal point is a function of  $T_{es}$ . This arrangement can be called a modulated pilot-signal, total-power receiver.

Another system that achieves two-point stabilization uses a ratio indicator for the output. Figure 3.8 shows the block diagram of such a receiver with two reference sources time shared with the signal and two



DETECTOR OPERATING POINT CONSTANT BUT CALIBRATION CHANGES

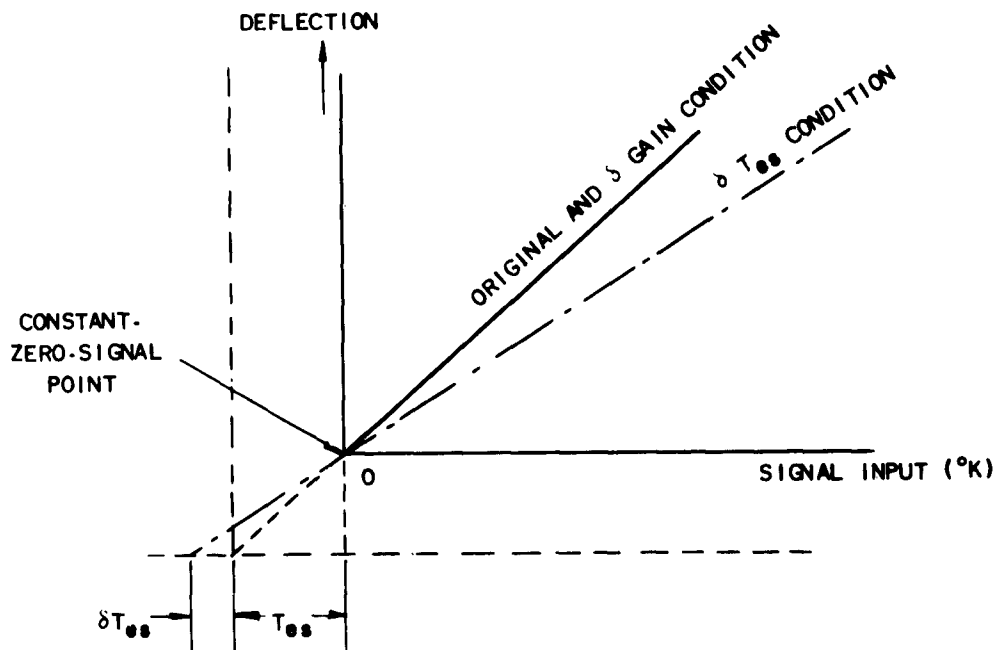
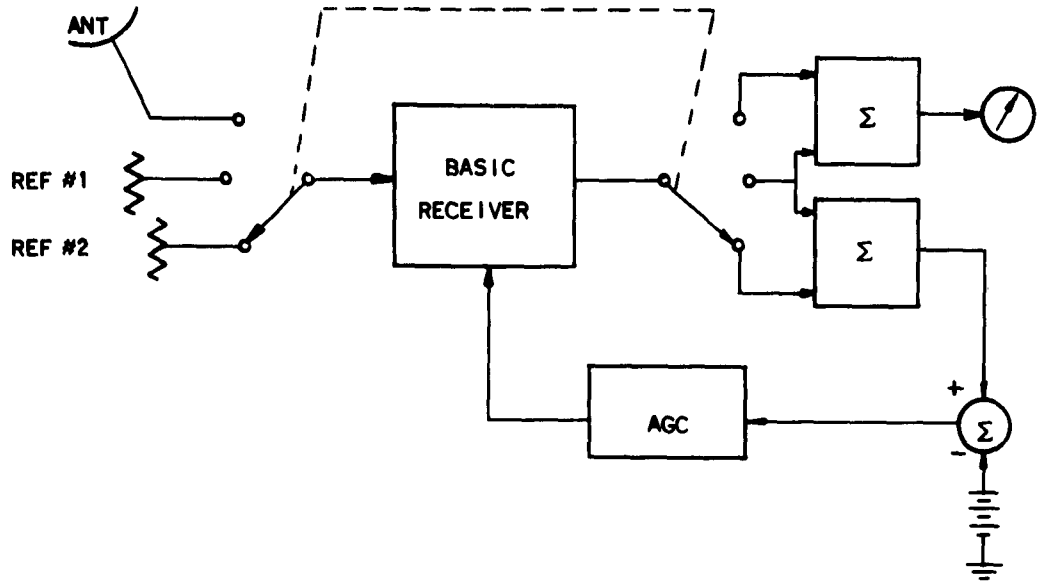


FIG. 3.4 GATED AGC DICKE RECEIVER WITH ZERO-SIGNAL POINT STABILIZATION.



CALIBRATION DEPENDS ON DETECTOR OPERATING POINT

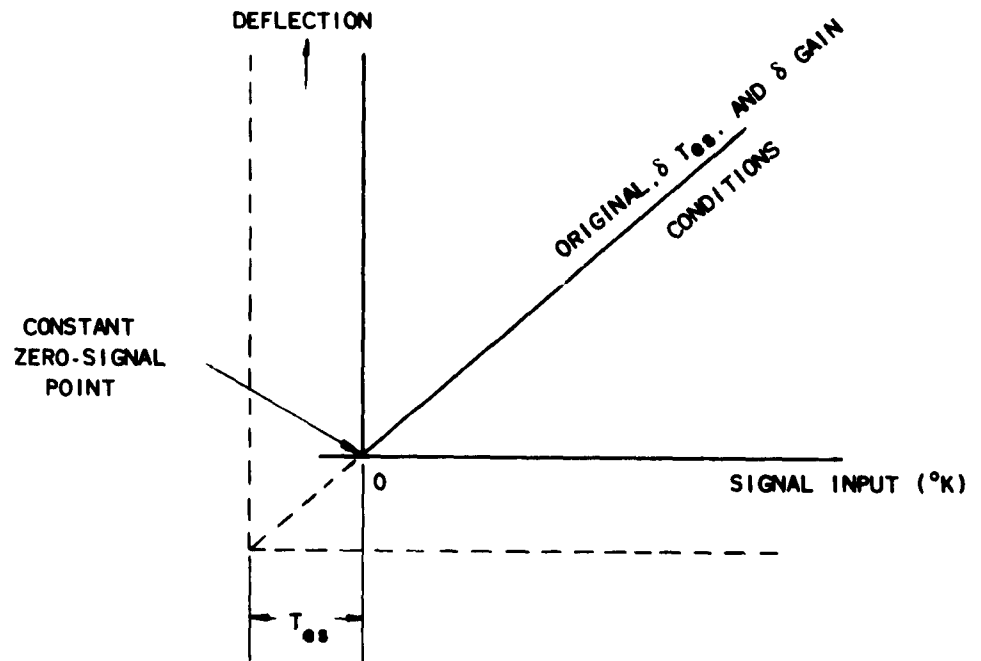
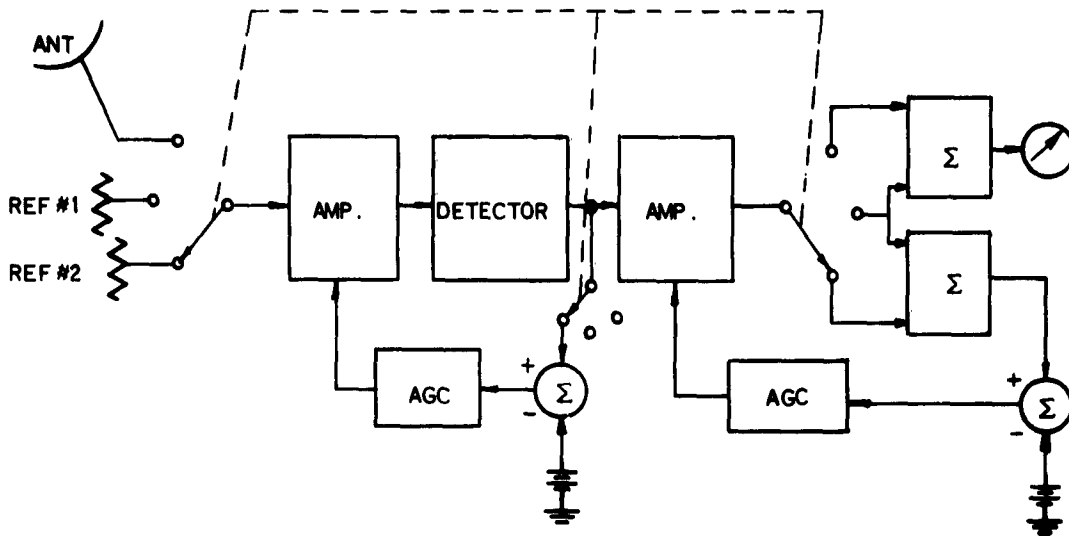


FIG. 3.5 DUAL-REFERENCE MODULATED RECEIVER WITH ONE SERVO GAIN CONTROL PRODUCING TWO-POINT STABILIZATION.



CALIBRATION UNCHANGED WITH  $\delta T_{e.s.}$  OR  $\delta$  GAIN CHANGES.

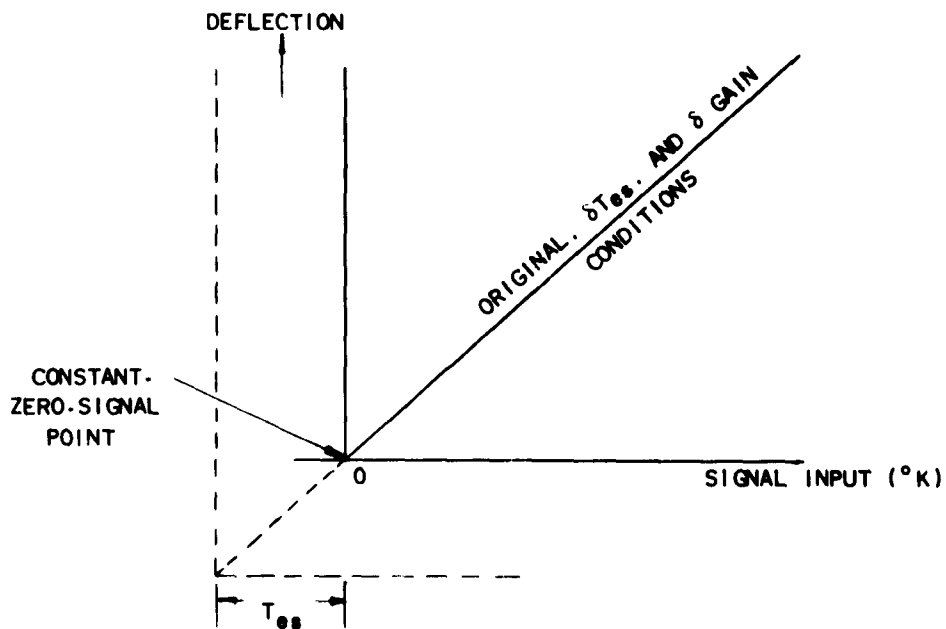
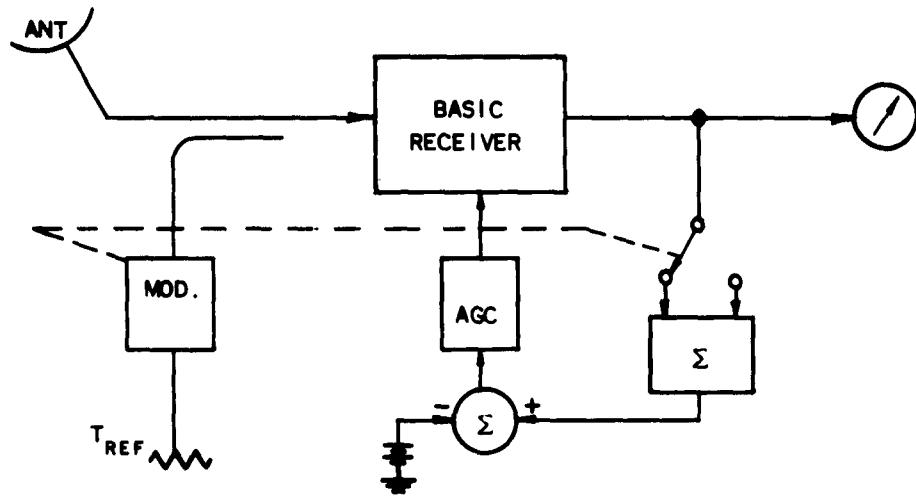


FIG. 3.6 DUAL-REFERENCE MODULATED RECEIVER WITH TWO SERVO GAIN CONTROLS PRODUCING TWO-POINT STABILIZATION AND CONSTANT DETECTOR OPERATING POINT.



CALIBRATION SLOPE CONSTANT BUT DETECTOR OPERATING POINT NOT

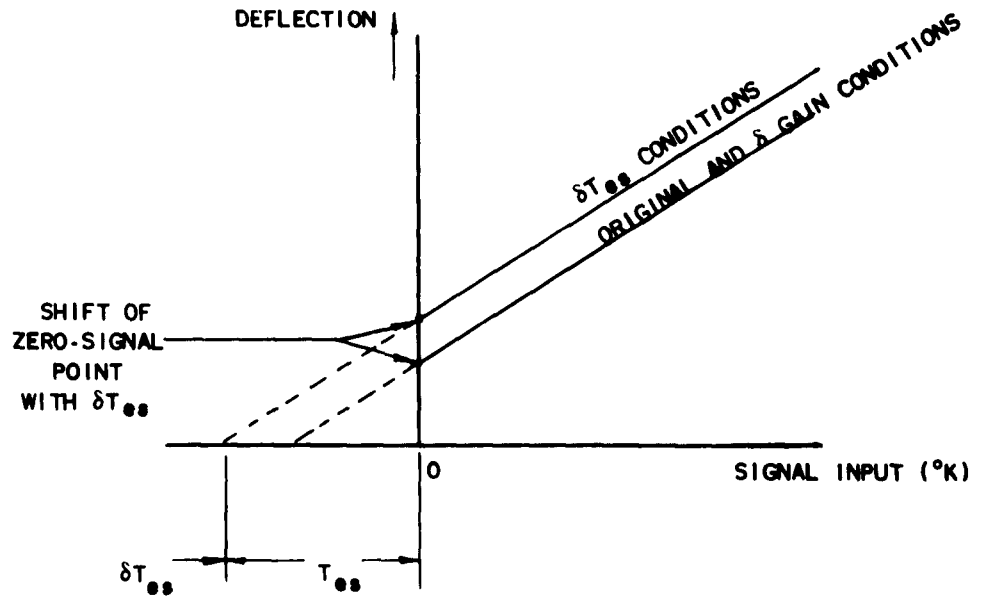
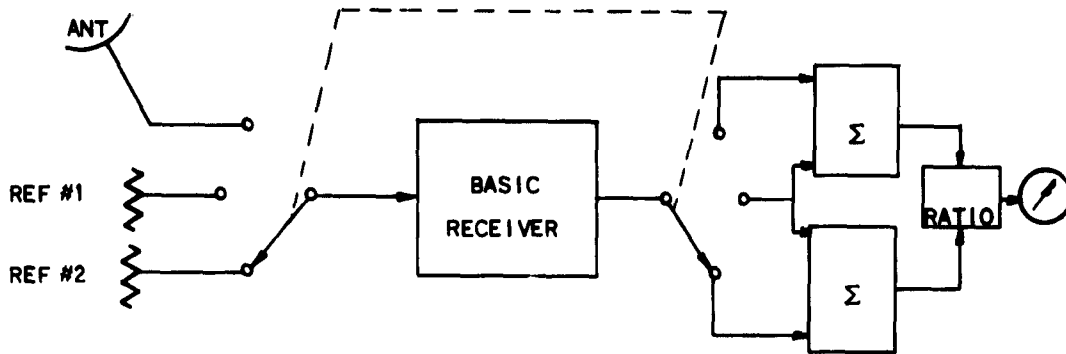


FIG. 3.7 MODULATED PILOT-SIGNAL TOTAL-POWER RECEIVER.



CALIBRATION DEPENDS ON DETECTOR OPERATING POINT

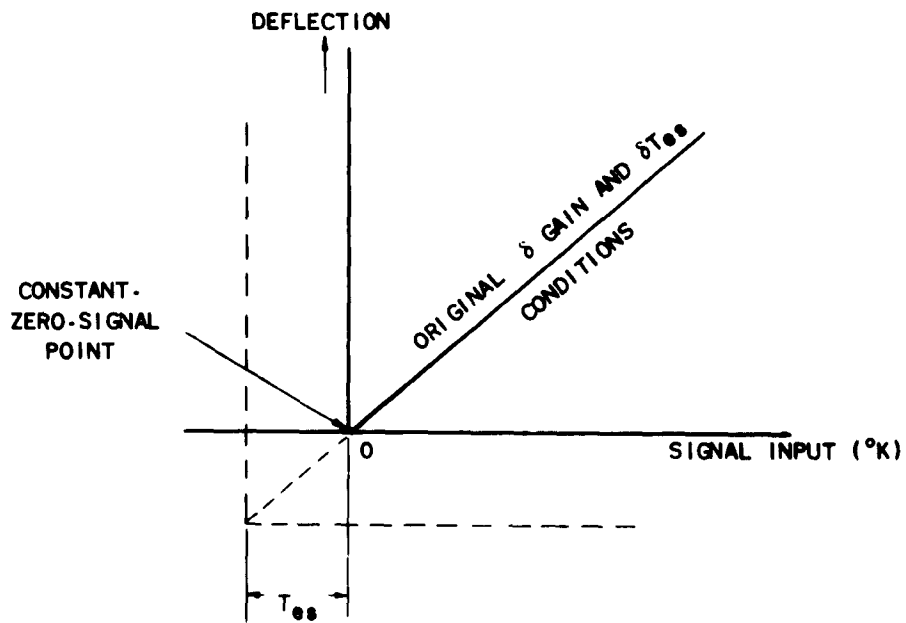


FIG. 3.8 RECEIVER GIVING TWO-POINT STABILIZATION USING A RATIO INDICATOR FOR THE OUTPUT.

coherent demodulators providing measures of the strength of the signal relative to one reference and the difference in strengths between the two references. The ratio of these two measures is zero for equal signal and compared reference strengths, regardless of gain or  $T_{e,s}$  conditions. The calibration depends on the detector operating level but is otherwise stabilized.

Still another approach to stabilizing the calibration curve for changes in receiver characteristics is the use of a null-balance principle. The receiver acts as an error-detecting device, which then actuates a control system to reduce the error to zero. The difference between the signal and a controllable reference source is the error. Consequently the system operates to maintain the signal and reference source in equality and a record of the reference level is a record of the signal level. In a static situation, the calibration of this system is free from changes in receiver characteristics but its dynamic performance depends on stability within the receiver. As would be expected, a large decrease in gain would result in a sluggish system and large lag errors for rapidly changing signals. Ryle and Vonberg [Ref. 17] described such a system for measurement of solar r-f radiation. Figure 3.9 shows a block diagram of a Ryle and Vonberg type receiver.

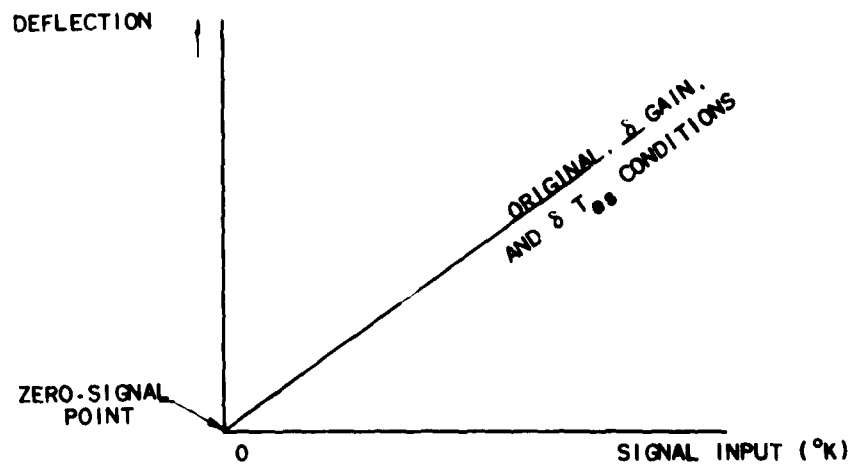
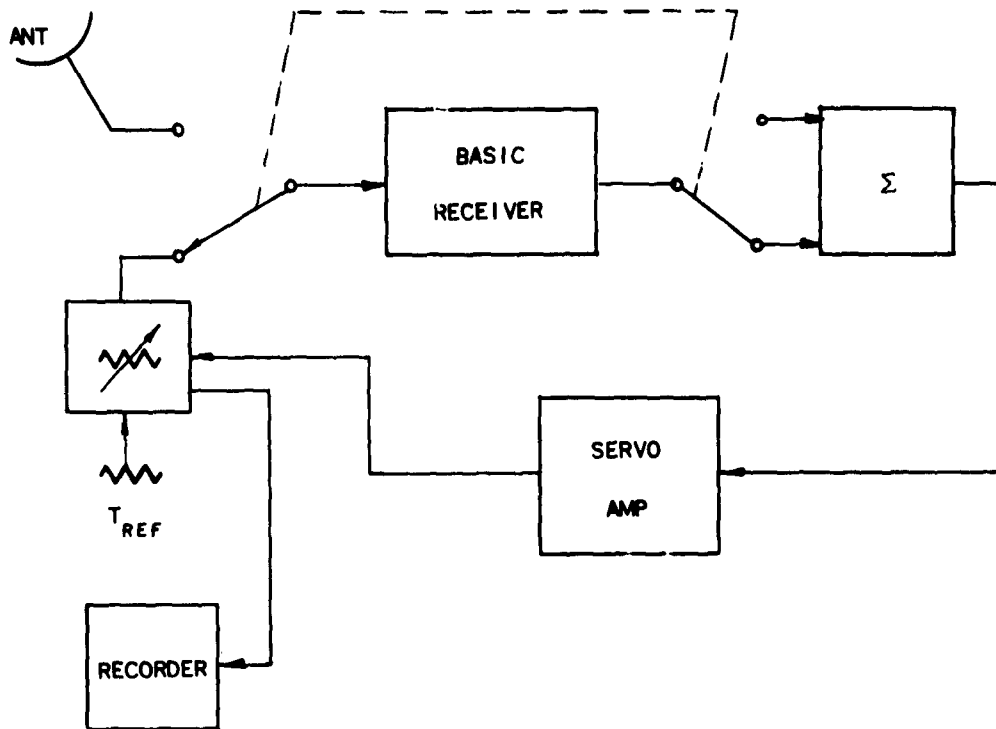


FIG. 3.9 NULL-BALANCING RECEIVER STABILIZED AGAINST GAIN AND  $T_{00}$  CHANGES AND INDEPENDENT OF DETECTOR OPERATING POINT.

#### IV. MORE-COMPLEX RECEIVERS

##### A. STABILIZED RECEIVERS WITH UNMODULATED SIGNAL

As mentioned earlier, two of the approaches to achieve freedom from instabilities applied to radio-astronomy receivers are d-c comparison techniques such as reported by Selove and correlation techniques such as discussed by Goldstein. Both of these methods use two channels and depend on the statistical independence of the two sources of equivalent input noise.

##### 1. Selove-Type Receivers

Zero-point stabilization is the goal of receivers of the Selove type. The zero signal output of the total-power receiver depends on the gain and  $T_{e_s}$  of the equipment, and subtraction of a fixed d-c level from the output does not alter this dependency. However, if it were possible to subtract a level which was a function of gain and  $T_{e_s}$ , the resulting output could be zero-point stabilized. Consider a receiver which has twin channels for amplification, detection, and smoothing. To the first order of approximation, gain and  $T_{e_s}$  changes are the same in both channels, so that, if a fixed noise-temperature input is provided for both channels, the outputs (including instability contributions) will have the same mean values and a resulting zero mean difference. To the extent that this approximation is true in a practical system, the Selove-type receiver is zero point stabilized. Figure 4.1 shows a block diagram for receivers of this kind.

The output of each channel will have an equal rms variation about its mean and the difference between these two will have an rms variation that is  $\sqrt{2}$  times an individual value. If one of the two identical channels has

$$U_L = 1/\sqrt{\tau\Delta f}$$

then the Selove-type receiver has

$$U_L = \sqrt{2} / \sqrt{\tau\Delta f} \quad (8)$$

In order to compare this with other receivers, the extra channel bandwidth should be accounted for by allotting the total signal and

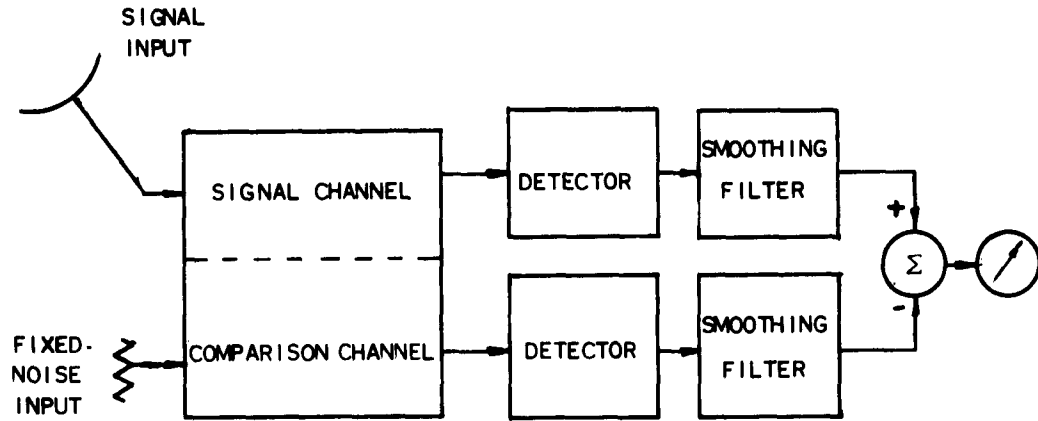


FIG. 4.1 BLOCK DIAGRAM OF A SELOVE TYPE "D-C COMPARISON" RECEIVER.

comparison bandwidth to the other receiver. When this is done the Selove receiver has a value of  $\Delta T$  twice that of a total power receiver. The ratio

$$\frac{\Delta T_{\text{Selov}}}{\Delta T_{\text{Total Power}}} = \frac{\sqrt{2} / \sqrt{\tau \Delta f}}{1 / \sqrt{\tau 2 \Delta f}} = 2$$

Operation with a comparison channel using parameters different from those of the signal channel is possible. In general, the signal, by its nature, will determine the integration time required. If the comparison channel had less integration time, the output would be noisier than necessary, and if it had more the instability spectrum above the cutoff frequency of the comparison channel smoothing filter and below the cutoff of the signal channel smoothing filter would tend to produce pseudo-signal outputs. Therefore, equal integration times is a reasonable situation

For differences in reception-filter bandwidths, consider the following. For an ideal d-c comparison receiver we have plotted  $\Delta T / \Delta T_{\text{std}}$ , (the dashed curve in Fig. 4.2) the ratio of its  $\Delta T$  to that for a standard total-power receiver with the same signal bandwidth  $\Delta T_{\text{std}}$ , against the ratio of comparison-channel bandwidth  $\Delta f_c$  to signal-channel bandwidth  $\Delta f_s$ . As the comparison-channel bandwidth becomes larger, the performance approaches that of the standard receiver and at low-comparison bandwidths it is much worse. When  $\Delta f_c / \Delta f_s = 1$  the value of the ratio is  $\sqrt{2}$ , as would be expected from Eq (8). A further comparison is provided by the solid

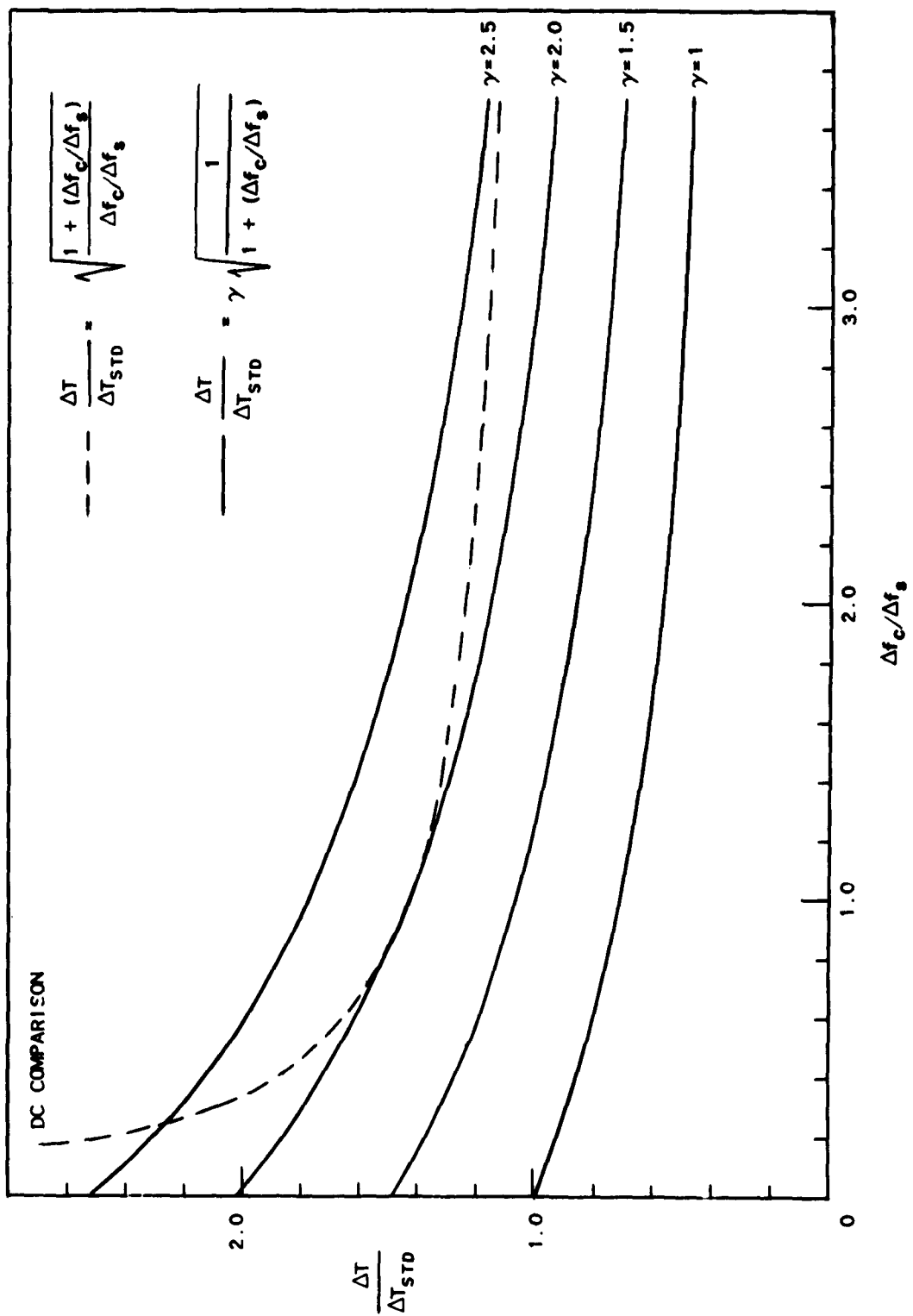


FIG. 4.2 CONDITIONS OF RELATIVE BANDWIDTH AND INSTABILITY FACTORS WHEN A TOTAL-POWER RECEIVER IS SUPERIOR TO A d-c COMPARISON RECEIVER. THE STANDARD MINIMUM DETECTABLE SIGNAL  $\Delta T_{STD}$  IS THAT FOR A TOTAL-POWER RECEIVER WITH  $\gamma = 1$  AND TWO EQUAL BANDS,  $\Delta f_c$  AND  $\Delta f_s$ , USED FOR THE SIGNAL.

curves in Fig. 4.2, which show the ratio  $\Delta T/\Delta T_{std}$  for a family of total-power receivers with different instability factors  $\gamma$ . The bandwidth for these receivers is taken to be equal to  $\Delta f_s [1 + (\Delta f_c/\Delta f_s)]$  or all the bandwidth is used in the signal channel. When  $\gamma = 2$  the d-c comparison receiver yields larger  $\Delta T$ 's for all bandwidth ratios except unity, in which case the two are equal.

For a stable receiver with  $\gamma$  small, the total-power configuration has an advantage, but as  $\gamma$  increases the d-c comparison receiver has a smaller  $\Delta T$ . In practice, the comparison receiver will be non-ideal, so that its curve would be raised and its relative advantage would be reduced. Thus we can say that, for conditions under which the total usable bandwidth is not limited for other reasons and a reasonably stable receiver can be achieved, the extra bandwidth of a second channel is more useful for signal than for d-c comparison purposes.

To approximate the condition of identical instability behavior, the two channels would have to be obtained by band filtering at the input and output of a sufficiently wideband amplifier. This requirement places a strict condition on relative bandwidth stability for the channels and is probably the most difficult requirement to meet in obtaining good performance from a receiver of this type.

## 2. Correlation-Type Receivers

This classification could well be called autocorrelation receivers when used to describe operation using a single signal input, in contrast to interferometer radiotelescopes using two inputs. Signal processing begins with a splitting of the input into two equal and necessarily fully correlated signals. These are separately equally amplified and invariably degraded with independent receiver noise and then multiplied together. The product signal is then smoothed with some integrating time and the result appears at the receiver output as a meter deflection. The ideal process can be described in mathematical terms as follows, letting  $s/\sqrt{2}$  be one half the signal on a power basis:

$$z(t) = [(s/\sqrt{2})(t) \cdot (s/\sqrt{2})(t)] * h(t).$$

The smoothing filter impulse response is  $h(t)$ , which can be written out as

$$z(t) = \frac{1}{2} \int_{-\infty}^t s^2(t') h(t-t') dt'. \quad (9)$$

This equation can be compared with

$$\rho_s(t, \tau) \Big|_{\tau=0} = \lim_{T \rightarrow \infty} \int_{t-T}^t s(t') \frac{1}{T} dt', \quad (10)$$

the value of the autocorrelation function for  $s(t)$  at any epoch  $t$  and with zero time displacement between  $s(t)$  and itself. When  $T$  grows large the function  $\rho_s(0)$  changes very slowly, so that Eq. (9) will be nearly equal to Eq. (10) when the equivalent width of the smoothing filter impulse response corresponds to large  $T$  values. To the degree that this approximation holds, an autocorrelation is being performed; hence the name.

A prime problem in receivers of this type is the necessity of splitting the signal and at the same time preventing the coupling of noise from the input of one receiver channel to the other. This coupled noise would appear at the multiplier as a correlated component and hence produce a zero-signal deflection. Since the idea is to have no zero-signal deflection in order to stabilize the system against gain changes, such coupled noise is undesirable.

A matched-tee junction in a waveguide, or its equivalent in other transmission lines, is a convenient method of splitting the signal equally. Coupling is still present, however, therefore, further steps must be taken to control this factor. When isolators are inserted between the tee and each receiver an improvement is possible since the source of the coupled noise then is divorced from the input of each channel and becomes well behaved. The equivalent coupled-noise-source temperatures are then equal to the isolator temperatures. A step beyond this configuration is to use circulators in place of isolators as shown in Fig. 4.3. Then the noise sources are not only known but are terminations that can be refrigerated if desired. In any event, the analysis of the circulator case covers the other two and makes the noise sources easily visualized.

In Fig. 4.3 the noise voltages  $s(t)$ ,  $v_1(t)$ ,  $v_2(t)$ ,  $n_1(t)$  and  $n_2(t)$  are all related to an equivalent noise source by a relation such as

$$\langle s^2 \rangle = 4kTR \int_{-\infty}^{\infty} G(f) df$$

or

$$\langle v_1^2 \rangle = 4kT_{C_1} R \int_{-\infty}^{\infty} G(f) df$$

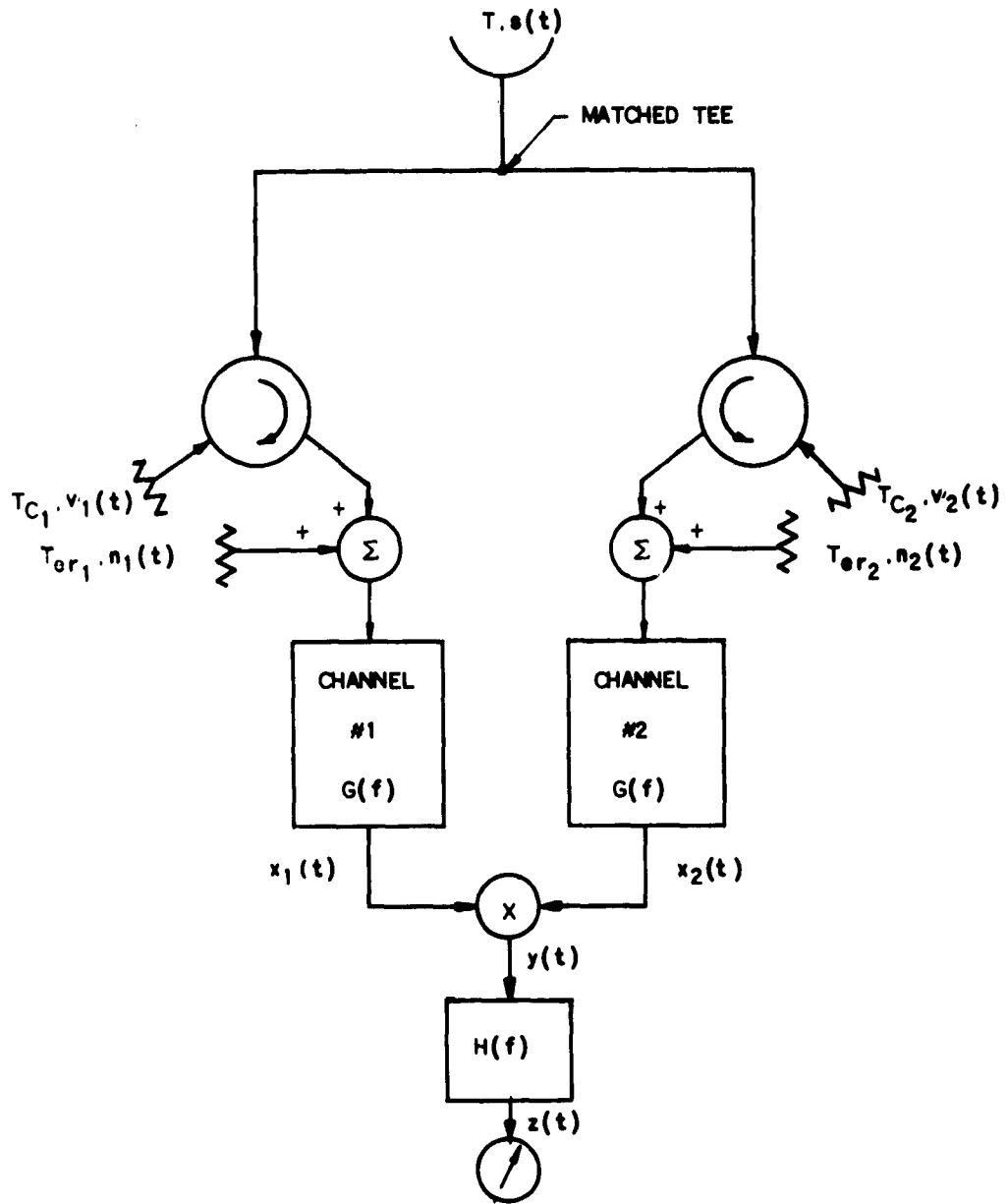


FIG. 4.3 CORRELATION RECEIVER USING CIRCULATORS.

The matched-tee junction splits the energy coming from the antenna so that a power  $\langle s^2 \rangle / 2$  appears in each branch along with the voltage  $s/\sqrt{2}$ . Energy flowing from the circulator load towards the matched tee meets a mismatch at the junction and an unequal division of energy occurs. The power in the antenna line is one half, the power in the line to the other receiver is one quarter, and the power reflected is also one quarter of the input power. Energy flowing toward the antenna will be radiated while the components flowing from the junction to the receivers will constitute a completely correlated but opposite-polarity signal. Thus each circulator load produces at the output a negative meter deflection. Noise sources at the receiver inputs produce energy flowing toward the circulators, where it is absorbed in the circulator load.

For this receiver the mean meter deflection will be

$$\langle s_r \rangle = \langle s^2 / 2 \rangle - \langle v_1^2 / 16 \rangle - \langle v_2^2 / 16 \rangle$$

In practice the zero-signal condition will not mean  $T = 0$  because of the equivalent noise temperature of the system before the tee junction. The mean meter deflection with zero signal can be nulled if the temperatures  $T_{C_1}$  and  $T_{C_2}$  are properly maintained.

Appendix B contains the analysis for the correlation receiver of Fig. 4.3. With the approximation that the smoothing filter is much narrower than the reception filters or the integration time much longer than the correlation time of the random voltages at the multiplier input, the analysis is straightforward. In evaluating the autocorrelation function  $\rho_y(\tau)$  for the multiplier output we have used the general relationship below for gaussian random-noise voltages with zero mean values from well behaved processes, which gives the time average for a product of four such variables in terms of products of pairs of the variables [Ref. 18]. For the term involving the receiver noise, for instance,

$$\begin{aligned} \langle n_1(t)n_2(t)n_1(t+\tau)n_2(t+\tau) \rangle &= \langle n_1(t)n_2(t) \rangle \langle n_1(t+\tau)n_2(t+\tau) \rangle \\ &+ \langle n_1(t)n_1(t+\tau) \rangle \langle n_2(t)n_2(t+\tau) \rangle \\ &+ \langle n_1(t)n_2(t+\tau) \rangle \langle n_2(t)n_1(t+\tau) \rangle \\ &= \rho_{n_1}(\tau) \rho_{n_2}(\tau). \end{aligned}$$

After reducing the expression for  $\rho_y(\tau)$  to the sum of terms obtained as above, its Fourier transform is taken to obtain  $B_y(f)$ , the power spectral density at the multiplier output. The smoothing-filter power-transfer characteristic is then applied to obtain the receiver-output power spectrum. From this we can write

$$\langle z \rangle = k[H(0)]^{1/2} \int_{-\infty}^{\infty} G(f) df [(T/2) - (T_{C_1}/16) - (T_{C_2}/16)]$$

for the meter deflection and

$$S = k[H(0)]^{1/2} \int_{-\infty}^{\infty} G(f) df (\Delta T/2)$$

for the signal or mean meter deflection increment due to an input temperature increment  $\Delta T$ . The noise output will be

$$N = \left[ \int_{-\infty}^{\infty} H(f) df \right]^{1/2} k[G \cdot G|_0]^{1/2} T_{e.s.}$$

Now, using unity signal to noise ratio to define  $\Delta T$ , we write

$$S/N = 1 = \frac{k[H(0)]^{1/2} \int_{-\infty}^{\infty} G(f) df (\Delta T/2)}{k \left[ \int_{-\infty}^{\infty} H(f) df \right]^{1/2} [G \cdot G|_0]^{1/2} T_{e.s.}}$$

and

$$\Delta T = (\sqrt{2}/\sqrt{\tau \Delta f}) T_{e.s.}$$

following the definitions for bandwidth and integration time discussed above.

The system effective noise temperature  $T_{e.s.}$  contains contributions from all the noise sources as given below:

$$\begin{aligned}
T_{es} = & (T_{er1} T_{er2} + (T/2)(T_{er1} + T_{er2}) + [(T_{er1} T_{C1} + T_{er1} T_{C2})/16]) \\
& + [(T_{er2} T_{C1} + T_{er2} T_{C2})/16] + (T^2/2) + (T_{C1} T_{C2}/64) \\
& + [(T_{C1}^2 + T_{C2}^2)/128]^{1/2}
\end{aligned}$$

For the case when

$$T_{er1} = T_{er2} = T_{er}$$

and

$$T_{C1} = T_{C2} = T_C$$

we have

$$\begin{aligned}
T_{es} & = [T_{er}^2 + TT_{er} + (T_{er} T_C/4) + (T^2/2) + (T_C^2/32)]^{1/2} \\
& = T_{er} [1 + (T/T_{er}) + (T_C/4T_{er}) + (T^2/2T_{er}^2) + (T_C^2/32T_{er}^2)]^{1/2}
\end{aligned}$$

When

$$T/T_{er} < 1$$

and

$$T_C/T_{er} < 1$$

we can write

$$\begin{aligned}
T_{es} & \approx T_{er} \{1 + (1/2T_{er})[T + (T_C/4)]\} \\
& \approx T_{er} + (T/2) + (T_C/8)
\end{aligned}$$

Gain changes produce changes in the output when  $[T - (T_C/4)]$  does not equal zero. Following Bracewell [Ref. 8], we form the ratio of mean meter deflection for the correlation receiver to that for a total-power receiver to obtain an instability-reduction factor

$$\zeta = \frac{[T - (T_C/4)]/2}{T + T_{er}}$$

to be applied to the contribution I (see Eq. (6)).

The correlation receiver of Fig. 4.3 has been shown to have a 1.414-times larger minimum detectable signal than a total-power receiver, but again using twice the total reception-filter bandwidth because of two channels. On this basis the comparison factor should be two. Zero-signal-point stabilization is possible by temperature control of the circulator loads and partial stabilization is assured since receiver noise contributions are eliminated.

When a matched tee without circulators is used, the receiver noise sources feeding the antenna take the place of  $T_{C1}$  and  $T_{C2}$  in the analysis of cross-coupled noise. Since little, if any, control is possible on these noise sources, the receiver has mainly the advantage of removing mean meter deflections due to receiver equivalent input noise  $T_{er}$  plus a minimum detectable signal only 1.414 times that of a total-power receiver.

With isolators a similar statement holds, but with the advantage, as mentioned above, of well defined sources at known temperatures for the cross-coupled noise.

When a matched hybrid junction or magic tee is used to split the signals, the multiplier input consists of voltages similar to those of the previous discussion. In Fig. 4.4, the fourth port of the magic tee has a termination at a temperature  $T_J$  that provides noise energy for the two channels of opposite polarity but correlated voltage. This energy splits equally, so that the voltage in the channels will be  $\pm k/\sqrt{2}$ . The corresponding value for  $T_{es}$  for this receiver will then be

$$T_{es} = [T_{er}^2 + TT_{er} + T_J T_{er} + T^2 + T_J^2]^{1/2}$$

$$\approx T_{er} + (T/2) + (T_J/2)$$

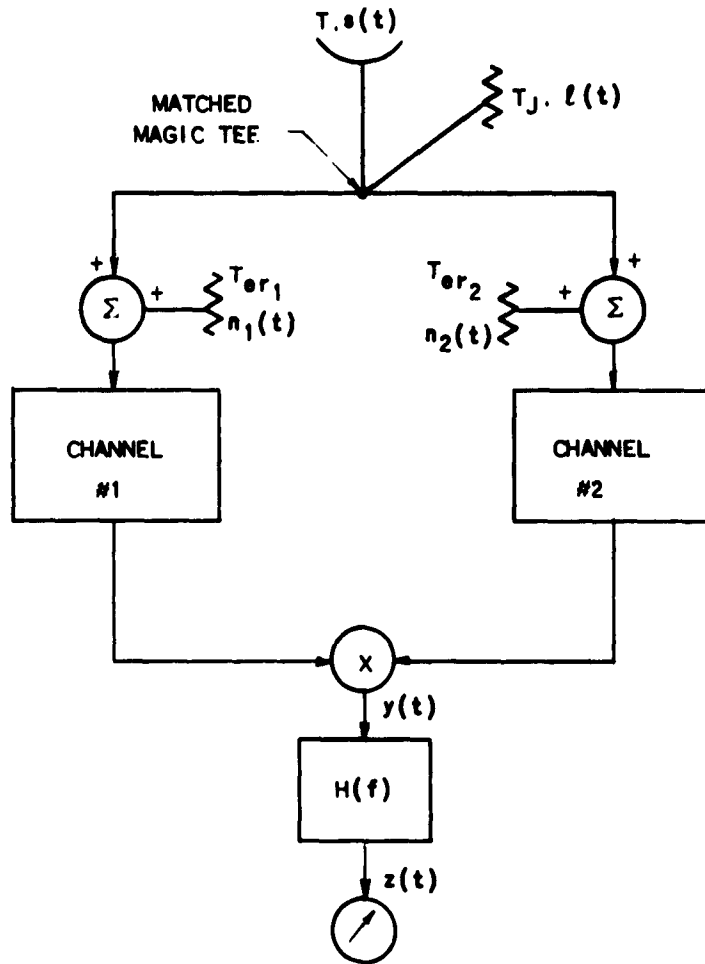


FIG. 4.4 CORRELATION RECEIVER USING A MAGIC TEE AT THE INPUT.

while the mean meter deflection will be proportional to

$$(T/2) - (T_J/2)$$

Although  $T_J$  would have to be maintained at a lower temperature than  $T_C$  in order to null the zero-signal mean meter deflection, the magic tee has the advantage of avoiding any signal-path loss of circulators.

Thus far in discussing correlation receivers, the multiplier has been assumed to be an ideal element. Practically they represent a difficult portion of the receiver to implement. Blum [Ref. 9] discusses a type of multiplier that uses essentially the quarter-square-difference principle. He suggests connecting the two-channel outputs to two ports of a hybrid junction, with the result that sum and difference signals appear at the other two ports. Each of these is squared in a square-law detector and finally the detector outputs are subtracted to get the product term. When this method of multiplication is used with the receiver of Fig. 4.4 the mean meter deflection will be

$$\begin{aligned} \langle z \rangle &= \langle s^2 \rangle - \langle l^2 \rangle \\ &= k[H(0)]^2 \int_{-\infty}^{\infty} G(f) df (T - T_J) \end{aligned}$$

The relative noise output for this multiplier is the same as that of an ideal device and, consequently, the minimum detectable signal is the same, i.e.,

$$\Delta T = \sqrt{2} T_{es} 1/\sqrt{\tau \Delta f}$$

where

$$T_{es} = T_{er} \{1 + [(T + T_J)/2T_{er}]\}.$$

From these considerations we see that the correlation receiver can be realized in this manner without sacrificing performance if care is taken with the practical difficulties such as balancing of the hybrids and duplication of detector responses

## B. STABILIZED RECEIVERS WITH MODULATED SIGNALS

### 1. Introduction

Several receivers fall into a mixed classification. For instance, a correlation receiver can be designed to use time sharing of a single channel, using the quarter-square multiplication process. With this process, alternately, the sum and the difference of a split input signal are squared, with alternate-period outputs subtracted from each other and a final smoothing performed. This process could also be described as a signal modulation, since in the sum periods the signal power is present while in the difference periods the signal power is cancelled out. Furthermore, this process has the characteristics of a phase-switched system in that sum and difference signals can be formed by switching a 180-deg phase shift in and out of one split-signal channel.

Receivers that fit these descriptions will be handled as modulated-signal receivers. The method of stabilizing a receiver as described by Dicke [Ref. 1] is the classic example of a receiver that uses a modulated signal. This type of receiver keeps the signal information identifiable in the total noise with a signal modulator ahead of as much of the noisy portion of the system as possible. At the output, knowledge of the characteristics of this modulation allows the extraction of the signal and at the same time, the suppression of the d-c component due to  $T_{es}$ .

### 2. Dicke-Type Receivers

In Dicke receivers the effective input-temperature modulation is proportional to the signal strength and demodulation is performed coherently after detection to obtain a measure of the signal. This measure is presented on a meter, which, in the absence of signal and hence of modulation, has a zero mean deflection.

The receiver input is commutated between the signal source and the reference source by the modulator. This commutation occurs periodically at a frequency  $f_m$  and the effective modulated input temperature can be written

$$T_{\eta} = \eta(t) T + [1 - \eta(t)] T_{ref}$$

where  $T_{ref}$  is the noise temperature of the reference source and  $T$  is that of the signal source. This form of expression comes from considering a variable attenuator in the signal path whose power-transfer characteristic

as a function of time is  $\eta(t)$  and whose attenuating element is at temperature  $T_{ref}$ . For sinusoidal modulation the function

$$\eta(t) = (1 + \cos 2\pi f_m t)/2$$

or, for square-wave modulation,

$$\eta(t) = \frac{1}{2} \{1 + (4/\pi) [\cos 2\pi f_m t - (1/3) \cos 2\pi 3f_m t + (1/5) \cos 2\pi 5f_m t - \dots]\}$$

or, in general,

$$\begin{aligned} \eta(t) &= \frac{1}{2} + \frac{1}{2} \sum_{n=-\infty}^{n=\infty} K_{\mu_n} \exp(jn2\pi f_m t) \\ &= [1 + \mu(t)]/2 \end{aligned}$$

The function  $\mu(t)$  determines the modulation waveform. For sinusoidal modulation  $\mu(t)$  is sinusoidal, for square-wave modulation  $\mu(t)$  is square-wave, etc. The restriction that  $T_\eta$  be positive requires that

$$\mu(t) \Big|_{\max} = 1$$

A rather qualitative discussion that gives the minimum detectable input-temperature increment for square-wave modulation follows.

An ideal switch alternately connecting the signal source and the reference source to the receiver input will produce square-wave modulation. The effective receiver-input noise temperature source is connected at all times. On the average, the detector output during the two halves of the cycle will be proportional to the sum of  $T$  and  $T_{er}$  and the sum of  $T_{ref}$  and  $T_{er}$ . The standard deviation from the mean for an individual half-period ( $1/2f_m$ ) average of the detector output can be written

$$\sigma_S \propto (T + T_{er}) \sqrt{2f_m/\Delta f}$$

for the signal and

$$\sigma_{ref} \propto (T_{ref} + T_{er}) \sqrt{2f_m/\Delta f}$$

for the reference. The receiver output will be proportional to the difference between the mean value in the two conditions, and this measurement will have a standard deviation that is the quadratic sum of  $\sigma_S$  and  $\sigma_{ref}$ . For the case in which  $T$  and  $T_{ref}$  are equal, the standard deviation for the output expressed as the minimum detectable input-temperature increment will be

$$\begin{aligned} \Delta T &= \sqrt{2} (T + T_{er}) \sqrt{2f_m/\Delta f} \\ &= 2(T + T_{er}) \sqrt{f_m/\Delta f} \end{aligned} \quad (25)$$

We see that the  $M$  factor for this mode of operation equals 2, twice that for total-power operation using a smoothing filter with  $\tau = 1/f_m$ . One  $\sqrt{2}$  factor (from the value of  $M$ ) comes from the need to compare two equally noisy levels and the second because the time spent observing either level is half that possible with total-power operation. (This reduction in observing time enters into the expression for  $\Delta T$  above as a value of  $\tau$  one-half that possible with total-power operation.) Further smoothing affects both systems equally and hence does not change the modifying factor  $M = 2$ .

For a switch that spends unequal times in the two positions,  $\beta$  being the fraction of the switching period spent in one position,

$$\Delta T = (T + T_{ref}) \sqrt{f/\Delta f} \sqrt{1/\beta(1-\beta)} .$$

Since this expression is a minimum for  $\beta = 1/2$ , square-wave switching can be considered optimum and the value of  $M = 2$  a minimum.

Appendix C contains a detailed analysis of a modulated receiver. The block diagram in Fig. 4.5 shows the generalized form for this receiver. The modulation considered here is a power modulation; i.e., the modulator output power is made to vary in a specified manner. Dicke's [Ref. 1] receiver used a rotating attenuator in the input waveguide and obviously falls in this category. Goldstein [Ref. 19] and Strom [Ref. 20] discuss sinusoidal-voltage modulation, which seems to be an artificial

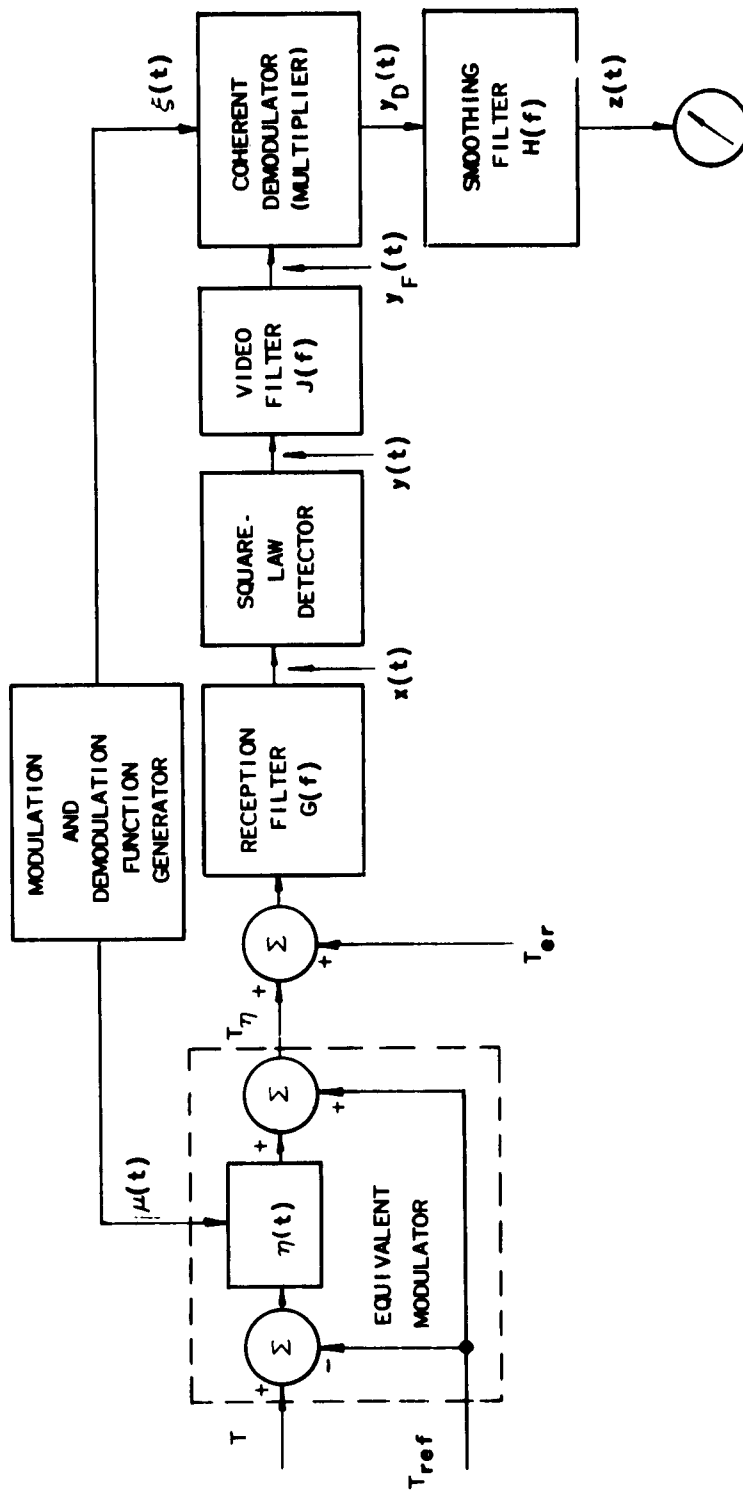


FIG. 4.5 BLOCK DIAGRAM OF THE MODULATED RECEIVER.

situation, although it can be shown to yield the same results as sinusoidal power modulation in the cases they considered.

After the detector, two components are added that are not present in the total-power receiver--the video filter and the coherent demodulator. The second of these is essential while the use of the first is controlled mainly by practical considerations. Frequently, in order to avert overloading in stages just prior to and in the coherent demodulator, it becomes advisable to limit the noise power by a rather narrow filter. This filter, whose power-transfer characteristic is  $K(f)$ , is made wide enough to avoid trouble with phase shifts and amplitude changes produced by drifts of tuned circuits and modulation generators. Therefore, the smoothing filter determines the noise bandwidth after detection.

The coherent demodulator can be described as a multiplying element in which the product of a signal and a reference voltage is produced. The signal output is at a d-c voltage level depending on the amplitude of the signal input and its phase relative to that of the reference voltage. A simple form for a coherent demodulator and smoothing filter is shown in Fig. 4.6.

The first step in the analysis consists of setting up a form for the voltage  $x(t)$  that gives the proper power levels out of the detector. Then, using this expression, the signal and noise powers through the rest of the receiver are calculated from autocorrelation functions and their transforms. It is necessary to take averages over statistically long periods in order to apply autocorrelation-function techniques. Since these long periods must be short compared with modulation periods, we are left with the requirement that has been assumed for this analysis, that  $f_m$  is much smaller than  $\Delta f$ .

The resulting expression for  $\Delta T$  is a function of  $\mu(t)$  and  $\xi(t)$ . After combining these into a factor  $M$ , we have the expected form

$$\Delta T = M(T + T_{ref}) \sqrt{1/\tau \Delta f}$$

The values of  $M$  for different modulation  $[\mu(t)]$  and demodulation  $[\xi(t)]$  waveforms have been calculated. When, for the video filter,  $J(f) = 1$ ,

$$M = 2 \sqrt{\langle \xi(t)^2 \rangle / [(1/T) \int_0^T \mu(t) \xi(t) dt]^2}$$

and values are given in Table 4.1.

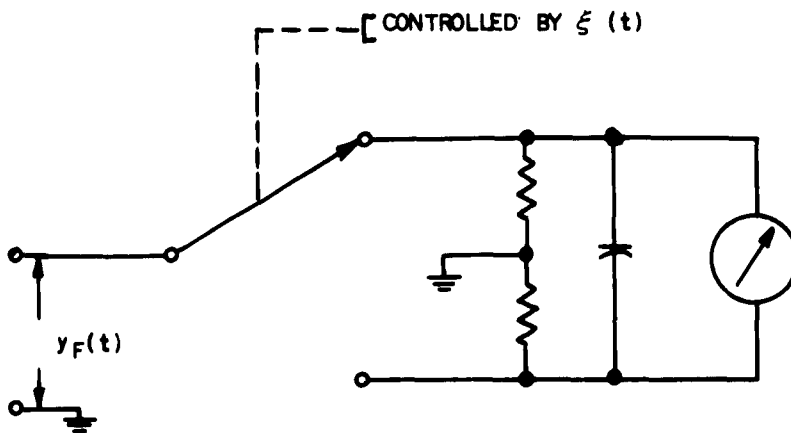


FIG. 4.6 COHERENT DEMODULATOR WHICH IS AN IDEAL SWITCH DRIVEN BY THE REFERENCE VOLTAGE  $\xi(t)$ . THE SWITCH ACTION MULTIPLIES  $y_F(t)$  BY A SQUARE WAVE.

TABLE 4.1. VALUES OF THE MODIFYING FACTOR M IN THE FORMULA FOR  $\Delta T$  FOR THE CASE OF NO VIDEO FILTER [ $J(f) = 1$ ].

Demodulation Waveform $\xi(t)$	Values of M for Modulating Waveform $\mu(t)$		
	Square-wave	Sinusoidal	Sawtooth
Square-wave	2.00	$\pi = 3.14$	4.00
Sinusoidal	$\pi/\sqrt{2} = 2.22$	$2\sqrt{2} = 2.83$	$\pi\sqrt{2} = 4.44$
Sawtooth	$4/\sqrt{3} = 2.31$	$2\pi/\sqrt{3} = 3.63$	$2\sqrt{3} = 3.46$

When the video filter passes only the fundamental component of the modulation,

$$M = \sqrt{2}/|K_{\mu_1}|$$

where  $|K_{\mu_1}|$  is the magnitude of the coefficient for  $n = 1$  in the following expression for  $\mu(t)$ :

$$\mu(t) = \sum_{n=-\infty}^{n=\infty} K_{\mu_n} \exp(jn2\pi f_m t)$$

Values for M in this case are given in Table 4.1.

TABLE 4.2. VALUES OF THE MODIFYING FACTOR M IN THE EQUATION FOR  $\Delta T$  FOR A NARROW-BAND VIDEO FILTER THAT PASSES ONLY THE FUNDAMENTAL COMPONENT OF THE MODULATION WAVEFORM  $\mu(t)$ .

Modulation Waveform $\mu(t)$	M
Square-wave	$\pi\sqrt{2} = 2.22$
Sinusoidal	$2\sqrt{2} = 2.83$
Sawtooth	$\pi\sqrt{2} = 4.44$

The qualitative discussion that led to a square-wave operation for a least  $\Delta T$  is upheld with the value  $M = 2$  applying in the case of  $\mu(t)$  and  $\xi(t)$ , both being square-waves, and  $J(f) = 1$ . In this case also we can state that, for a given modulation waveform, the least M occurs when  $\xi(t)$  is of the same form. With the narrow video filter, M is seen to be independent of  $\xi(t)$  except for its relative phase. Only the amplitude of the fundamental frequency component of  $\mu(t)$  enters the expression. In the presence of instabilities, the modulated receiver provides stabilization of the zero point on the calibration curve. When operating optimally in this sense, the condition of zero-signal input results in a zero-mean meter deflection. The manner in which instabilities affect the modulated receiver's performance is discussed below

Instabilities in receiver components ahead of the detector modulate the power into the detector and contribute to the power spectral density of the detector output  $B_{y_j}(f)$ . These contributions can be avoided by proper choice of  $f_m$  as discussed above. Instabilities after detection and before demodulation increase the noise-power spectrum uniformly across the band passed by the video filter and hence contribute to output-noise

power even under zero-modulation-component conditions. Considering these instabilities also as a modulation effect, the spectrum of the noise into the demodulator will be that of the video-filter output convolved with the spectrum of instabilities producing the modulation and an impulse function of unit area representing stable transfer conditions. The noise spectrum will be widened and increased in amplitude in this process. Figure 4.7 shows typical spectra involved in this effect.

Therefore, even with a zero-mean meter deflection, an increase in the fluctuating meter-deflection component occurs, depending on the stability of the receiver components between the detector and the demodulator. Fortunately, the gain required in this section of the receiver can be achieved with amplifiers using heavy negative feedback and having consequently a high degree of stability. In the following paragraphs we assume that the effect is negligible.

At times, operation with a fixed difference in temperature between the antenna and the reference is necessary. For instance, the reference may be at room temperature and the antenna temperature may be much lower. The zero point of calibration will have a fixed offset depending upon  $T - T_{ref}$ . Partial stabilization of the zero-point compared to total-power operation will occur as long as the ratio [Ref. 8]

$$\zeta = (T - T_{ref}) / (T + T_{er}) < 1.$$

This ratio compares the zero-signal deflection of the modulated receiver with that of the total-power receiver and is defined as the instability-reduction factor for the contribution I (see Eq. (6)).

The expression for  $\Delta T$  in the presence of instabilities and a fixed temperature difference  $T - T_{ref}$  is

$$\Delta T = M \{ T_{er} + [(T + T_{ref})/2] \} U_L \sqrt{1 + (I\zeta/U_L)^2}$$

## C. RECEIVERS WITH SERVO STABILIZATION

### 1. Introduction

The possibility of using automatic gain control (AGC) for achieving receiver stabilization has been mentioned above. Three general ways of carrying this out are:

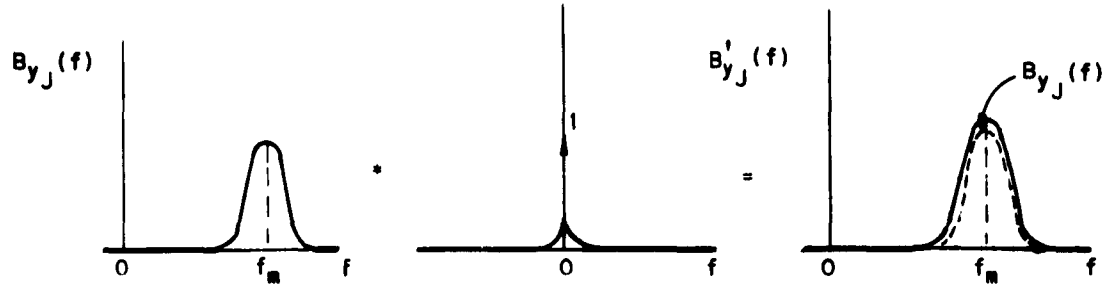


FIG 4.7 EFFECT OF INSTABILITIES IN THE RECEIVER COMPONENTS BETWEEN THE DETECTOR AND DEMODULATOR ON THE POWER SPECTRUM  $B_{y_J}(f)$ .

1. By utilizing the difference in spectral content of signals and instabilities.
2. Through the addition of a second channel from which AGC information is obtained.
3. By means of time sharing techniques.

Each of these methods has characteristics which will be pointed out. As was suggested in Chapter III, the control may be applied to amplifiers before or after detection, or both.

## 2. Automatic-Gain-Control Theory

Consider an AGC loop on a total-power receiver that is designed to maintain an average level  $\langle y \rangle$  at the detector output depending on the d-c reference level  $L$ . Figure 4.8 presents the block diagram for this situation. The power-gain-control characteristic for the variable-gain amplifier is  $G_v(v)$  and it relates the input power  $\langle x_1^2 \rangle$  and the detector output  $\langle y \rangle$  thus:

$$\langle y \rangle = G_v(v) \langle x_1^2 \rangle$$

In the sense used above,  $\langle y \rangle$  is a function of time, with the time average taken over times long compared with significant correlation times of  $x(t)$  but short compared with variations in detector output that are of interest. Hence  $\langle y \rangle$  can be considered as the envelope of a noise-modulated signal  $x_1(t)$  and the analysis presented by Oliver [Ref. 21] can be applied.

For small signals, let

$$G_v(v) = G_0 + G_1 v$$

so that the a-c open-loop gain will be

$$\Gamma = \langle x_1^2 \rangle G_1 D(f)$$

The expression for sensitivity of a control loop to a parameter such as  $\langle x_1^2 \rangle$  is

$$(d\langle y \rangle / \langle y \rangle) / (d\langle x_1^2 \rangle / \langle x_1^2 \rangle) = 1 / (1 + \Gamma)$$

When the loop gain is high the stability of the average detector output is improved by a factor nearly equal to the loop gain. As  $\Gamma$  drops off with frequency according to  $D(f)$  the instabilities begin to pass so that above the frequency where  $\Gamma = 1$  almost no control exists. This behavior is necessary, however, since signal information must pass through undiminished. As a result, such AGC systems are useful only where the d-c and very low-frequency components of the signal are not necessary.

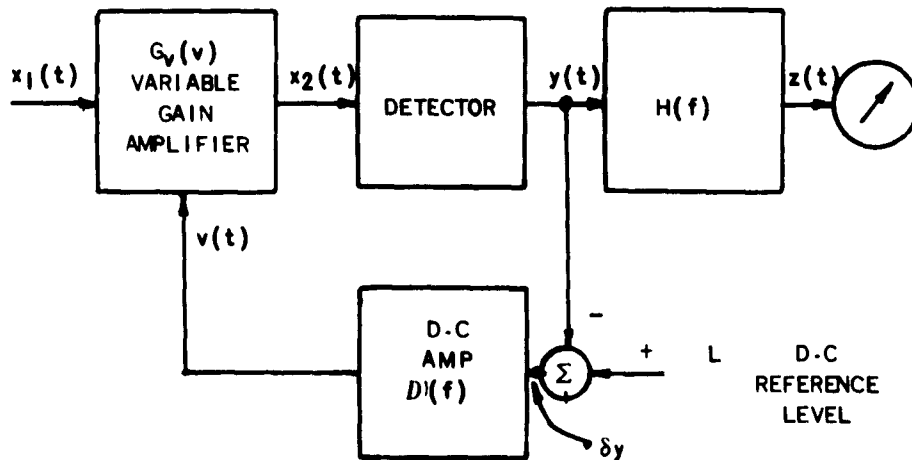


FIG. 4.8..BLOCK DIAGRAM OF AN AGC LOOP IN A TOTAL POWER RECEIVER

As an example, in a case where the lowest signal frequency of interest  $f_{\min}$  is 0.001 cps and an improvement factor of 100 is desired, two possible filter functions  $D(f)$  have been examined. The asymptotic frequency-response plots for these two filters and the resulting receiver-response plots are shown on Fig. 4.9. A guard band of a decade width below  $f_{\min}$  has been allowed, fixing the frequency ( $f_g = 10^{-4}$  cps) at which  $\Gamma = 1$ . The improvement factor of 40 db means a  $\Gamma(0)$  also of 40 db so that, for the first case with a single section RC filter (illustrated by the solid curves) the slope of  $D(f)$  is 20 db/decade and the break frequency  $f_b$  for the filter turns out to be  $10^{-6}$  cps. With a two-section RC filter response shown with dotted lines, the break frequency must be  $10^{-5}$  since the whole 40-db gain is lost in the first decade above  $f_b$  when the slope is 40 db/decade. The normalized receiver response plotted is

$$Y'(f) = Y(f)/Y(0)[1 + G_1 \langle x^2 \rangle D(f)]$$

on a db scale.  $Y(f)$  is the voltage transform of the detector output  $\langle y \rangle$  on the average and is assumed to be flat throughout the range of interest. The frequencies  $10^{-5}$  and  $10^{-6}$  cps are easier to comprehend when expressed in terms of a time constant. In Fig. 4.10 the stability-improvement-factor requirements on  $f_b$  and single-section time constants are presented. The factor of 100 and a time constant of 43 hr is probably outside a reasonable range of practical values. Even with the two-section filter a total time constant of 4.3 hr is necessary. In general,

$$f_{b_i} = f_g^i / \Gamma(0), \quad i = 1, 2 \text{ for 1 or 2 sections}$$

A steep-slope filter is desirable; however, when combined with high loop gains, troubles with oscillations in the AGC loop will arise.

### 3. Pilot-Signal Receivers

If by some means a standard signal can be passed through the receiver in such a way that it remains isolated from the normal signal channel, an AGC voltage can be derived from this standard or pilot signal. One possible standard signal is a sinusoid, just outside the signal channel, which is separated with a suitable filter before detection. The pilot signal is detected, compared with a reference level, and used to provide the necessary gain control. The objection to this system is that

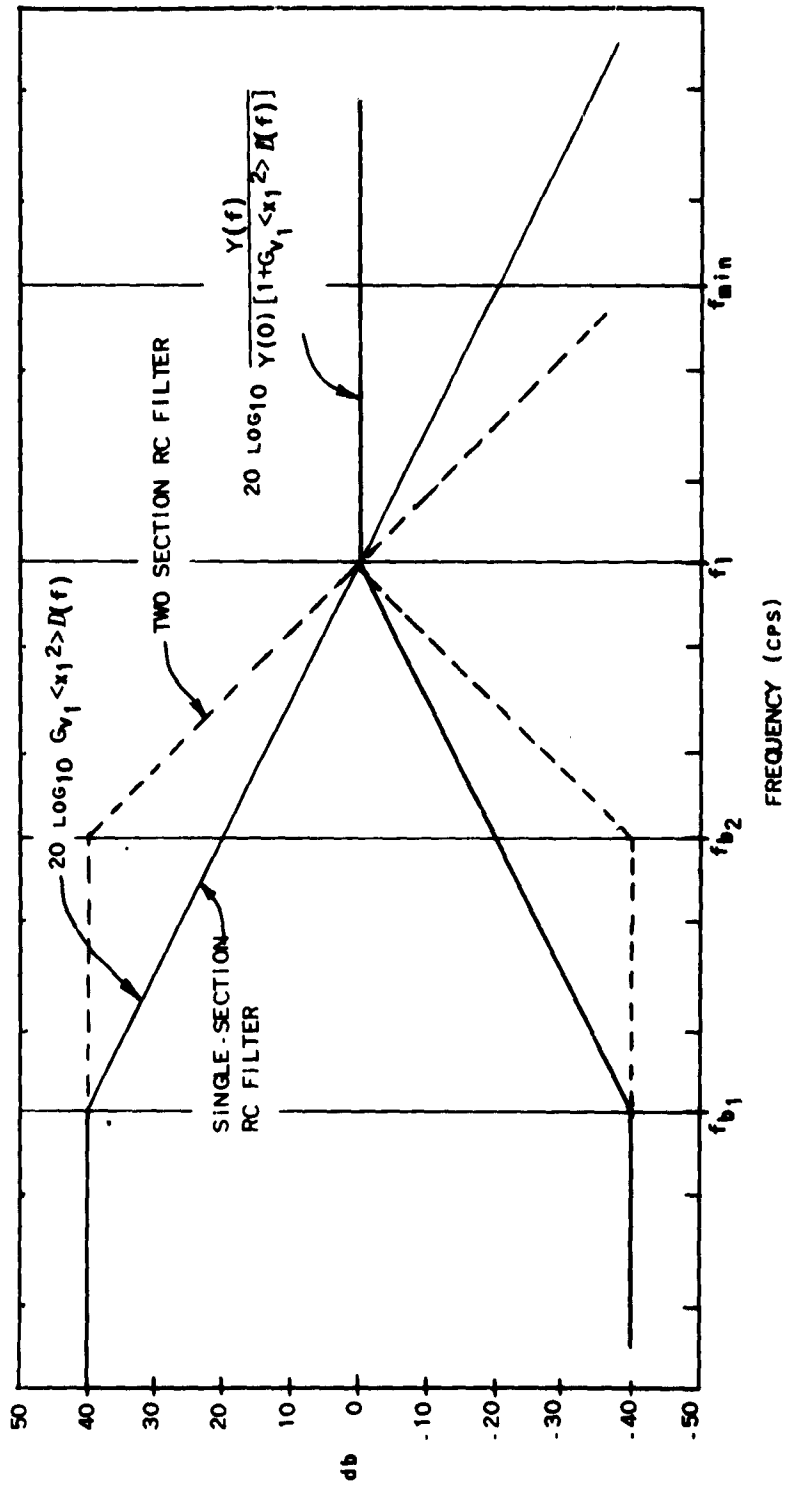


FIG. 4.9 ASYMPTOTIC-FREQUENCY-RESPONSE CURVES FOR THE RECEIVER WITH AGC (HEAVY LINE) AND THE AGC LOGS (LIGHT LINE). SOLID CURVES ILLUSTRATE A SINGLE-SECTION RC FILTER FOR  $D(f)$  WHILE THE DASHED LINES ARE FOR A TWO-SECTION RC FILTER.

the gain at a particular frequency at which no signal power occurs is being stabilized. One can imagine a bandpass amplifier stabilized in this manner which would still have instabilities in the average gain over the passband.

An improvement over the above pilot system can be achieved by using a modulated-noise pilot signal added to the input of a total-power receiver. A coherent demodulator selects the pilot signal at the receiver output from which the gain control is derived. Since the whole reception filter is used for both signal and pilot, stabilization occurs similarly for both. Such a system is shown in Fig. 4.11.

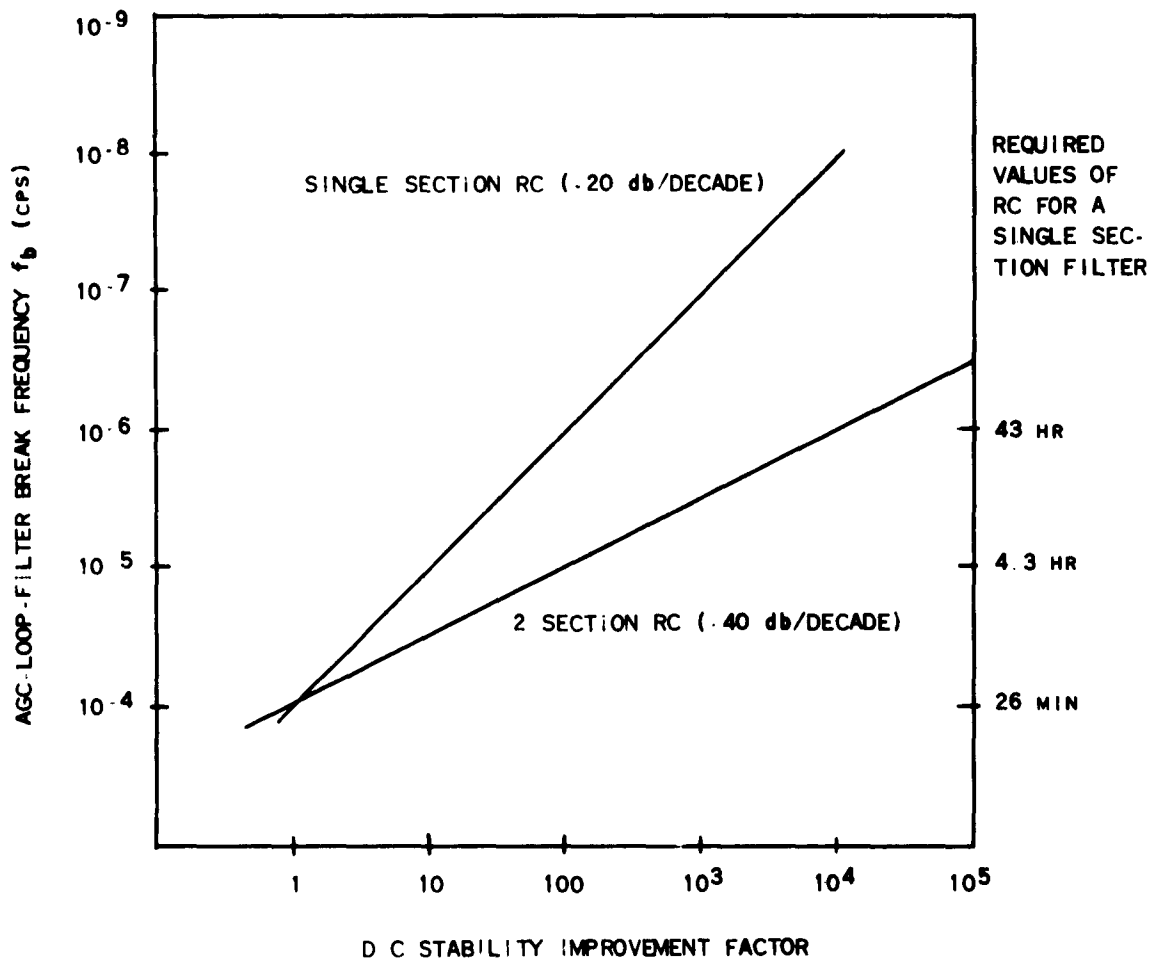


FIG. 4 10 REQUIREMENTS ON FILTER BREAK FREQUENCIES WITH IMPROVEMENT FACTORS FOR 1. AND 2. SECTION RC FILTERS FOR AN  $f_{min} = 10^{-3}$  CPS.

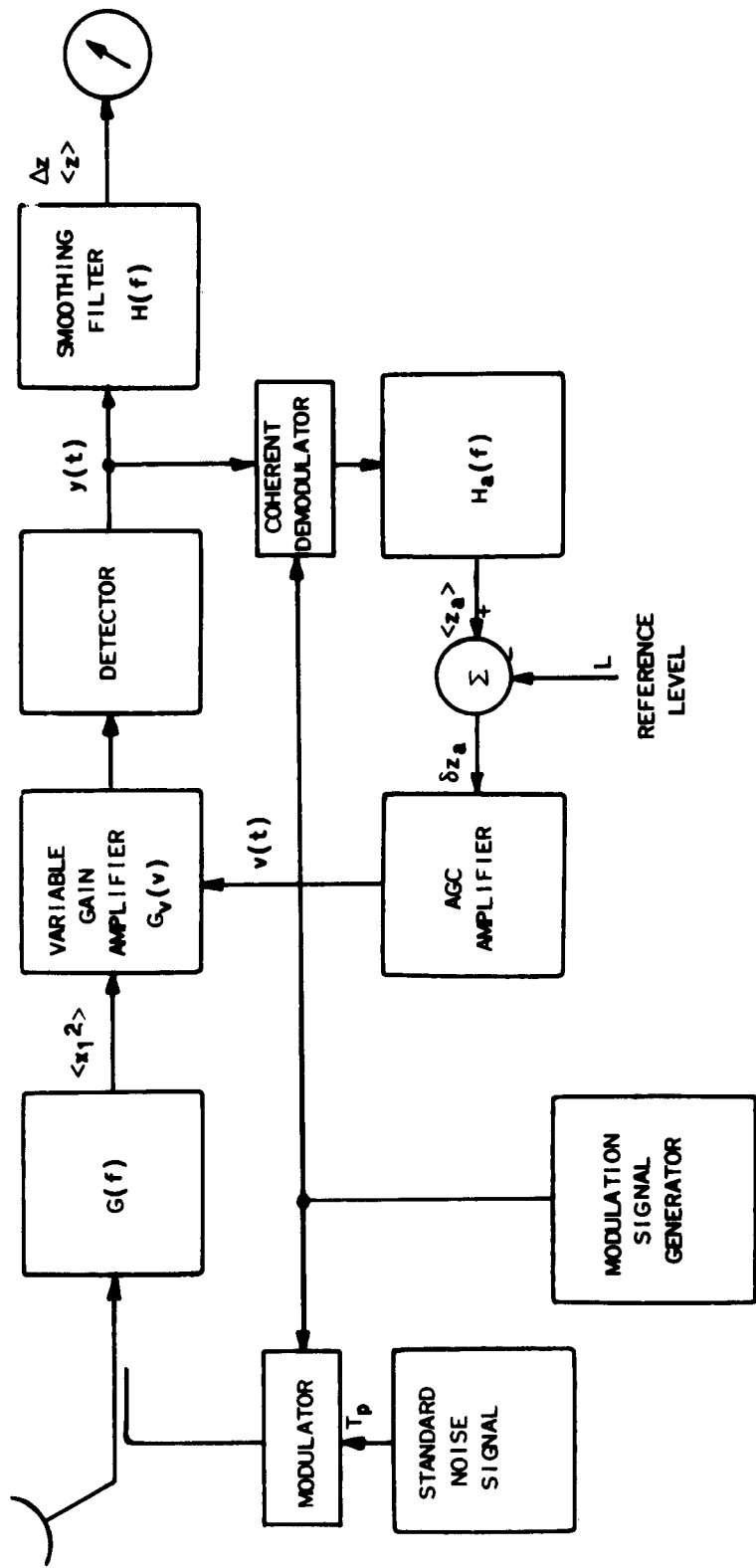


FIG. 4.11 BLOCK DIAGRAM FOR A MODULATED PILOT-SIGNAL-STABILIZED RECEIVER .

The measurement of the standard noise signal  $T_p$  is made with a modulated-signal or Dicke-receiver system. At its output the level  $\langle z_a \rangle$  is produced with a standard deviation

$$\sqrt{\langle \delta z_a^2 \rangle} = \Delta z_a = 2 T_{00} / \sqrt{\tau_a \Delta f}$$

when square-wave modulation is used. (We assume a one-to-one calibration between signals  $T$  at the input and deflections  $z$  at the output and between pilot signals  $T_p/2$  and  $z_a$ .) The variation of  $\langle z_a \rangle$ ,  $\delta z_a$ , has two components,

1. That due to receiver instabilities which produce a  $\delta z_a$  proportional to  $\langle z_a \rangle$  and
2. That due to receiver noise which produces a  $\delta z_a$ ,

satisfying the equation above. For variations of the first type, the AGC loop will provide improvements (as discussed above with the total-power receiver) depending on loop gain. This improvement is effective for both  $\langle z_a \rangle$  and  $\langle z \rangle$ . The major difference between this case and that of Section 2 above is that the additive nature of the pilot signal has allowed stabilization of the receiver without affecting signal changes with a d-c component.

The second type of variation produces some interesting effects. While the first type arises from a change in  $\langle x_a^2 \rangle$  and  $\langle x_f^2 \rangle$ , the second type is of the same nature as a change in  $L$ . This variation of course results in a gain change of such a sense that the average value of  $\langle z_a \rangle$  remains constant. This situation is evident when the system is presented in block form as in Fig. 4.12. The primed symbols below indicate values when the AGC loop is closed. Since

$$\langle z_a \rangle = G_v \langle x_a^2 \rangle [H_a(f)]^{1/2}$$

during AGC action

$$\langle z_a \rangle = G'_v \langle x_a^2 \rangle [H_a(f)]^{1/2} + \delta z_a$$

and

$$G'_v/G_v = 1 - (\delta z_a / \langle z_a \rangle).$$

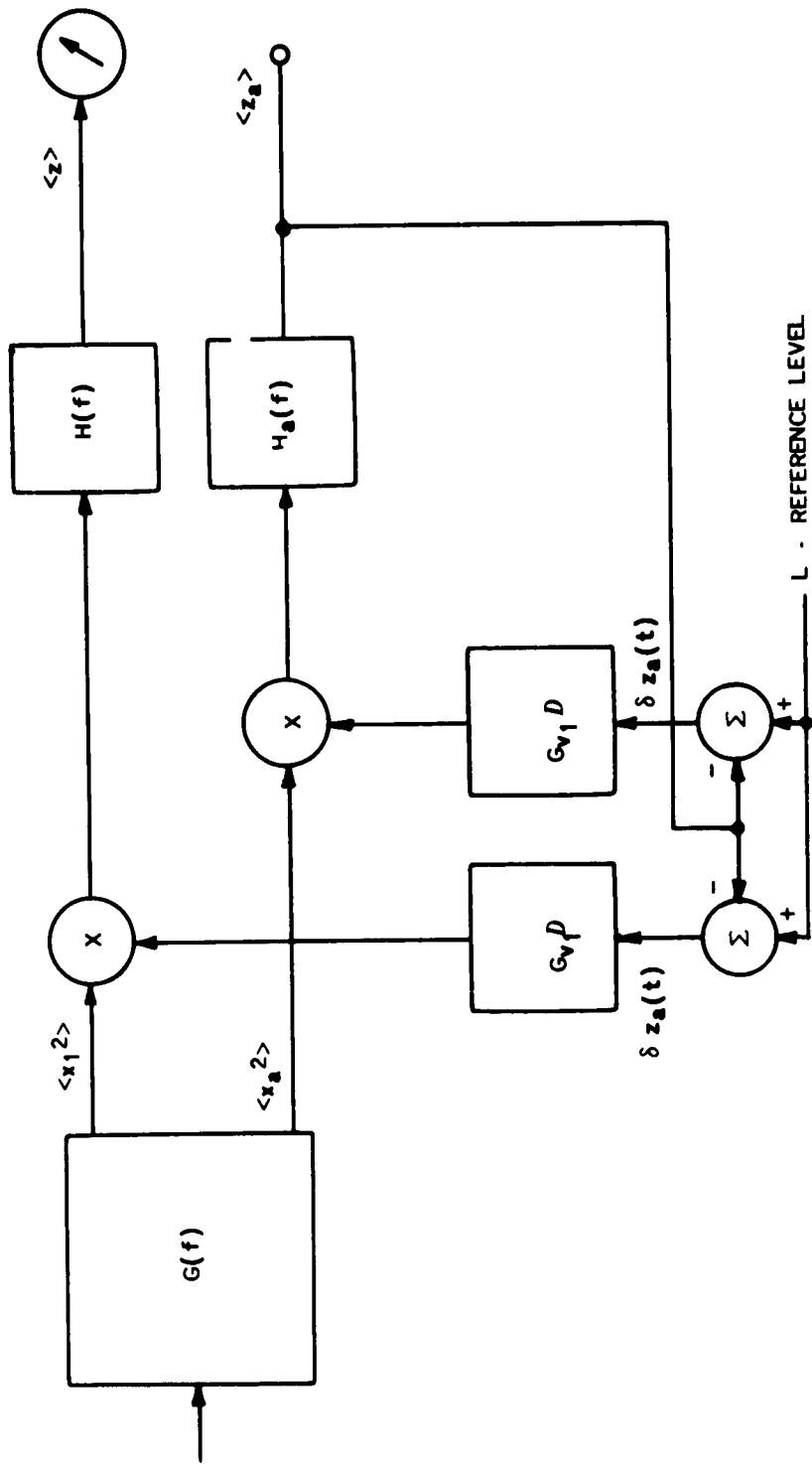


FIG. 4.12 REPRESENTATION OF THE AGC LOOP IN THE MODULATED PILOT-SIGNAL RECEIVER.

This change in gain produces a variation in the receiver output  $\delta_a z^*$  in addition to the random noise variation  $\delta z$  such that

$$\delta_a z = (G'_v/G_v) \langle z \rangle - \langle z \rangle$$

or

$$\delta_a z = - \langle z \rangle \delta z_a / \langle z_a \rangle$$

The total variation at the output will be

$$\delta z_T = \sqrt{\delta_a z^2 + \delta z^2}$$

The variance of the output

$$\begin{aligned} \Delta z_T'^2 &= \Delta z'^2 + [\delta_a z^2]_{av} \\ &= \Delta z'^2 + (\langle z \rangle^2 / \langle z_a^2 \rangle) [\delta z_a^2]_{av} \end{aligned}$$

Now, if

$$\langle z \rangle / \langle z_a \rangle = a$$

and

$$\Delta z' / \Delta z_a = \epsilon = \sqrt{\tau_a / 4\tau}$$

then

$$\begin{aligned} \Delta z_T'^2 &= \Delta z'^2 + a^2 \Delta z_a^2 \\ &= \Delta z'^2 [1 + (a^2 / \epsilon^2)] \\ &= \Delta z'^2 [1 + (4a^2 \tau / \tau_a)] \end{aligned}$$

---

\* Note that the symbol  $\delta_a z$  indicates receiver-output changes due to AGC while  $\delta z_a$  indicates AGC-channel-output changes.

The addition of the pilot signal increases the system noise by one half the pilot signal equivalent noise temperature; hence

$$\begin{aligned} T'_{e_s} &= T_{e_s} + (T_p/2) \\ &= T_{e_s} [1 + (1/a)] \end{aligned}$$

The minimum detectable signal for the receiver will then be

$$\begin{aligned} \Delta z'_T &= \Delta z' \sqrt{1 + (4\tau a^2/\tau_a)} \\ &= T'_{e_s} \sqrt{(\tau_a + 4\tau a^2)/\tau_a} \tau \Delta f \end{aligned}$$

Comparing this with a simple total-power receiver we find

$$\Delta z'_T/\Delta z = [1 + (1/a)] \sqrt{1 + (4\tau a^2/\tau_a)}$$

This function has been plotted for Fig. 4.13 with the factor  $a$  as a parameter. With very small pilot signals, such as with  $a$  equal to 100, the required integrating time in the AGC loop becomes very large. The value of AGC loop gain  $\Gamma$  can be as large as loop stability will allow in the pilot-signal system, since signals are not influenced by the AGC action. The requirement of  $\tau_a$  as shown by Fig. 4.13 has a conflicting specification that is the desirability of maintaining a large  $\Gamma$  over the whole signal spectrum. If a minimum is set for  $\Gamma$  at the maximum signal frequency, the value of  $\Gamma(0)$  required with a particular filter to achieve a particular value of  $M$  can be determined. As an example illustrated in Fig. 4.14 under the conditions of  $\Gamma(f_{max}) = 40$  db,  $\tau = 5$  sec,  $a = 10$ , a value  $M = 2$  requires about 88-db gain in the AGC loop when a single-section RC filter is used.\* Interestingly enough, the two-section RC filter requires about 123-db gain under the same conditions. This requirement can be understood by realizing that, while the minimum

---

\*The filter break frequencies are defined as:

$$f_{b_1} = 1/\pi\tau_a \quad ; \quad f_{b_2} = 2/\pi\tau_a$$

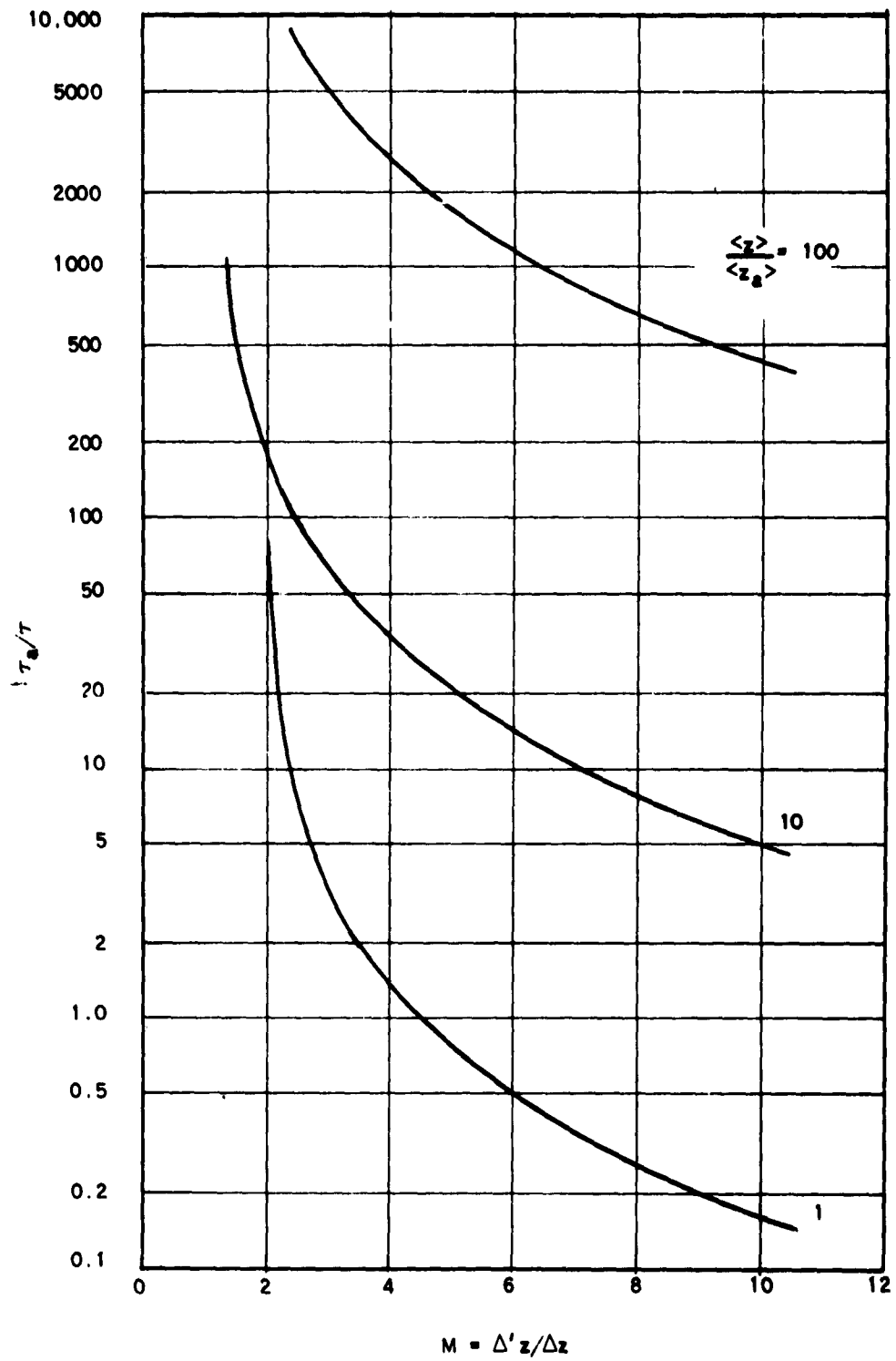


FIG. 4.13 RATIO OF PILOT-SIGNAL TO SIGNAL INTEGRATING TIMES AS A FUNCTION OF M FACTOR FOR A PILOT-SIGNAL AGC RECEIVER.

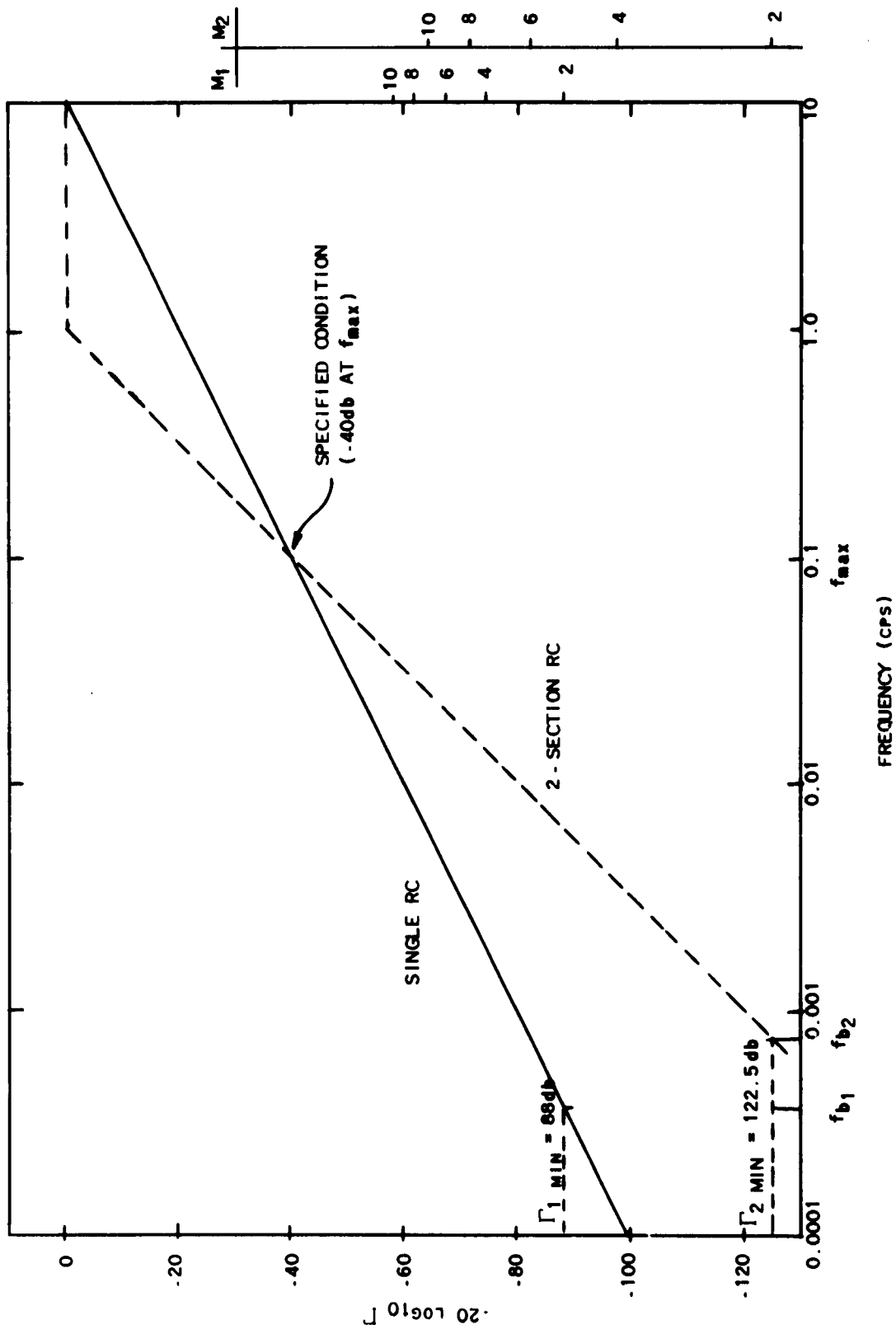


FIG. 4.14 NORMALIZED ASYMPTOTIC RESPONSE TO INSTABILITIES OF A MODULATED PILOT-SIGNAL RECEIVER.  $M = 2$ ,  $\tau = 5$  SEC  
 $\alpha = 10$  AND RESPONSE AT MAXIMUM SIGNAL. FREQUENCY  $f_{MAX}$  SPECIFIED AT -40db.

detectable signal-modifying factor  $M$  depends on total noise power under the smoothing-filter response, the AGC requirement depends on the tail of the voltage response of the smoothing filter. In this case the extended response of the single section relative to that of the two-section is an advantage.

The modulated pilot-signal receiver has the capability of equaling the minimum detectable signal of a modulated signal receiver and has the advantage that throughout the linear-response range of the receiver, the improvement factor on instabilities remains constant. As was discussed in Chapter III, and shown in Fig. 3.7, the slope of the calibration curve is held constant but the zero point can change with changes in  $T_{es}$ .

#### 4. Other AGC Systems

Two possibilities for applying AGC to receivers with modulated or switched inputs are:

1. Connecting the servo loop to stabilize the receiver output for one state while the signal is measured during the other state.
2. Connecting the servo loop to stabilize the receiver for one input state while the signal is measured from the difference between the the two states.

Time-sharing or switching techniques that isolate signal information from the AGC channel will deteriorate the  $\Delta T$  value.

A white noise that is square-wave gated does not change its spectral character, although it does lose 3 db in strength. It undergoes an irreversible process since aliased bands overlap, causing information to be lost. The band-limited gain-instability noise can be sampled adequately and detailed information of its waveform can be recovered. Consequently, AGC voltages derived from switching systems will contain information on the gain-instability fluctuations in the signal output, which can therefore be reduced, but they will not have information on receiver noise fluctuations in the signal output. They do carry a similar noise fluctuation which will add quadratically to the receiver-noise fluctuation in the signal output.

An example of this type of receiver is shown in Fig. 3.2 which has an  $M = 2$ . The factor  $\zeta$  for instabilities will be equal to  $1/\Gamma$ , the inverse of the AGC-loop gain.

When the signal output is derived from the difference between the antenna and reference temperatures, and gated AGC is applied as shown in

Fig. 3.4, the effect of changes in gain and  $T_{ea}$  is opposite that of a Dicke system (see Fig. 3.3). The value of M will be

$$M = 2\{1 + [T/(T_{er} + T_{ref})]\}$$

and

$$\zeta = [(T - T_{ref})/(T + T_{er})] (1/\Gamma)$$

This system improves the dynamic range over which instability effects are reduced compared with the Dicke system.

A process of further time sharing using three switch positions and two reference temperatures as shown in Fig. 3.5 changes M even more, but it results in a greater calibration stability. As shown neither gain nor  $T_{ea}$  changes affect the calibration. Whether this three-position switching system can be achieved in practice without introducing undesirable effects is not known.

In a critical application, an auxillary AGC loop might be incorporated, as shown in Fig. 3.6 to assure a constant detector operating point. This additional AGC loop of course increases M even more. Each stage in these stabilization processes must be justified in practice, considering the many factors involved in a particular application. Simplicity has many virtues as a design criterion.

## V. RYLE AND VONBERG TYPE RECEIVERS

### A. GENERAL DESCRIPTION

In previous chapters the null-balancing concept was introduced as a means of stabilizing receiver calibration. The equipment described by Ryle and Vonberg [Ref. 17] and later in more detail by Machin, Ryle and Vonberg [Ref. 22] successfully demonstrated the method applied to radio-astronomy measurements at meter wavelengths.

The necessary components required to perform the null balance consist of:

1. A comparison device to indicate the difference or error between a controllable reference source and the signal source.
2. An amplifier for the error voltage.
3. A controller for the reference source.

These components are connected to form a servo system that acts to null the error voltage. Figure 5.1 illustrates such a system. Each of these components will be discussed below with a viewpoint of presenting their transfer functions and characteristics for inclusion in the servo loop.

#### 1. Controllable Reference Sources

The basic requirement for the reference source is that its range of variation coincide with the range of expected signal strengths. At the same time a reliable measure of the reference-source strength must be available for recording. Since the receiver will be designed for particular measurements, the transfer function of the controlled source must be satisfactory in terms of frequency response when considered as part of the servo loop.

Ryle and Vonberg used a saturated-noise diode whose filament supply was readily variable. They chose to use 10-kc alternating current supplied from a voltage-controlled source to heat the filament. A 350-ohm anode load resistor was used which provided a 30,000 °K noise temperature (when transformed to the transmission line impedance of 70 ohms) at an anode current of 15 ma. From their measurements the transfer function for their diode was of the form  $K_d/(T_d s + 1)$ , with  $T_d = 0.09$  sec during heating and  $T_d = 0.06$  sec while cooling. To achieve stability in the complete equipment, feedback proportional to the derivative of the anode current was applied to the input of the control stage. The resulting transfer function can be written in this form

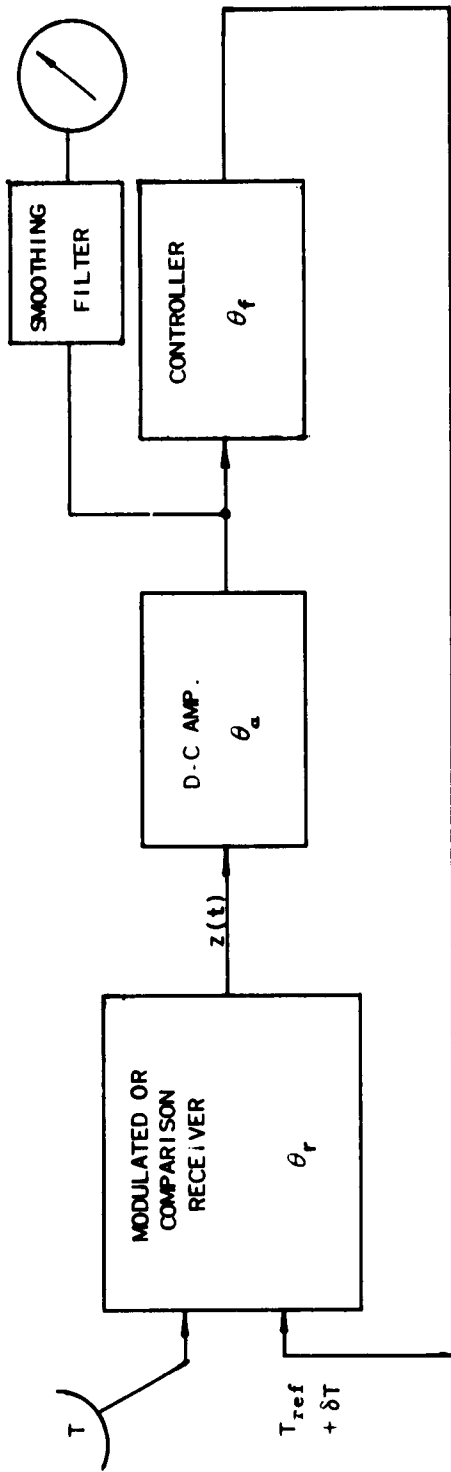


FIG. 5.1 SIMPLIFIED BLOCK DIAGRAM FOR A RYLE AND VONBERG TYPE NOISE-BALANCING RECEIVER.

$$\frac{K_d(T_\phi s + 1)}{(T_d s + 1)(T_\phi s + 1) + K}$$

where  $T_\phi$  is the time constant of the feedback path.

A second convenient source of noise is a gas-discharge tube coupled to a transmission line. The characteristics of such a source are relatively independent of conditions of the discharge; hence, control of the temperature to permit use of this tube as a reference source requires the addition of a controllable attenuator. If the noise source is in a waveguide a motor-positioned attenuator of the conventional kind can easily be used. A simple scheme under some conditions is to utilize a self-balancing, potentiometer-type recorder that has been modified to move the recording pen and an attenuator card simultaneously for control of the noise temperature. The measuring circuit must be disabled also, so that the instrument operates as a servomechanism. When the attenuator card is designed to give a linear temperature output as a function of recorder-pen position, a very satisfactory means of control and recording is achieved. One disadvantage of such a system is the relatively slow response time of mechanical recorders and attenuators, which limits the usefulness of the receiver to slowly varying signals.

The simplest transfer function of motor-driven attenuators will be of the form  $K_M/s(T_M s + 1)$ , which includes an integrating term  $1/s$  typical of motors and a time constant  $T_M$ .

Another controllable attenuator is a resonant-absorption ferrite device with a variable magnetic field. A transfer function between a field-coil current and noise temperature at the attenuator output could be arranged with the form  $K_f/(T_f s + 1)$ , with the time constant  $T_f$  dependant on the L/R ratio of the coil and driving circuit. Although this device could be made with a satisfactory frequency response it still suffers from an inherent nonlinear characteristic that would have to be corrected either in the driving circuit or in the data reduction.

## 2. Error-Voltage Amplifiers

The main requirement for these amplifiers is sufficient gain. Their noise level must, of course, be satisfactory and their frequency response must be adequate. By making the frequency response of one stage dominant, we can for our purposes describe the amplifier with a transfer function such as  $K_a/(T_a s + 1)$ . The available output-voltage swing must

of course be large enough to drive the controlled noise source over its full range.

### 3. Comparison Devices

Detecting a difference in temperature between two sources is the fundamental operating principle for a Dicke-type receiver, and the logical extension of this idea is the Ryle and Vonberg system. Therefore, we shall consider Dicke-type receivers as comparison devices.

A requirement of rapid operation may result in a minimum of smoothing within the comparison receiver itself; in fact, the determining element in frequency response may be the video filter. The action of the coherent demodulator translates the center of response of the video filter to zero frequency, resulting in a low-pass response. A single tuned filter after this operation has the transfer function  $K_f/(T_f s + 1)$ .

Of course, when a smoothing filter is used at the comparison-receiver output, the voltage-transfer function corresponding to the power-transfer characteristic  $H(f)$  must be used to write the transfer function for the comparison device. In the simplest case it would be the same as the function shown above.

The discussion so far has not considered system noise. The comparison receiver will have a minimum detectable error signal as described by the applicable  $\Delta T$  expression. For our purposes we can assume that the other components in the servo loop contribute no additional noise, so that the loop noise output will be a modified version of that produced by the comparison receiver. The details of the modification are presented below.

#### B. NOISE ANALYSIS

For this study we shall assume that the system is balanced, so that only small changes  $\delta T$  in  $T_{ref}$  are present because of noise. Then  $\delta T$  has a zero mean value and its mean-square value will be the total noise-power output for the system.

For fluctuations from the mean for the closed loop we can write, using the notation of Fig 5.1

$$\begin{aligned} \delta T &= (z - \langle z \rangle) \theta_a \theta_f - \delta T \theta_r \theta_a \theta_f \\ &= \frac{(z - \langle z \rangle) \theta_a \theta_f}{1 + \theta_r \theta_a \theta_f} \end{aligned}$$

Now we use the relation between power spectral densities at the input and output of a linear system to find the power spectral density for  $\delta T$ . From Eq. (C.11) the spectrum for  $\langle z \rangle$  is

$$C_c(f) = p_z H(f),$$

where  $p_z$  is the uniform strength that is weighted by the filter response  $H(f)$ . Thus, letting  $D(f)$  be the power spectral density for  $\delta T$  we have

$$D(f) = C_c(f) \left| \frac{\theta_a \theta_f}{1 + \theta_r \theta_a \theta_f} \right|^2$$

We can then write

$$\langle T_{ref} \rangle = T \frac{\theta_r \theta_a \theta_f}{1 + \theta_r \theta_a \theta_f} \Big|_{f=0}$$

and

$$\Delta \langle T_{ref} \rangle = (T' - T) \frac{\theta_r \theta_a \theta_f}{1 + \theta_r \theta_a \theta_f} \Big|_{f=0}$$

When  $\Delta \langle T_{ref} \rangle = \sqrt{\langle \delta T^2 \rangle}$ ,  $(T' - T) = \Delta T$  the minimum detectable signal, by definition, so that

$$\Delta T = \sqrt{\langle \delta T^2 \rangle} / \left[ \theta_r(0) \frac{\theta_a \theta_f}{1 + \theta_r \theta_a \theta_f} \Big|_{f=0} \right]$$

Now

$$\theta_r(0) = \langle z \rangle / (T - T_{ref}) = \sqrt{p \langle z \rangle} H(0) / (T - T_{ref})$$

which can be evaluated from Eq. (C.8). The complete expression for  $\Delta T$  then, is

$$\Delta T = \sqrt{\frac{2k^2(T_{er} + T_{ref})^2 [G \cdot G] \Big|_0 \sum_{n=-\infty}^{n=\infty} |K_{\xi_n}|^2 \int_{-\infty}^{\infty} H(f) |\theta_a \theta_f / (1 + \theta_r \theta_a \theta_f)|^2 df}{(k^2/4) \left[ \int_{-\infty}^{\infty} G(f) df \right]^2 \left[ (1/T) \int_0^T \mu(t) \xi(t) dt \right]^2 H(0) |\theta_a \theta_f / (1 + \theta_r \theta_a \theta_f)|^2_{f=0}}$$

$$= M (T_{er} + T_{ref}) 1/\sqrt{\tau' \Delta f},$$

where M is defined by Eq. (C.15) and

$$1/\tau' = \frac{\int_{-\infty}^{\infty} H(f) |\theta_a \theta_f / (1 + \theta_r \theta_a \theta_f)|^2 df}{H(0) |\theta_a \theta_f / (1 + \theta_r \theta_a \theta_f)|^2_{f=0}}$$

Since  $H(f)$  and  $|\theta_r|^2$  are related by a frequency-independent factor, we can rewrite the above equation as

$$\tau' = \frac{|\theta_r \theta_a \theta_f / (1 + \theta_r \theta_a \theta_f)|^2_{f=0}}{\int_{-\infty}^{\infty} |\theta_r \theta_a \theta_f / (1 + \theta_r \theta_a \theta_f)|^2 df}$$

From the above analysis we see that the Ryle and Vonberg type receiver depends on the behavior of the modulated-signal receiver used for comparison or error indication. The minimum-detectable-signal expression is that for the comparison receiver, except that the integrating time is modified by the closed-loop transfer function

### C. DYNAMIC BEHAVIOR

The transfer function for the receiver can contain an undetermined number of poles and zeros, depending on the complexity of the individual components. Two possible forms are those with a  $1/s$  term and those without. Without the pole at the origin the device is a proportional-control system, in which the error is reduced to as small a value as desired by providing sufficient loop gain. This device then would have a fixed percentage error but would always operate with a stable zero-signal point. Changes

in  $K$ , the loop gain, would result in calibration changes; however, for large gains, the deviation from a unity proportionality factor would be small, since the functional form for this factor is

$$K/(1+K) \approx 1 \quad (K \gg 1).$$

When a  $1/s$  term is present the control system nulls with a zero error, at which time excitation within the loop is noise only. The system response will equal a step input signal after the decay of transients but will have a fixed error for a given ramp-input signal. Errors are present whenever the signal changes. The advantage of zero-steady-state error is gained at the expense of more difficulty in stabilization of the control system.

The general problem of describing control-system behavior in terms of error coefficients has been discussed by Truxal [Ref. 23]. Figure 5.2 shows a single-loop system and the notation to be used for the discussion of error coefficients:  $E(s)$  is the transform of the error signal,  $R(s)$  is the transform of the input signal, and  $G(s)$  is the transfer function of the forward path. The expression

$$E(s)/R(s) = 1/[1+G(s)]$$

when expanded in a Maclauring series, can be written as

$$1/[1+G(s)] = [1/(1+K_p)] + (s/K_v) + (s^2/K_A) + \dots \quad (11)$$

where the  $K_i$  are the error coefficients. When this series expansion is a valid representation of  $E(s)/R(s)$  with only a few terms, then the error coefficients have meaning as follows:

- $K_p$  is inversely proportional to an error depending directly on the signal
- $K_v$  is inversely proportional to an error depending on the derivative of the signal.
- $K_A$  is inversely proportional to an error depending on the second derivative of the signal.

A more useful interpretation, from the viewpoint of radio astronomy, is the relationship between the error coefficients and the moments of

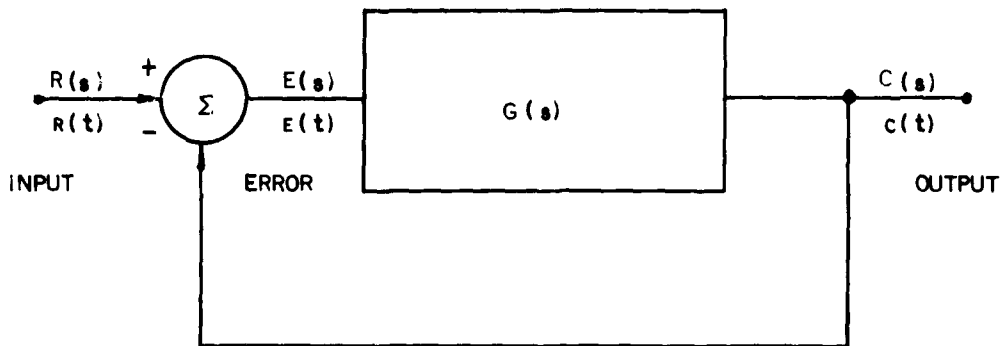


FIG 5.2. SIMPLE SERVO-SYSTEM BLOCK DIAGRAM

the closed-loop response  $h'(t)$  Following Truxal's presentation, we first write the transfer function

$$C(s)/R(s) = G(s)/[1 + G(s)] = 1 - \{1/[1 + G(s)]\}$$

Then, after inserting Eq (11) we have

$$C(s) = [K_p/(1 + K_p)] R(s) - [s R(s)/K_v] - [s^2 R(s)/K_A] - \dots$$

The impulse response  $h'(t)$  will equal  $c(t)$  when  $r(t)$  is an impulse;  $R(s)$  is then unity, so that

$$C(s) = [K_p/(1 + K_p)] - (s/K_v) - (s^2/K_A) - \dots \quad (12)$$

Using the central value theorem we find

$$K_p/(1 + K_p) = C(0) = \int_{-\infty}^{\infty} c(t) dt, \quad (13)$$

which are expressions for the area under the impulse response. When  $K_p$  is infinite the area is unity. Differentiation of Eq. (12) with respect to  $s$  gives

$$C'(s) = - (1/K_V) - (2s/K_A) - \dots$$

From this we can write

$$1/K_V = - C'(0) = \int_{-\infty}^{\infty} t c(t) dt. \quad (14)$$

Thus  $1/K_V$  is the first moment of the impulse response. A second differentiation of Eq. (12) with respect to  $s$  gives

$$C''(s) = - (2/K_A) - \dots$$

From this we can write

$$1/K_A = - C''(0)/2 = \frac{1}{2} \int_{-\infty}^{\infty} t^2 c(t) dt,$$

which shows the relationship between  $K_A$  and the second moment of the impulse response. Similar relations exist for the higher-order moments.

In the next section, data-interpretation problems that can be discussed with the aid of impulse-function moments will be presented. The effect of variations of the moments of the impulse response can be related to the parameters of the control system or receiver through the error coefficients.

#### D. LIMITATIONS

The performance of a Ryle and Vonberg type receiver has been shown to be excellent for the measurement of changes in input level. The advantages of the modulated-signal receiver regarding zero-point stabilization are achieved over the whole range of measurement with no further increase in the minimum detectable signal. The usable integration time is usually set by some observational requirement, so that the effect of the control loop can be included in the original design to insure the desired value for  $\tau$ .

The question of integration time, however, does bring out two features of the Ryle and Vonberg system that must be considered. First, inasmuch

as the loop design is an important factor in determining  $\tau$ , a difficulty arises in regard to readily changing  $\tau$  for different measurements. Second, the value of  $\tau$  that results from a given design is dependent on loop gain. Here then is a characteristic of the receiver that does depend on gain stability.

Up to now the input to the receiver has been considered at a constant level. However, in the discussion of the Ryle and Vonberg type receiver, the behavior with more general signals is an essential consideration.

When a source passes through the antenna pattern, the receiver output has a time-varying level. This output has a band-limited waveform and differs from the true representation of the source distribution because of antenna smoothing and smoothing in the receiver. The effects of receiver smoothing will be considered below. In Fig. 5.3 a typical source observation is presented in terms of spectra and waveforms.

The details of the source distribution have to be determined from the receiver output, with such things as position, angular extent, and total flux of interest. Let us consider position measurements. The position of a signal in time can be described by the time coordinate of its centroid  $\bar{t}$ , defined as

$$\bar{t} = \int_{-\infty}^{\infty} t z(t) dt / \int_{-\infty}^{\infty} z(t) dt$$

relative to an arbitrary zero. The operation of smoothing produces a shift in the abscissa of the centroid, depending on the smoothing function. This process can be described by the following theorem, which is proved in Appendix D.

**THEOREM** The centroid of the signal waveform will be located  $\bar{t}_h$  sec in time before the centroid of the recorded waveform where  $t_h$  is the time coordinate of the centroid of the impulse response of the receiver in relation to its origin or time of impulse.

Using error coefficients, we can write

$$\bar{t}_h = (1 + K_p) / K_p K_v$$

which displays the need for error coefficient stability if position measurements are to be accurately made. The fractional change in  $\bar{t}_h$

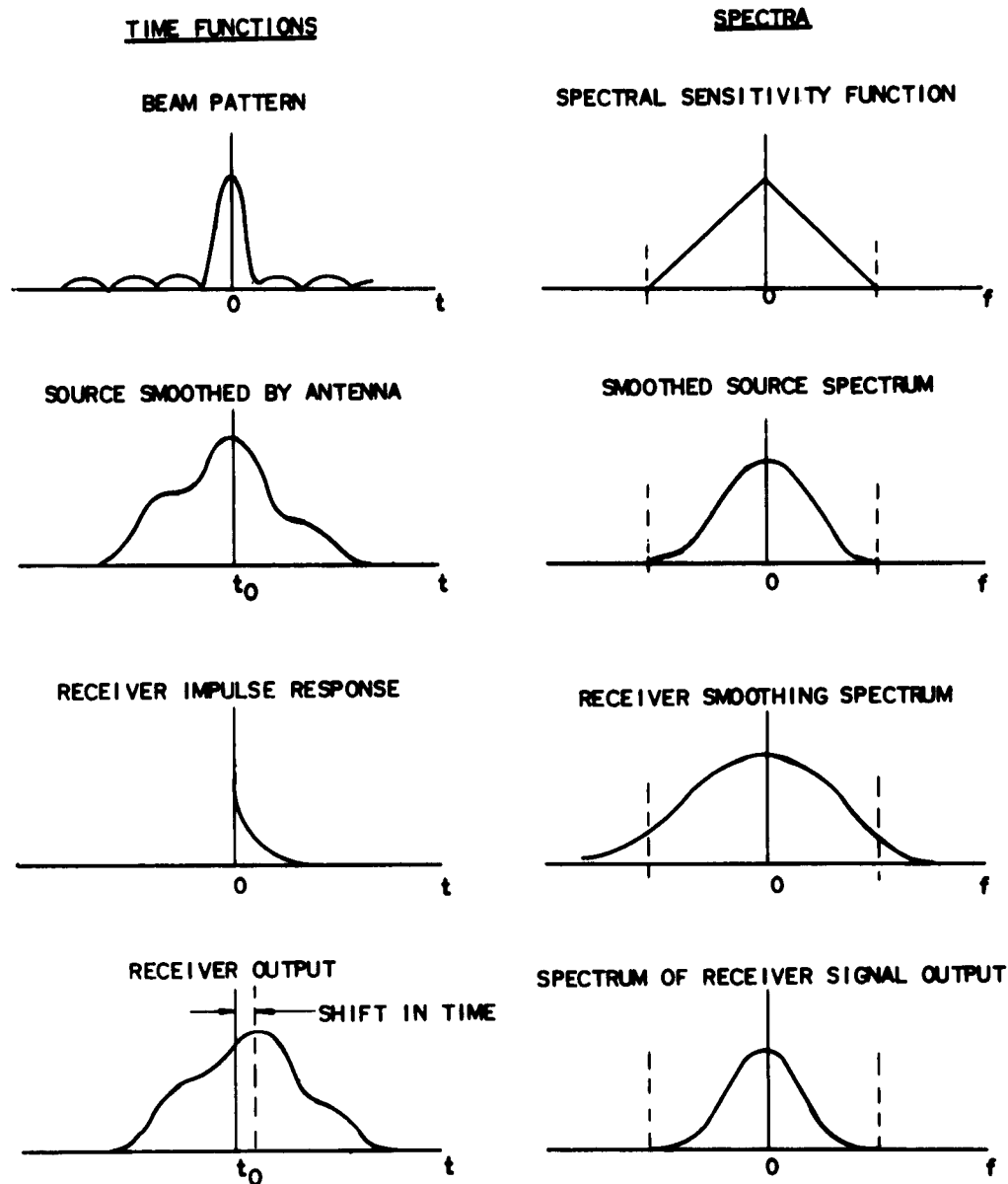


FIG. 5.3 SPECTRA AND TIME FUNCTIONS SHOWING THE TWO SMOOTHING OPERATIONS OCCURING DURING THE OBSERVATION OF A DISCRETE SOURCE.

relative to a fractional change in loop gain  $K$  can be defined as  $S_K$ , an important measure of sensitivity to this effect. Thus

$$S_K = (d \bar{t}_h / dK) \cdot (K / \bar{t}_h) \quad (16)$$

This expression can be evaluated for systems as shown in Fig. 5.2, letting  $G(s) = K F(s)$ , where  $K$  is the loop gain factor. Then

$$C(s) = K F(s) / [1 + K F(s)]$$

$$C(0) = [K F(0)] / [1 + K F(0)]$$

$$C'(s) = [K F'(s)] / [1 + K F(s)]^2$$

and

$$C'(0) = [K F'(0)] / [1 + K F(0)]^2$$

Then, from Eqs. (13), (14) and (15), we can write

$$\begin{aligned} \bar{t}_h &= -C'(0) / C(0) \\ &= -F'(0) / F(0) [1 + K F(0)] \end{aligned}$$

The derivative of  $\bar{t}_h$  with respect to  $K$ ,

$$d\bar{t}_h / dK = F'(0) / [1 + K F(0)]^2$$

Now, substituting into Eq. (16), we have

$$\begin{aligned} S_K &= -K F(0) / [1 + K F(0)] \\ &= -C(0) \end{aligned}$$

Since the null-balancing principle requires  $C(0)$  the d-c gain, to be very nearly unity,  $S_K$  will be the same for any configuration of components in the system.

A general statement for Ryle and Vonberg type receivers is that the accuracy of position measurement depends directly on loop gain stability,

with a 10-percent change in loop gain giving a 10-percent change in the position correction to be applied to account for the receiver smoothing.

Attempts to reduce the absolute error by using smoothing functions with small first moments and hence small  $\bar{t}_h$ 's, will lead to other difficulties associated with negative responses and longer times in which noise can introduce errors.

#### E. SUPPLEMENTARY SMOOTHING FILTERS

By designing rapid response into the receiver, so that the effective integrating time is short compared with those desired for measurement, it is possible to further smooth the output with a filter of the desired characteristics. This supplemental filter can be chosen to be stable and, since it provides the majority of the integration, gain changes do not cause trouble. A second feature is the improved ability to change integration times and smoothing characteristics readily without disturbing the receiver dynamic performance. When special complex smoothing functions are desired, operating on the signal outside the loop is a distinct advantage.

The device which provides the reference noise source will determine the manner in which it is possible to obtain an output signal for further supplementary smoothing. What is advantageous in general is to have no active element subject to instabilities between the signal output and the actual noise-level reference. In the case of the noise diode, the indication of noise is directly and simply related to the noise level and at the same time is an electrical signal that lends itself to supplementary smoothing. The difficulty with the noise diode is the inherent thermal delay in the heater, which may prevent one from achieving very small integrating times.

A ferrite attenuator designed with a linear relationship between noise level and driving signal would be capable of rapid response and have the electrical signal for further smoothing. This attenuator seems to be a desirable controller for the reference noise source.

## VI. STANFORD MICROWAVE-SPECTROHELIOGRAPH RECEIVER

### A. GENERAL REQUIREMENTS

The Stanford microwave-spectroheliograph antenna, described by Bracewell and Swarup [Ref. 24], is a pencil-beam interferometer composed of two, perpendicular, 16-element arrays, phase-switched together to form the multiple pencil beams. The arrays operate between 2700 and 3400 Mc, providing at 3292.1 Mc a half-power beamwidth of 2.3 min by 2.3 deg. Pencil-beams 3.1 by 3.1 min are formed by the complete antenna and, for solar observations, raster scanning is performed so that contour maps of solar-brightness temperature are obtained. Patrol observations on the sun using the east-west array provide one-dimensional scans of brightness every 3 to 5 min over an 8-hr period. Automatic-control equipment for the antenna allows patrol observations to proceed unattended.

The collecting area of the antenna and the transmission-system loss are such that equivalent input temperatures for the receiver will vary from about 200 °K (for cold-sky observation) to several thousands of degrees.

#### 1. Bandwidth and Beamwidth Relationship

Because the antenna is a multiple-element interferometer, the reception-filter bandwidth must be limited if a narrow beam is to be maintained in directions making a large angle  $q$  as measured from a plane perpendicular to the array. The nature of this beam broadening due to receiver bandwidth can be understood as follows. The field originating in a source with a flat power spectrum (or nearly so) in the frequency range of interest and incident on the antenna can be described over periods smaller than the reciprocal reception-filter bandwidth by a single frequency and amplitude of oscillation. During such an interval the antenna pattern is that given by monochromatic theory and an output contribution is produced from a point source according to its position relative to the particular monochromatic beam formed. Over long periods the detected power spectrum from the source is related to the power-transfer characteristic  $G(f)$  of the receiver. Each frequency  $\delta f$ , defined as  $f - f_0$ , produces a beam at a different angle around  $q_0$  defined by the central frequency  $f_0$  and an order-of-interference number  $m$ . We have

$$\sin q_0 = m\lambda/d = m c/d f$$

and

$$\delta q_0 = m c \delta f / d(\cos q_0) f_0^2$$

The distribution of beams around  $q_0$  is weighted according to the function  $G(\delta f)$  expressed in terms of  $\delta q$  using the relation above. If we call this  $G(\delta q)$  and use the antenna response around  $q_0$  [Ref. 25]

$$P(\delta q) = \frac{\sin N\pi d(\cos q_0) \delta q / \lambda}{(\pi d / \lambda)(\cos q_0) \delta q}$$

the effect of bandwidth broadening is described by the relation

$$P'(\delta q) = P(\delta q) * G(\delta q) \quad (17)$$

This convolution of the two functions describes the way in which the various contributions from different frequencies are combined to produce a resultant beam  $P'(\delta q)$ . Instead of using the half-power width of both  $P(\delta q)$  and  $G(\delta q)$  as parameters, one can achieve an advantage by introducing the ratio of the half-power width of  $G(\delta q)$ ,  $w_{G, 1/2}$ , to  $\phi_c$  the peculiar interval\* for the antenna. Since both of these functions vary with  $q$ , their ratio

$$W = \frac{w_{G, 1/2}}{\phi_c} = 16 \kappa m \delta f / f$$

where

$\kappa = 1$  for the cross

$= 2$  for an array

and where  $\delta f$  is the half-power width of  $G(f)$ . Equation (17) has been solved numerically to obtain the resultant beam half-power width. These results appear in Fig. 6.1 for a single array and the cross with both a rectangular and a single-tuned-response form for  $G(f)$ . The single-tuned

---

\*The peculiar interval  $\phi_c = \lambda / 16d \cos q$  for the cross and  $\lambda / 32d \cos q$  for a single array and is the reciprocal of twice the highest spatial frequency to which the antenna responds.

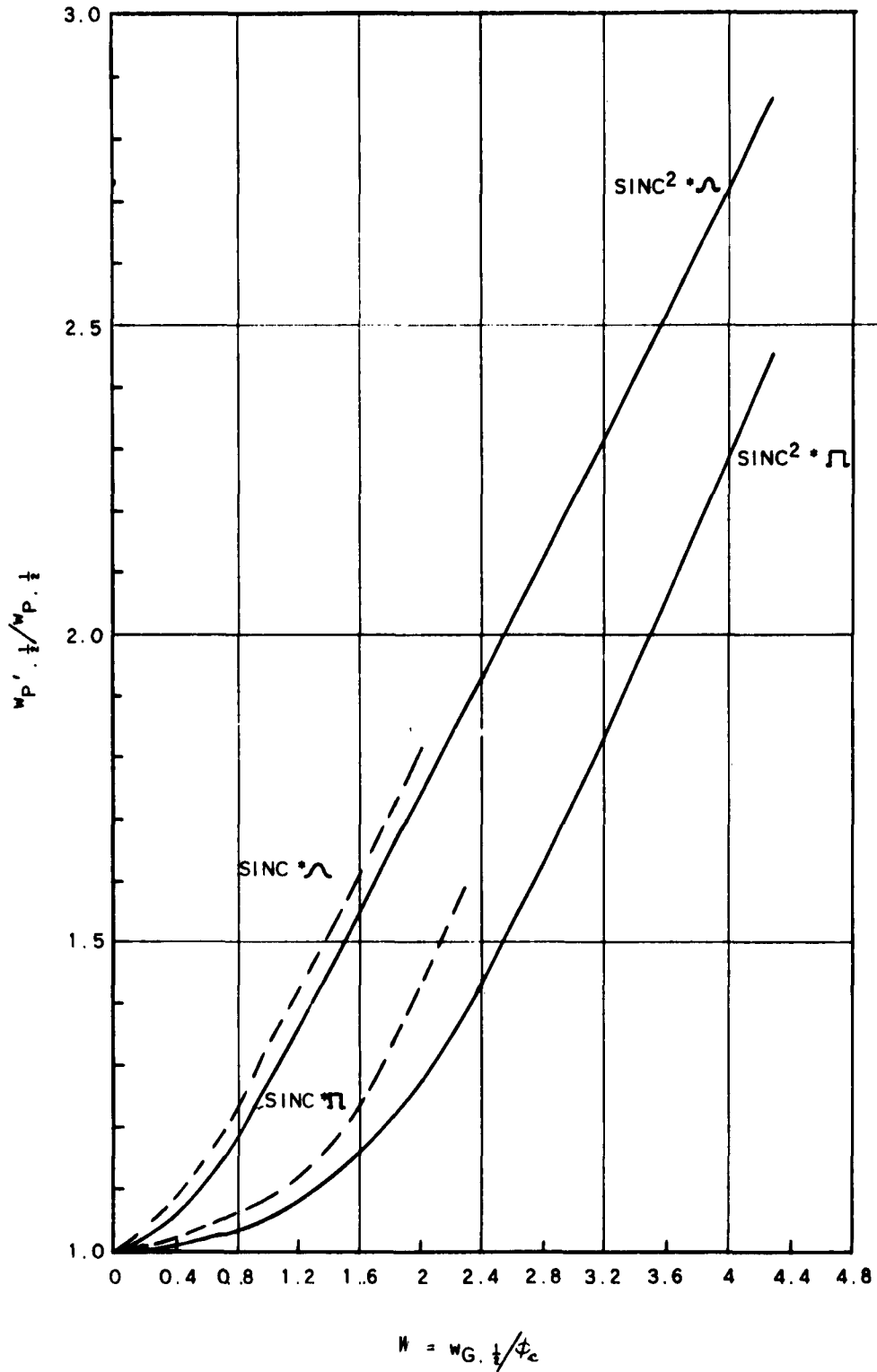


FIG 6.1 RELATIVE BEAM BROADENING DUE TO CONVOLUTION WITH RECTANGULAR AND SINGLE TUNED CIRCUIT POWER RESPONSE FUNCTIONS.

response results in a wider beam than the rectangular response. The theoretical half-power beamwidths for a single array and the cross have been plotted in Figs. 6.2 and 6.3 including the  $1/\cos q_0$  factor. Several reception-filter widths available in the receiver are shown to indicate the expected beamwidth for high-order interference numbers. For solar mapping with the cross, use of the 0.5-Mc bandwidth out to the  $m = 20$  response results in less than 5 percent broadening and less than 10 percent broadening out to the  $m = 30$  response.

## 2. Temporal Response of Receiver

The temporal response of the receiver as limited by the smoothing filter must be fast enough so that source-distribution information is not lost during scanning observations. The maximum-frequency component at the output of the receiver related to the source distribution is determined by the upper limit of the spectral-sensitivity function (SSF) for the radiotelescope and the scanning rate. If  $s_h$  is the highest spatial frequency in the SSF in cycles/radian and the scanning rate is  $\Omega$  radians/sec, the highest frequency out of the receiver will be

$$f_h = s_h \Omega$$

For the cross,  $f_h$  is 0.0488 cps and for the east-west array, 0.0976 cps with the earth's rotation. Consequently, the frequency and phase response of the smoothing filter at these frequencies must be such as to produce negligible distortion. The sampling theorem applied to the above outputs requires samples every 10.2 sec and 5.1 sec respectively.

## 3. Accuracy

The bandwidth and response-time requirements given above lead to a minimum level-uncertainty figure  $U_L$  for the radiotelescope. Allowing an integrating time ( $\tau$ ) of 0.5 Mc, we obtain

$$U_L = 1/\sqrt{\tau \Delta f} = 0.63 \times 10^{-3}$$

If we set a limit of 1 percent accuracy on measurements a 1-percent change in temperature should be detectable. For the 200 °K-sky case, this means a 2 °K minimum detectable signal. The product of modifying factor M and system equivalent noise temperature then must be given by the basic equation (rearranged)

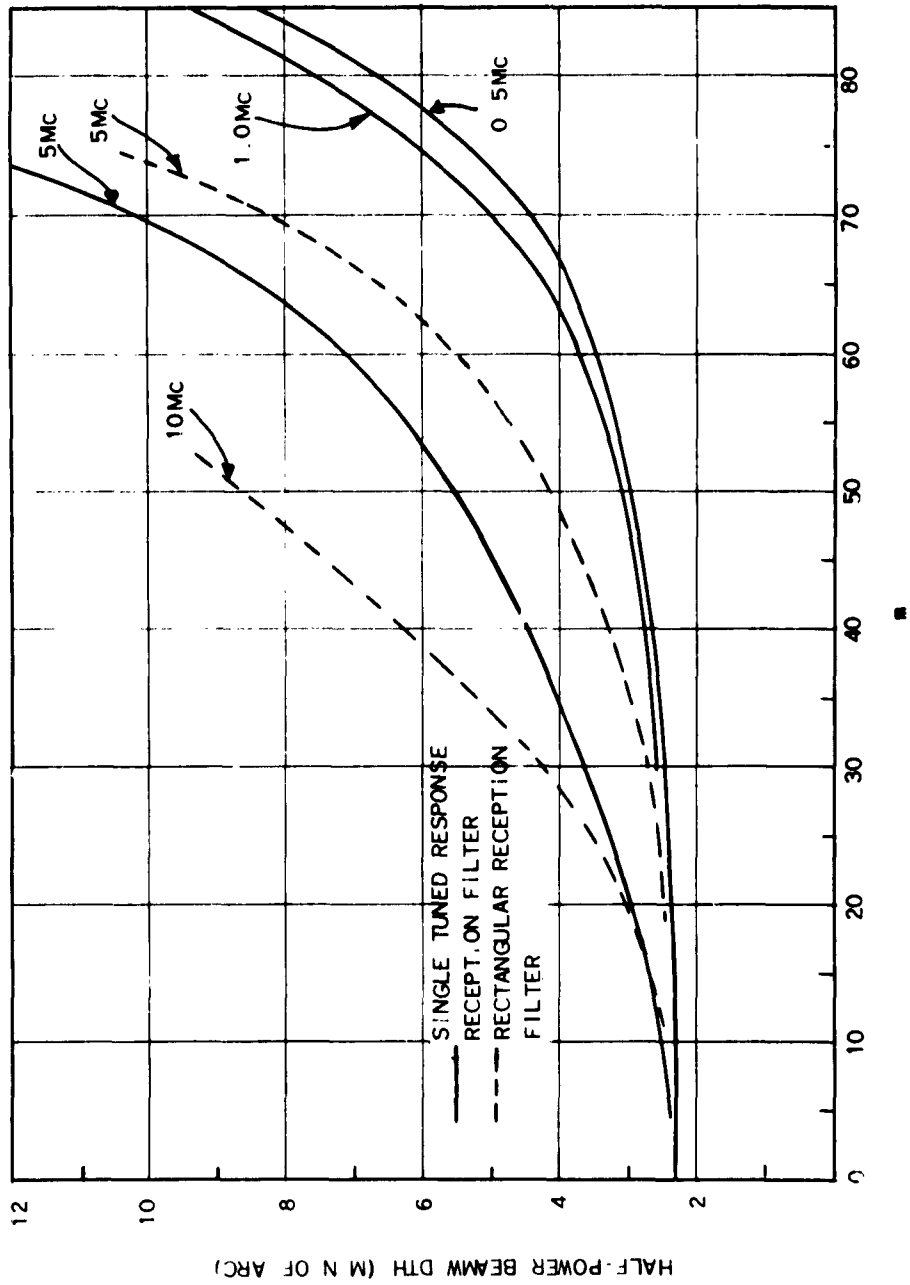


FIG 6 2 HALF-POWER BEAMWIDTH FOR A SINGLE ARRAY VS ORDER OF INTERFERENCE  $m$ , WITH VARIOUS RECEPTION-FILTER HALF-POWER WIDTHS

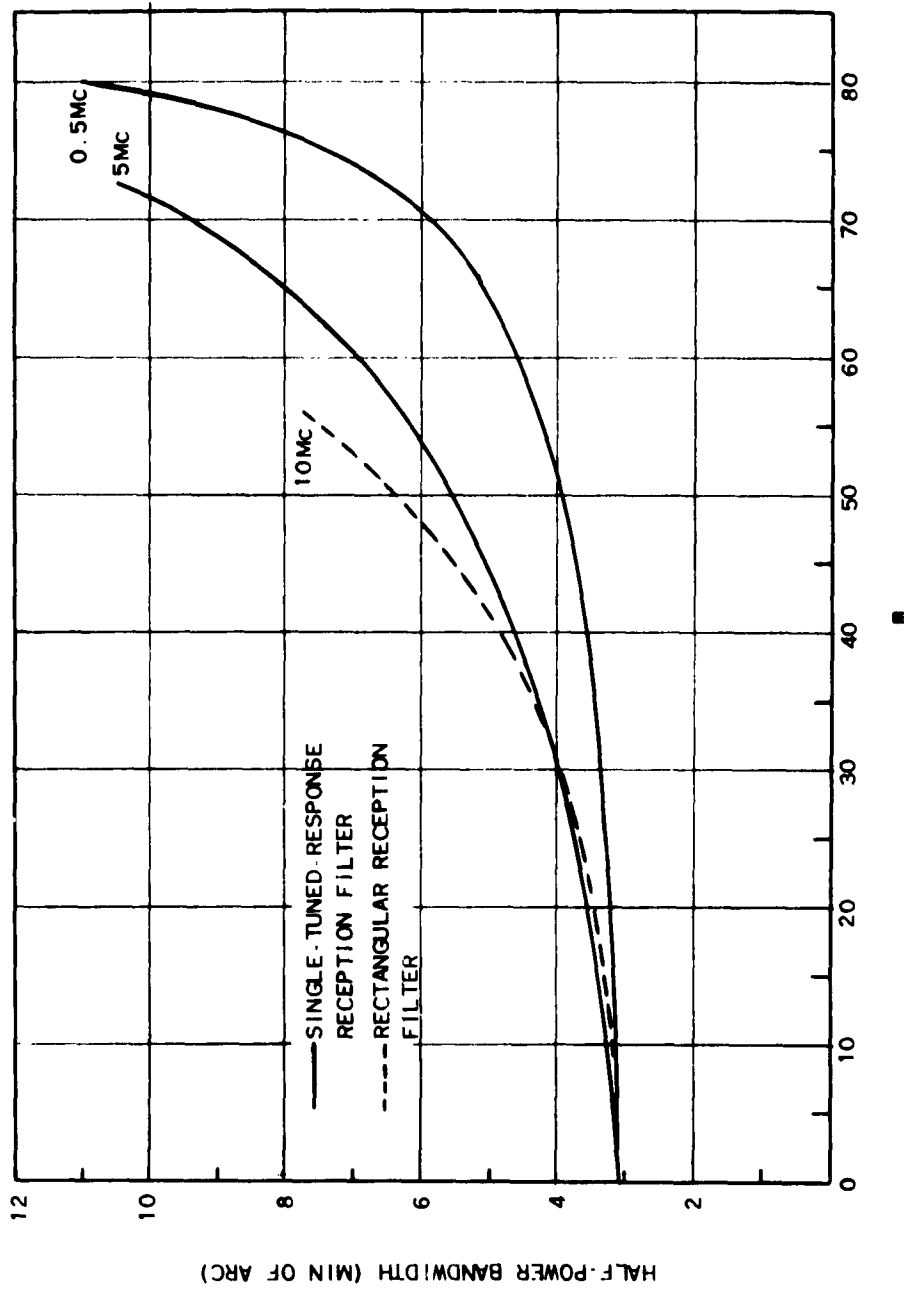


FIG. 6.3 HALF-POWER BANDWIDTH FOR THE CROSS ANTENNA VS. ORDER OF INTERFERENCE  $m$ , WITH VARIOUS RECEPTION-FILTER HALF-POWER WIDTHS.

$$MT_{e_s} = \Delta T/U_L = 3170^\circ\text{K}$$

For an ideal modulated-signal receiver with  $M = 2$ ,  $T_{e_s}$  must be on the order of  $1580^\circ\text{K}$  in order to satisfy the above requirements. The system used has a  $T_{e_s}$  of  $1800^\circ\text{K}$  and thus is satisfactory from this viewpoint.

## B DESCRIPTION OF THE RECEIVER

### 1 General

The solar observational receiver at Heliopolis on the Stanford University campus is shown in block diagram form in Fig. 6.4. It operates with a single array as a modulated-signal (Dicke) type receiver or as a phase switched receiver using both arrays. Provision has been made for calibration from a gas-discharge noise source up to  $2000^\circ\text{K}$  using a neon tube. A superheterodyne, high-frequency section with image rejection is fed by a traveling-wave amplifier that sets the effective receiver-noise temperature  $T_{er}$  and allows noncritical operation and adjustment of the image-rejection filter and mixer. The low-side local-oscillator signal comes from a reflex klystron operating in an oil bath with regulated supply voltages. Its frequency is adjusted so that the 0.5-Mc bandwidth of the i-f amplifier accepts the desired signal frequency of 3292.1 Mc. The wider bandwidths provided are symmetrically oriented about the narrow-band center.

From the mixer the signal passes through a 10-Mc wide, 90-db gain, i-f amplifier and then through a 0-20-db step attenuator before entering the narrow-band filter. The filter consists of a single-tuned circuit with coupling, trimmer capacitors, and resistive loading changed by a switch as different bandwidths are selected.

An infinite-impedance detector operated at low signal levels is used that closely approximates square-law operation. A disadvantage of this detector, however, is the necessity of balancing out the static d-c component of the output in order to observe the small changes due to signal. Consequently, total-power-receiver operation, which as an auxiliary feature is useful, requires the addition of external equipment.

After detection, the signal passes through a phase-shift network so that the relative phase of the signal as compared with the demodulation waveform can be adjusted to zero. A single-tuned LC amplifier stage, 40-cps wide at 465 cps (the modulation frequency) emphasizes the fundamental frequency component before further amplification and phase splitting.

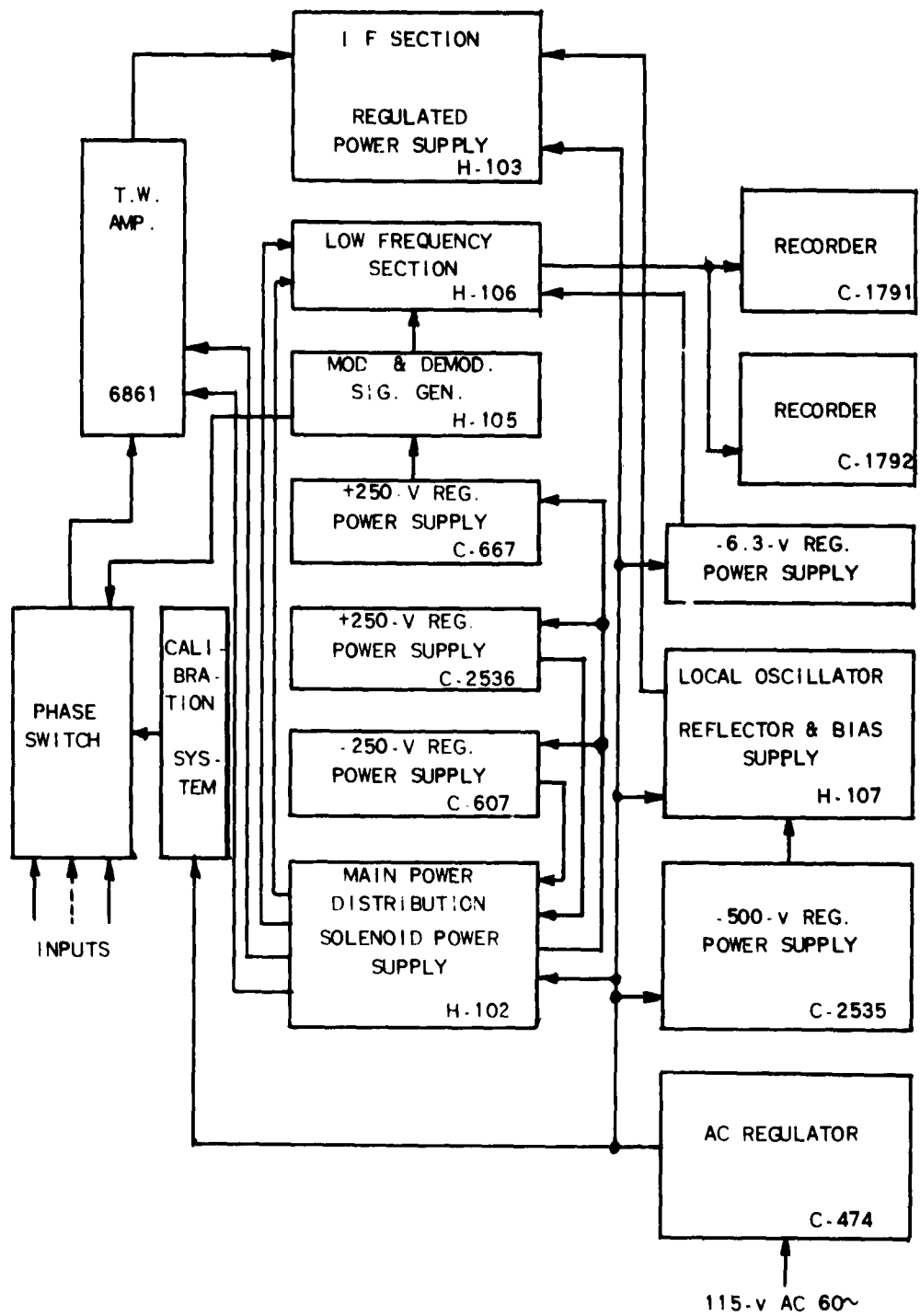


FIG 6 4 BLOCK DIAGRAM OF THE CROSS RECEIVER

occurs. The gain through this section is adjustable in two decades of nominal values (i.e., 0, 10, 20, ..., 100 and 100, 200, 300, ..., 1000).

The coherent demodulator accepts a balanced-signal input that is transmitted or shunted to ground depending on the state of two pairs of triodes connected back to back. The balanced demodulation input square wave drives the common grids of each pair to provide the switching action. The single ended output feeds the smoothing filter, which is a single section RC low-pass network loaded only by a cathode follower. A second cathode follower with an adjustable grid voltage provides a zero balance control for the potentiometer type recorder connected between the cathodes.

An adjustment of recorder deflection is provided with a continuous control followed by an accurate step potentiometer with 1.5 db steps of voltage into the 100 0 - 100 mv recorder.

## 2 Input Circuitry

Two types of observation performed at Heliopolis are the one-dimensional scanning obtained from a single array and the two-dimensional scanning obtained by phase switching the two arrays.

An input system has been developed that allows both of these observations to be performed with only a simple change in input waveguides. For phase-switched operation, the waveguide transmission lines from the two arrays terminate at a colinear pair of ports of a matched hybrid-tee junction. One of the side ports will provide the sum of the voltages from the two arrays and the other port will provide the difference. Now if the phase length of one of the array signal paths is changed by 180 deg. the outputs of the two side ports will be exchanged. Thus, at either side port, the signal changes from a sum to a difference or vice-versa when the phase length of one input is changed by 180 deg. The input circuit is diagrammed in Fig. 6 5.

A two-port device whose phase length changes by the required 180 deg at a frequency of 465 cps is the key component. The design and construction of this device using varactor diodes resulted in an efficient and reliable phase switch that is readily driven at 465 cps and that is capable of operation at much higher frequencies.

The input and output of the variable-phase element are the colinear ports of a matched hybrid tee junction. The side ports are connected to shorted sections of waveguide, each containing a varactor diode. When these sections are properly adjusted for one condition of the diodes

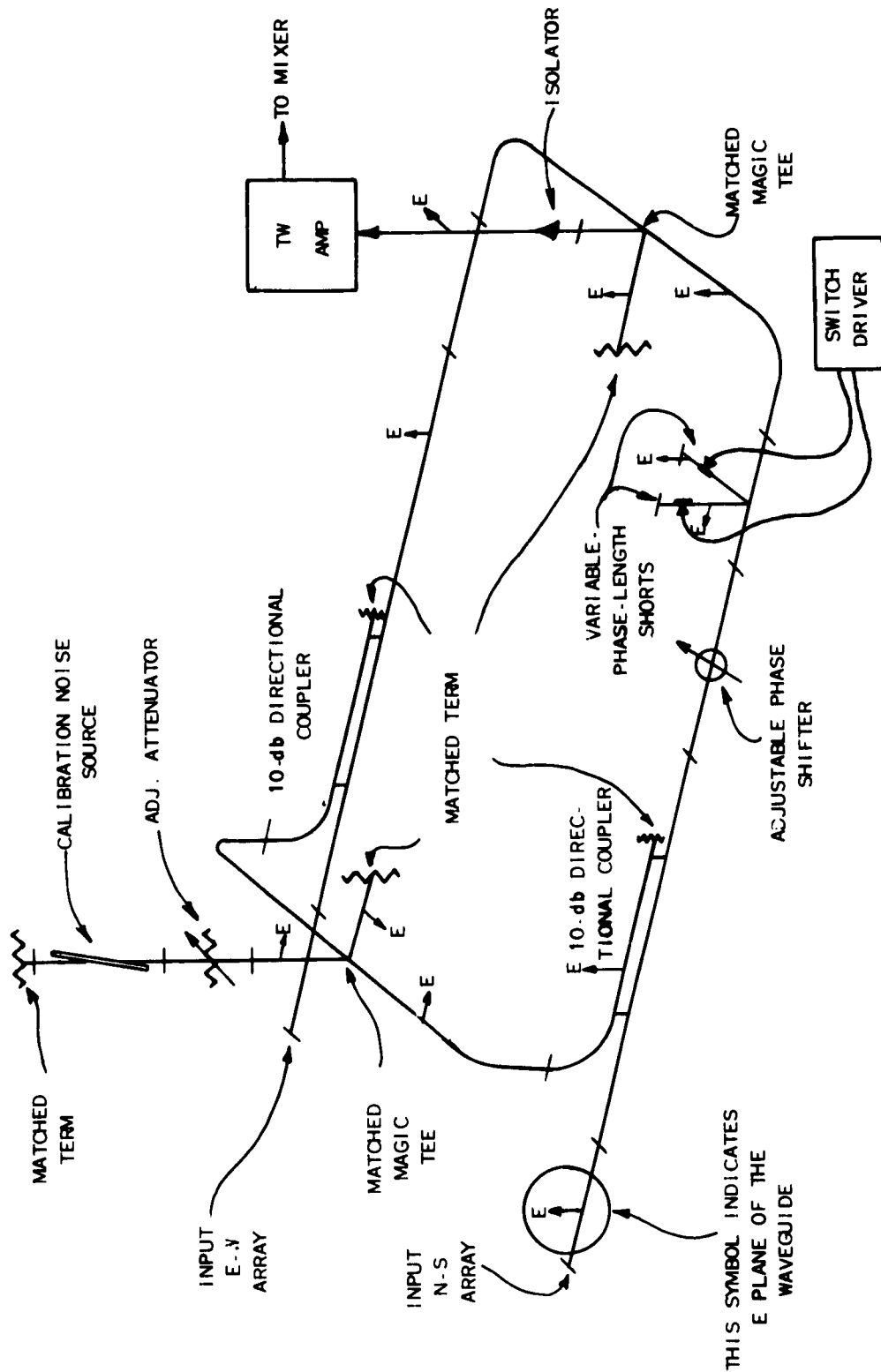


FIG. 6.5 DIAGRAM OF THE PHASE SWITCH FOR CROSS OPERATION.

the signal that enters the hybrid junction is divided between the two side arms, is reflected after traveling a certain phase length, and is then recombined in proper phase to proceed through the output port. When the diodes are in the opposite bias condition, the shorted sections appear a quarter-wavelength longer and hence a total phase length of 180 deg is added to the signal.

With careful construction and adjustment of the switch, the simultaneous amplitude modulation is negligible and the insertion loss less than 0.8 db. Since the variable phase element appears in one input line only, the switch-insertion loss in db is effectively only one half that of the element itself. A detailed description of the side-port shorting sections shown in Fig. 6.6 is given in Appendix E.

When single-array operation is desired, a waveguide section as shown in Fig. 6.7 is connected to the phase-switch inputs. The additional matched hybrid tee junction provides sum and difference outputs composed of antenna and reference source contributions. The action of the phase switch on these inputs is to yield either the antenna contribution or the reference-source contribution at the output for the two phase switch conditions. The result is a switching of the receiver input between the antenna and the reference source and consequently square-wave modulation of the antenna signal.

Included in the input circuitry shown in Fig. 6.5 is the calibration system. A high-directivity, 10-db, directional coupler is inserted in each input and these are fed from a single gas-discharge noise source whose output is attenuated and divided by a matched-hybrid-tee junction. This hybrid junction is important because it gives additional isolation between inputs for any signal which tends to couple through the calibration system. When properly connected, the known calibration signal from the noise source appears at the traveling-wave tube input in proper phase to provide the same-polarity output deflection as the antenna signal when the microwave switch configuration is in use.

### 3 R-F and I-F Sections

The output of the phase switch is connected to the traveling-wave amplifier through an isolator to minimize any effects of impedance modulation produced by the phase switch. An RCA 6861 low-noise traveling-wave tube (TWT) provides 23 db of gain with an effective noise temperature of 1200 °K. This tube has given excellent service, being in continuous operation for over 20,000 hr. The operating voltages for the TWT are

	MOUNT	
	No.	No.
A	8.8	6
B	5.9	1.9
C	5.7	5.5
D	3.4	3.2
	..E..	..H..

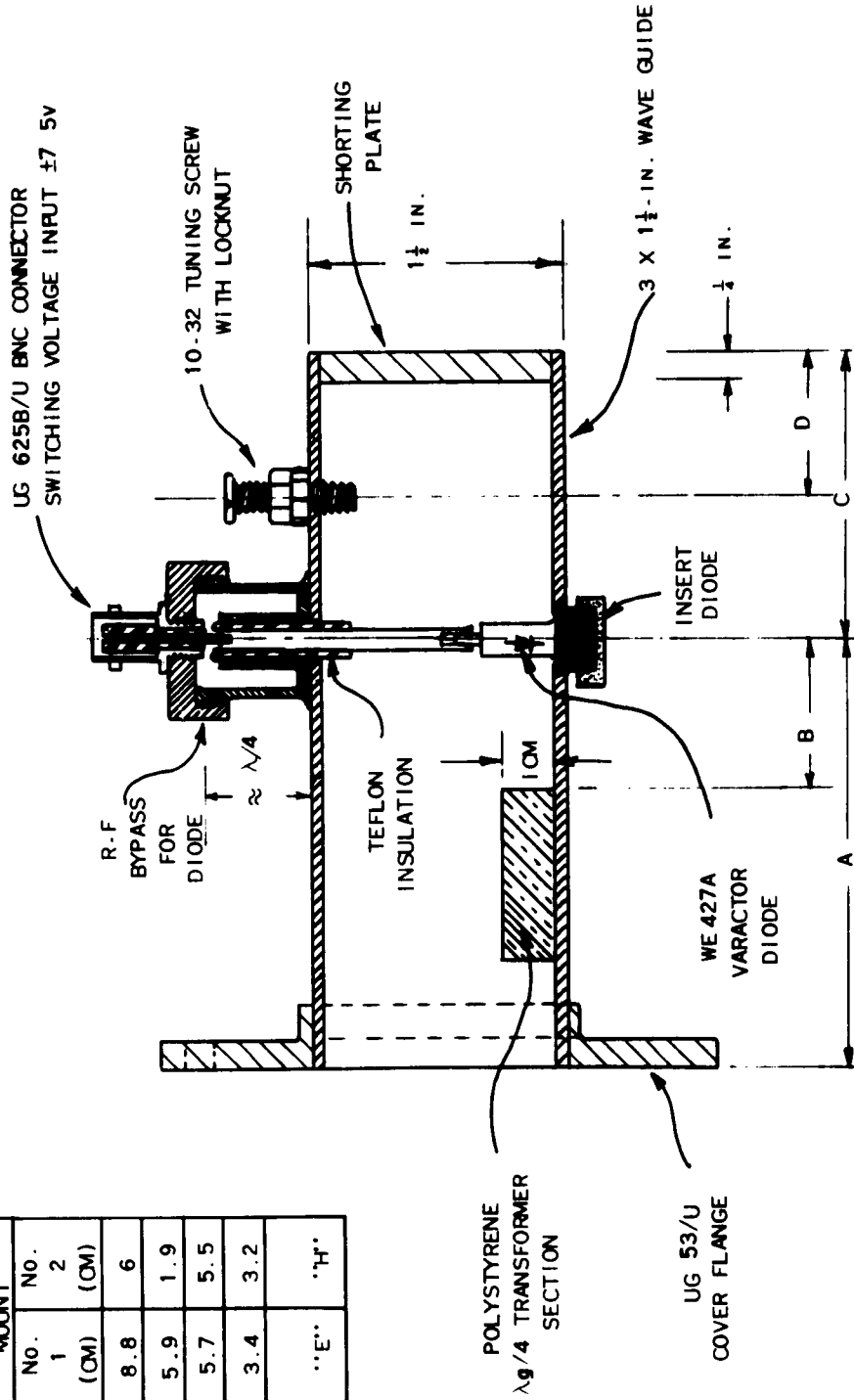


FIG. 6.6 VARIABLE PHASE LENGTH SHORTS FOR PHASE SWITCH. (CROSS SECTION ALONG CENTER-LINE OF GUIDE.)

obtained from an adjustable-tap resistive divider across the regulated  $\pm 250$  v supplies to allow the setting of voltages for optimum noise-temperature operation. For protection, the TWT voltages are controlled by a relay that senses the solenoid voltage, thus insuring a properly focused beam

From the traveling-wave amplifier (Fig. 6.8) the signal passes through the image-rejection filter. Over 20-db rejection of the image 120 Mc away from the signal is obtained with a re-entrant quarter-wave transmission filter. From this filter the signal goes on to the coaxial-line mixer. The local oscillator is a 2K42 reflex klystron operating at 3232.1 Mc. The necessary frequency stability is achieved through regulated supply voltages, an oil bath, and a high-Q transmission cavity coupled to the klystron output. Because the i f amplifier has a d-c path to ground at its input, a d-c block is used following the mixer to allow the mixer current of 0.6 ma to be monitored. A sample of the local-oscillator power into the mixer is detected and applied to a meter as a means of checking frequency. A daily check and adjustment of the reflector voltage to peak this meter when necessary assures the proper operating frequency.

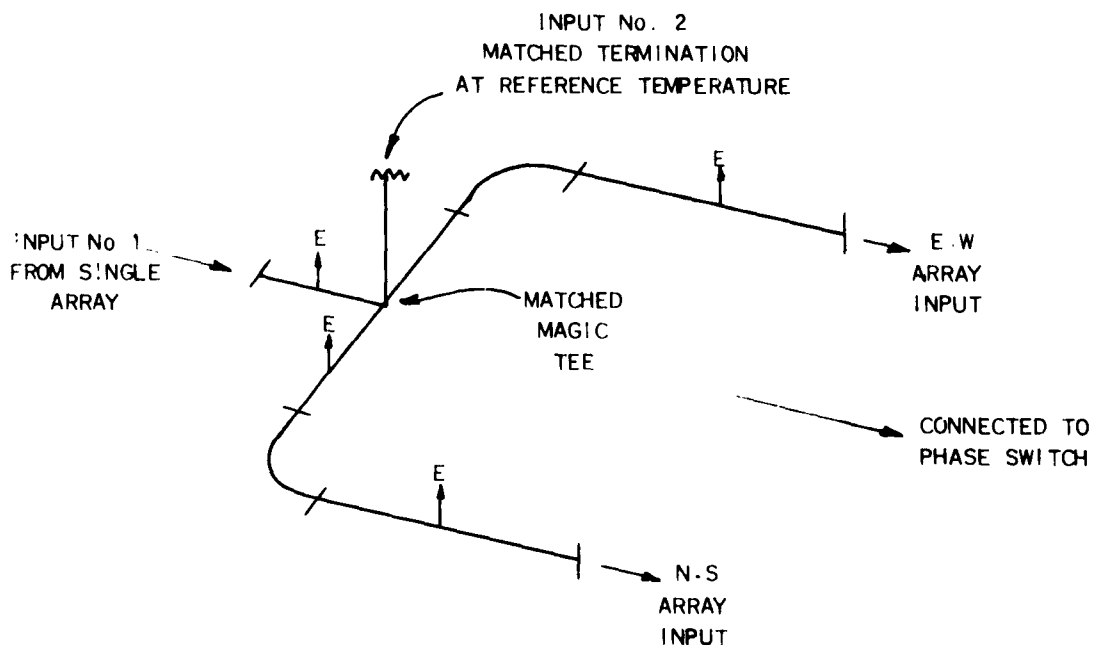


FIG. 6.7 ADDITION TO THE PHASE SWITCH WHICH PRODUCES A DOUBLE-THROW MICROWAVE SWITCH.

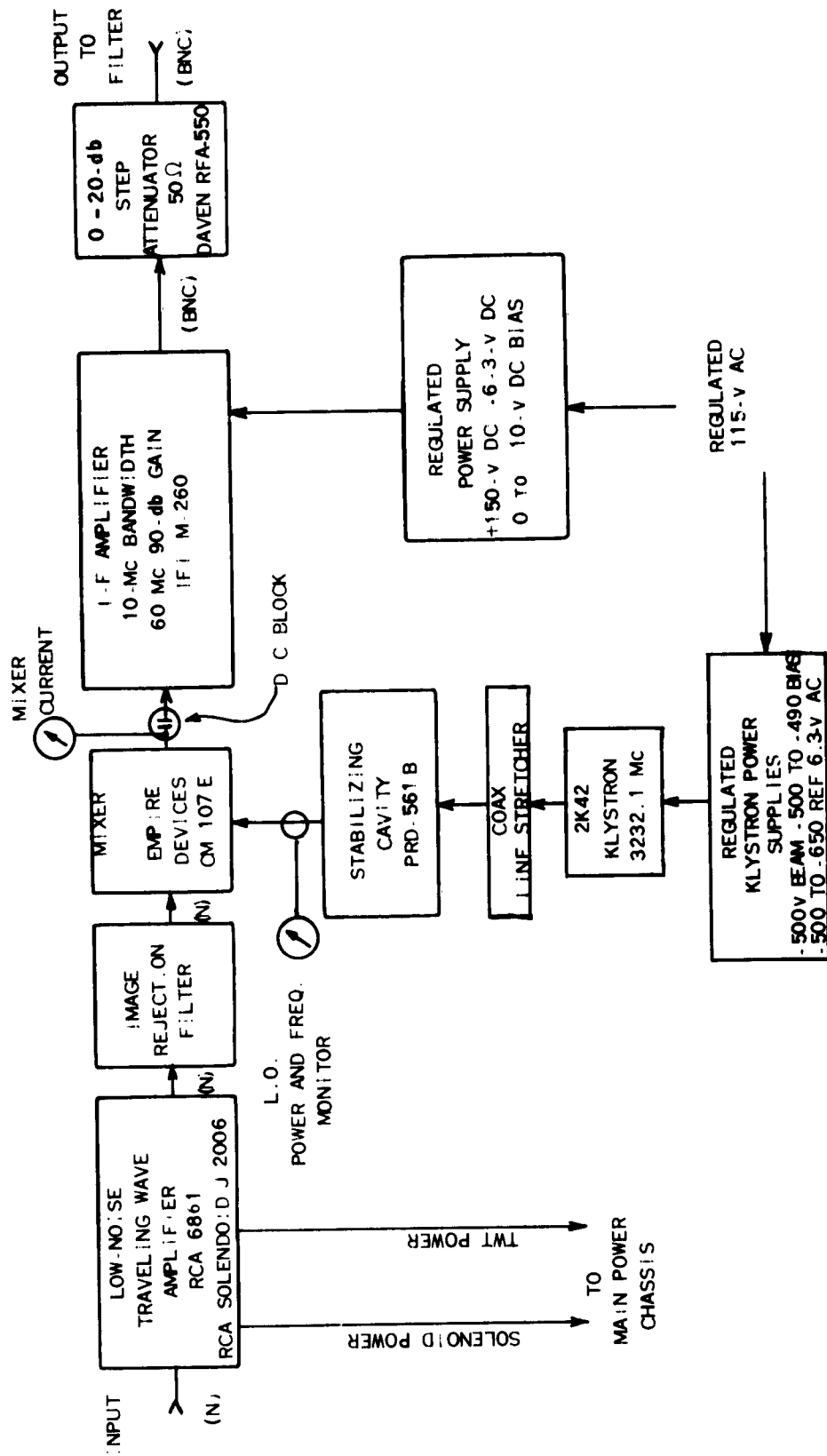


FIG. 6 8 BLOCK DIAGRAM OF R-F AND I-F SECTIONS OF RECEIVER .

The 60-Mc i-f amplifier is an unmodified commercial unit with 10-Mc bandwidth and is normally operated at maximum gain. The attenuator following the i-f amplifier has a range of 0 to 20 db in 1-db steps and is useful for performance checks as well as providing i-f gain control.

Because of bandwidth effects on the antenna pattern as discussed above, a range of bandwidths (0.5, 2.5, 5, and 10 Mc) is provided. The i-f amplifier output at a 10-Mc bandwidth is coupled into a single-tuned circuit adjusted to the desired 3-db bandwidth through resistive loading. A bandswitch changes coupling, trimming capacitors, and loading resistors as necessary. A cathode follower transfers the signal from this filter circuit to the detector.

#### 4. Detector and Low-Frequency Section

The receiver depends on square-law detection for proper operation. The infinite-impedance detector circuit, when operated with small signals, has a satisfactory square-law response, as demonstrated by the graph of Fig. 6.9, which is an over-all calibration-response curve for the receiver from input to output and has less than 1-percent rms error as measured from a best-fit straight line.

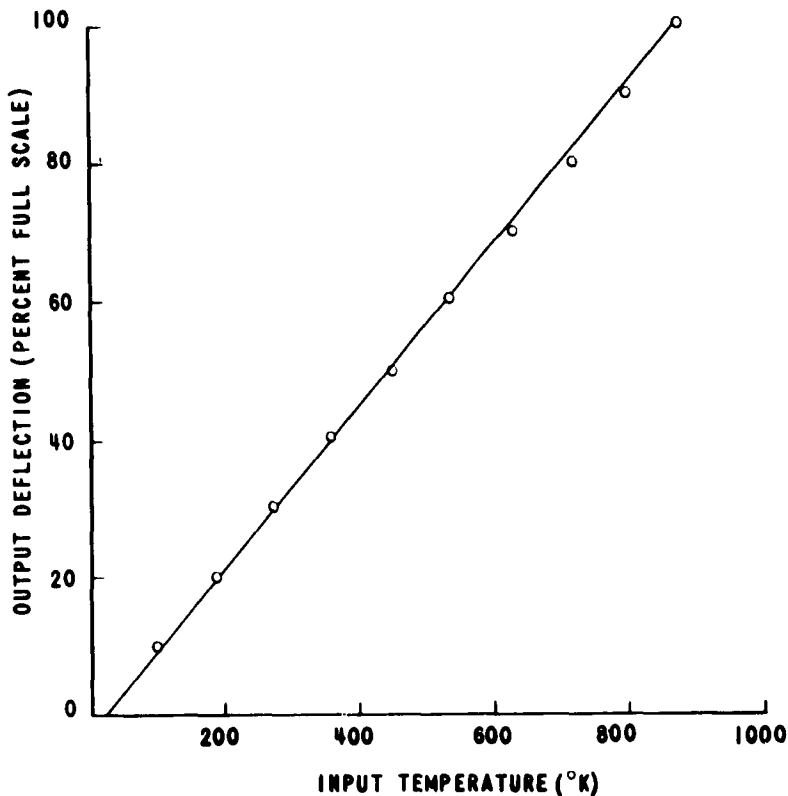


FIG. 6.9 POWER RESPONSE CURVE FOR THE COMPLETE RECEIVER. THE RMS DEPARTURE FROM A STRAIGHT LINE IS LESS THAN 1 PERCENT.

After detection, as shown in Fig. 6.10, the signal passes through a variable-phase-shift network which is set for maximum receiver output with a standard calibration signal. With the square-wave modulating-waveform generator used, no adjustment of the phase of the demodulating waveform can be made; hence this must be done in the signal channel.

A single-tuned LC amplifier follows the phase shifter with a bandwidth of 40 cps. This filtering sufficiently reduces the noise power that must be handled by the low-frequency amplifiers and coherent demodulator to avoid saturation problems on noise peaks. The bandwidth is not so narrow, however, that slight frequency drifts of the modulating-signal generator result in undue phase shifts and consequent output fluctuations.

Further amplification is provided by two RC-coupled stages. These have voltage dividers providing a range of gains from 10 through 1000. The coherent demodulator requires a balanced input which is obtained with a phase-splitting circuit.

#### 5. Demodulation and Output Sections

The coherent demodulator is a realization of the switching circuit shown in Fig. 6.11(a) by the vacuum-tube circuit (b).<sup>\*</sup> For zero input the d-c output is but a few millivolts and stable, so that satisfactory compensation can be made with the zero set control of the cathode-follower pair driving the recorder. The output impedance for the demodulator is high, so that the smoothing filter must necessarily also be high impedance and require the use of cathode followers to drive recorders and output meters satisfactorily.

The smoothing filters provided have the characteristics shown with the circuit diagram in Fig. 6.12. The recorder used may add a substantial amount of smoothing so that observations made where there is a question as to smoothing effects should include specific measurements for determining the over-all smoothing present. Impulse-response checks or frequency-response measurements may both prove of value in such cases.

The cathode followers mentioned above are connected as shown in the schematic in Fig. 6.13. Both impedance-matching and zero-set functions are present in this circuit. A mercury cell furnishes the grid

---

<sup>\*</sup>This circuit is an adaptation of one originating in the Radiophysics section of C.S.I.R.O. Sydney, Australia.

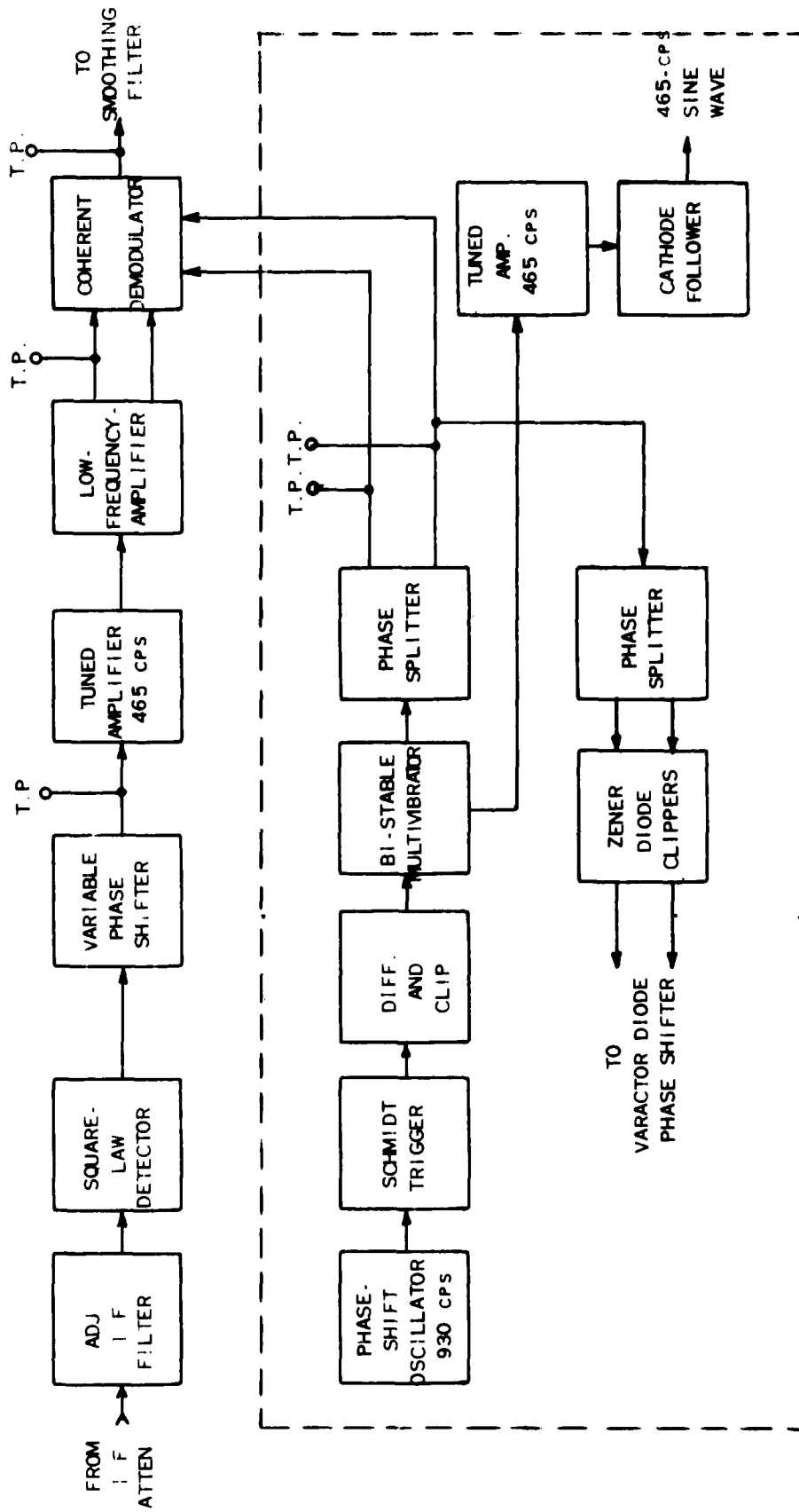
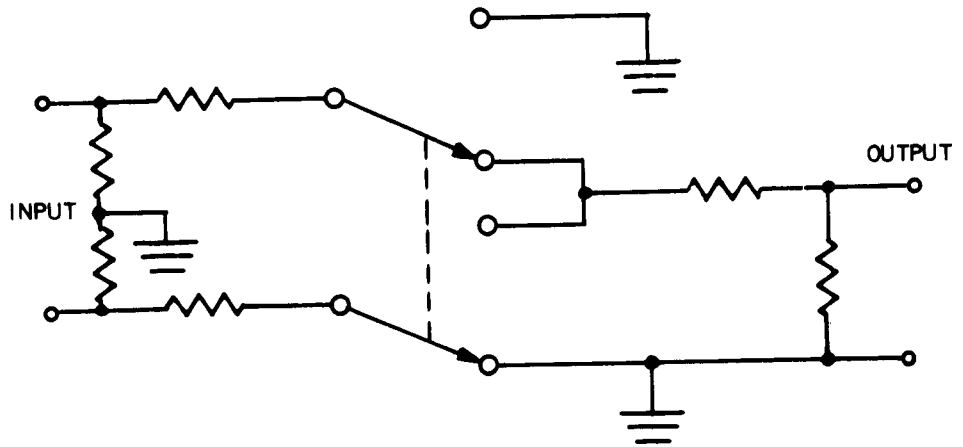
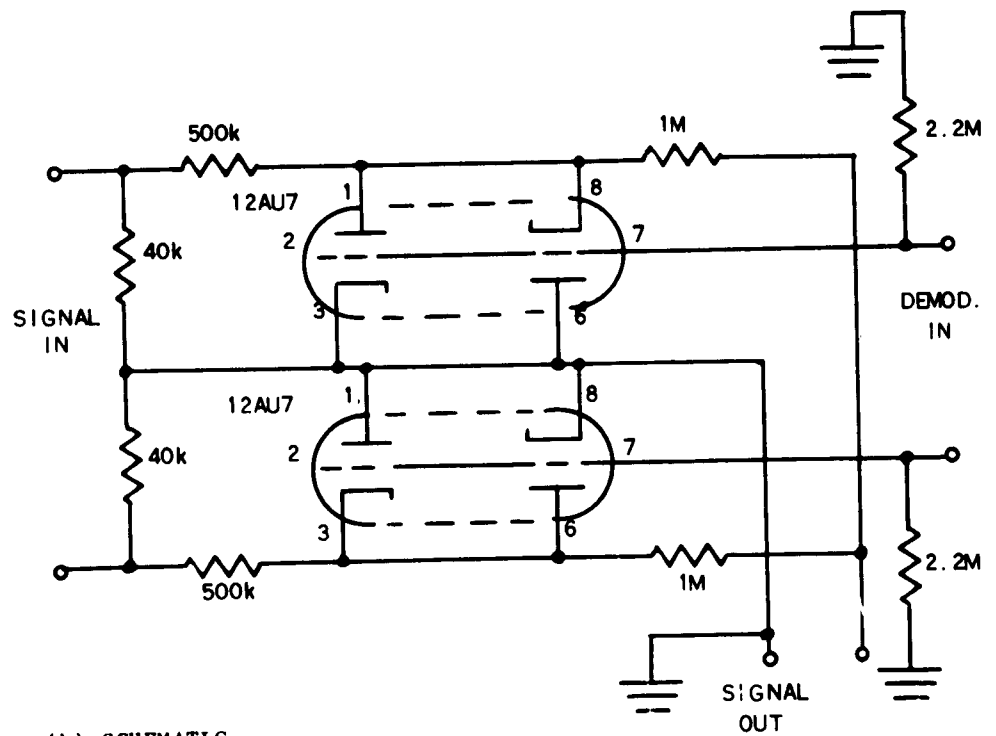


FIG. 6.10 BLOCK DIAGRAM OF RECEIVER FROM I-F ATTENUATOR THROUGH THE COHERENT DEMODULATOR, INCLUDING MODULATION AND DE-MODULATION SIGNAL GENERATOR BLOCKS WITHIN DASHED LINE SUPPLIED FROM SEPARATE +250-V SOURCE.



(a) SWITCHING-CIRCUIT REPRESENTATION



(b) SCHEMATIC

FIG 6.11 COHERENT DEMODULATOR.

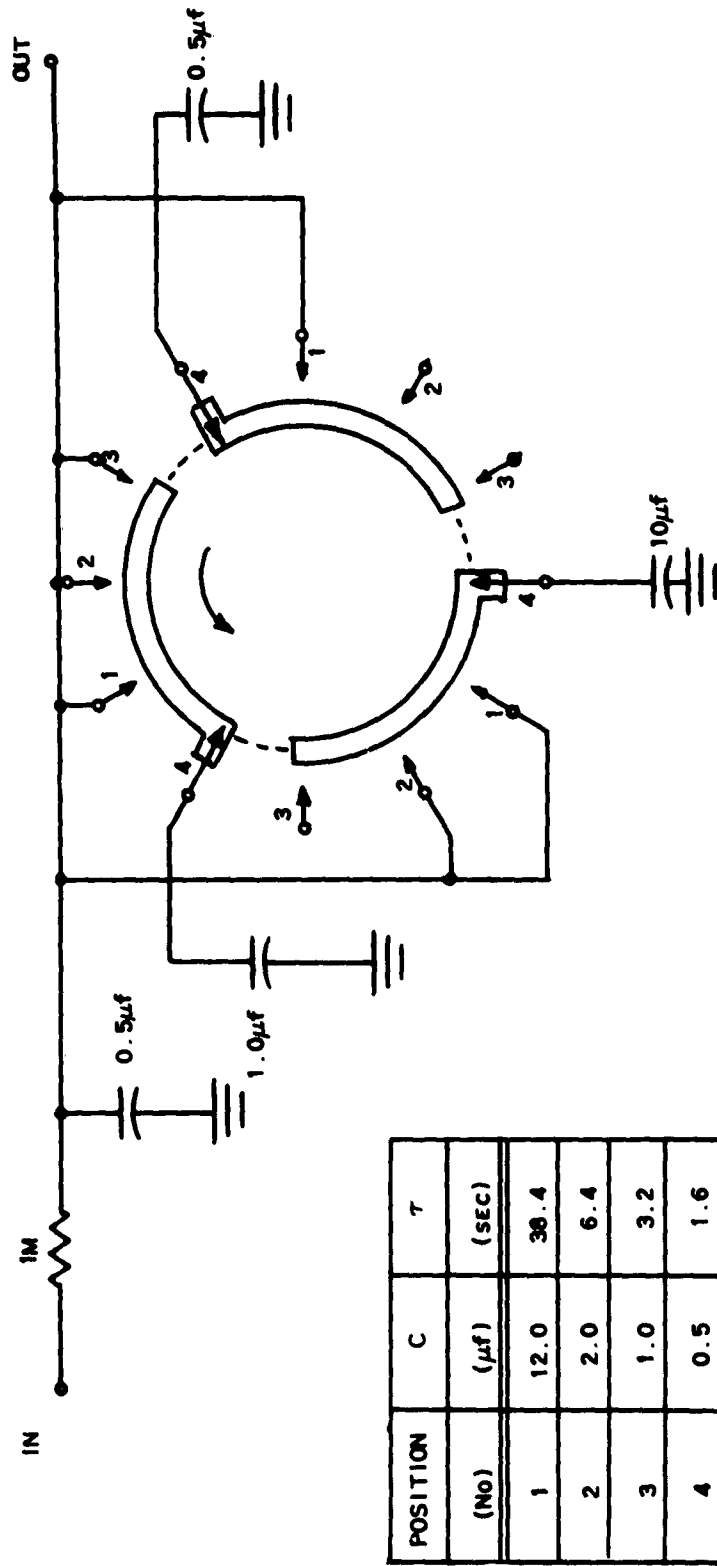


FIG. 6.12 SMOOTHING-FILTER SWITCHING AND INTEGRATING TIMES.

voltage for zero setting with a lifetime of about 60 days. In normal operation, a 100 0-100 microammeter and two 100-0-100-mv recorders are operated in parallel between the cathodes.

One recorder has a slow chart speed (1.5 in./hr) for use as a log of receiver operation. The second recorder produces the analog output of observations and has an adjustable attenuator for calibration and standardization of records. A continuous potentiometer followed by an accurate step potentiometer makes up this attenuator. Since the self-balancing-potentiometer, recorder-input impedance at balance is very high, loading of the final attenuator is very small and its accuracy is maintained.

#### 6. Auxiliary Apparatus

Power is supplied from the 115-v 60-cycle lines through an electronic regulator that furnishes a constant rms value of voltage. The receiver has regulated d-c supplies for -650, -500, -250, -6.3, and +250v.

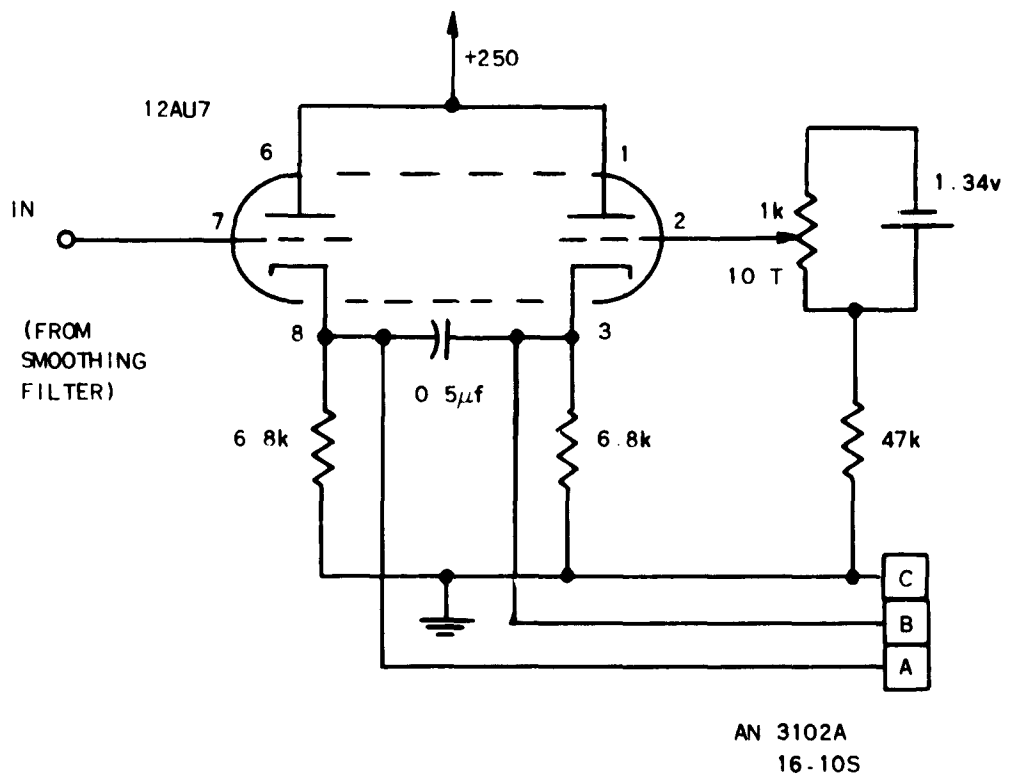


FIG. 6.13 CATHODE-FOLLOWER OUTPUT CIRCUIT

Of these, the -650 and -500 v supplies are used for the local-oscillator reflector and beam voltages respectively. Several critical circuits operate better with d c heater power so this has been provided from transistorized regulated supplies. While a single supply would have been satisfactory, the course of construction and development led to smaller separate units. The TWT has d-c heater power as well as the i-f amplifier, filter, and detector circuit, and also the tuned 465-cps amplifier, demodulator, and output cathode followers.

The TWT solenoid requires 110 v d-c at 1.5 a. Heating of the solenoid produces a large change in resistance, hence, during warm-up, the proper current must be maintained by changing an adjustable transformer feeding the rectifier-filter combination.

A separate +250-v regulated supply is used for the modulating and demodulating signal generator to prevent these signals from appearing throughout the receiver on the +250-v bus. The blocks enclosed by the dashed line in Fig. 6.10 are the circuits so supplied. In order to generate square waves without problems in asymmetry the scheme shown is employed. An R-C phase-shift oscillator at twice the desired frequency feeds a Schmidt trigger circuit adjusted to trigger on positive-going zero crossings. The resulting rectangular waveform is differentiated and clipped to provide a twice-frequency trigger pulse. When this waveform drives a bi-stable multivibrator a square-wave output is produced at the desired frequency. Various phase splitters, cathode followers, and reference diode clippers provide all the necessary output waveforms. From the square-wave at 465 cps, a tuned amplifier selects the fundamental component for a somewhat distorted sine-wave output.

Several test points are brought to the front panel through a selector switch so that waveforms can be monitored easily. These appear on positions of the test function switch: No. 1 (not used), No. 2, detector output, Nos. 3 and 4, two phases of the demodulating waveform, No. 5, one signal input to the demodulator; No. 6, the output of the demodulator.

## C CHARACTERISTICS AND PERFORMANCE

### 1. Critical Features

The TWT must be properly adjusted for lowest effective noise temperature and adequate gain. This adjustment results in a stable condition and requires little further care. Proper image rejection is

necessary to prevent simultaneous reception from two interference maxima at different positions in the sky resulting from the two bands. A minimum value of 20-db rejection is maintained.

The departure from ideal square-law detection has to be small but is readily measured and is repeatedly checked during calibration procedures. For a detector response with linear as well as a squared term, the departure from the best-fit square law can be shown to be linearly related to the linear-term coefficient and also to the range of input signals considered. Thus, for small ranges of input and a small linear coefficient, the approximation to square law operation is sufficiently accurate. When operated to keep the active sun response well on scale, inputs to over twice full scale remain on a linear portion of the system and do not show the effects of saturation.

The stability of the gain and the bandwidth is an important consideration. Although the modulated-signal mode of operation gives a considerable improvement factor for output fluctuations due to instabilities, their effect is present and must be responsible for the majority of the difference between actual and theoretical minimum-detectable-signal values.

Phase switching in practice has a tendency to introduce losses, unwanted responses, and inefficient operation. There may be a fixed loss for signals passing through the phase-reversing element. Half of this is the effective loss for the switch, since only half the signal passes through it. If the phase reversal is not complete, the output is less than optimum. For symmetrical antennas, with a difference  $\psi$  between 180 deg and the actual shift in phase the output is reduced according to the equation

$$P = P_{max} \cos \psi/2,$$

where  $P_{max}$  is the maximum output for  $\psi$  equal to zero and provided optimum phase-length compensation is introduced into one transmission line. For unsymmetrical antennas, the pattern is affected as well as the amplitude [Ref. 25].

In addition to a fixed loss, the switch may have a variable transmission efficiency. This shows up as an amplitude modulation at  $f_m$  superimposed on the phase-reversal modulation. The effect of this amplitude modulation is most deleterious when a solar observation is

made with the cross and a large source is in one array response and not the other. Such a condition can lead to the presence of a spurious fan-beam-response record superimposed on the cross record. These responses have to be held to a small value even with the extreme differences in array response possible from the active sun. Because of this, phase-switch adjustment is carried out to minimize amplitude modulation even at the expense of poor efficiency resulting from incomplete phase reversal. Fortunately, the loss for a small  $\psi$  is not serious. A ferrite isolator between the phase switch and the TWT also help to minimize the amplitude-modulation effects.

## 2. Minimum Detectable Signal

The measurement of  $\Delta T$  was made with the aid of a digitizer and printer. A series of digitized values of the output for a zero-signal condition was recorded, followed by a series after the introduction of a calibration step. From this data, the mean value of the level on each side of the calibration step was determined. Then the actual calibration slope in divisions per  $^{\circ}\text{K}$  was obtained. Following this, the standard deviation from the mean was calculated for both levels. Two values of  $\Delta T$  were thus obtained from this process.

With the following parameters for the receiver:

$$T_{e,s} = 1800 \text{ }^{\circ}\text{K}$$

$$M = \pi/\sqrt{2}$$

$$\tau = 2.67 \text{ sec}$$

$$\Delta f = 1.57 \times 10^6$$

the theoretical value for  $\Delta T$  is 1.95  $^{\circ}\text{K}$ . Using a calibration step of 16  $^{\circ}\text{K}$ , values of 2.44, 2.52, 2.43, and 2.36  $^{\circ}\text{K}$  were deduced from measurements. These values yield an average value of 2.43  $^{\circ}\text{K}$  for the experimental minimum-detectable signal.

## D SAMPLE RECORDS

### 1 Fan-Beam Solar Record

The repeated solar scans which the antenna provides from the E-W array while tracking are used as a patrol on solar activity. The record

in the absence of activity repeats with very little change from scan to scan, as can be seen from the record reproduced in Fig. 6.14.

## 2. Pencil-Beam Solar Record\*

When the antenna is operated as a cross, the successive scans appear with opposite polarity and exhibit great differences as the pencil-beam scans different portions of the sun. Such a record is reproduced in Fig. 6.15.

## 3. Weak-Source Record

As a contrast to the large signal-to-noise ratio of the solar records, a fan-beam observation of the moon's thermal emission is shown in Fig. 6.16.

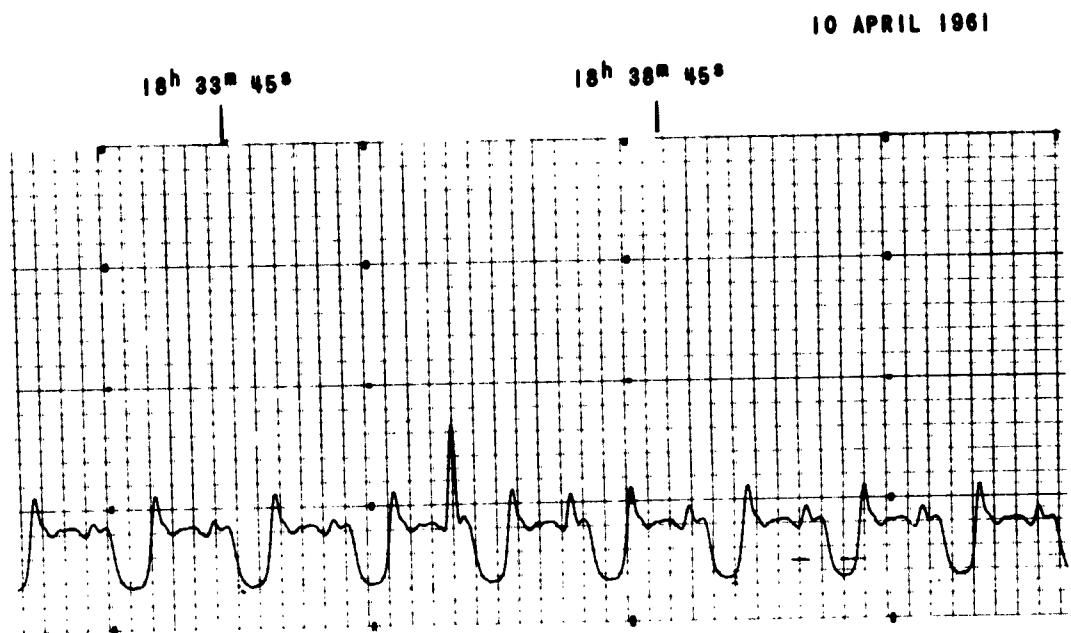


FIG. 6.14 SAMPLE SOLAR RECORD SHOWING FAN-BEAM SCANS. A SIMPLE MICROWAVE BURST IS PRESENT.

\*The solar observations have been reported by Swarup [Refs. 25,25].

20 JUNE 1961

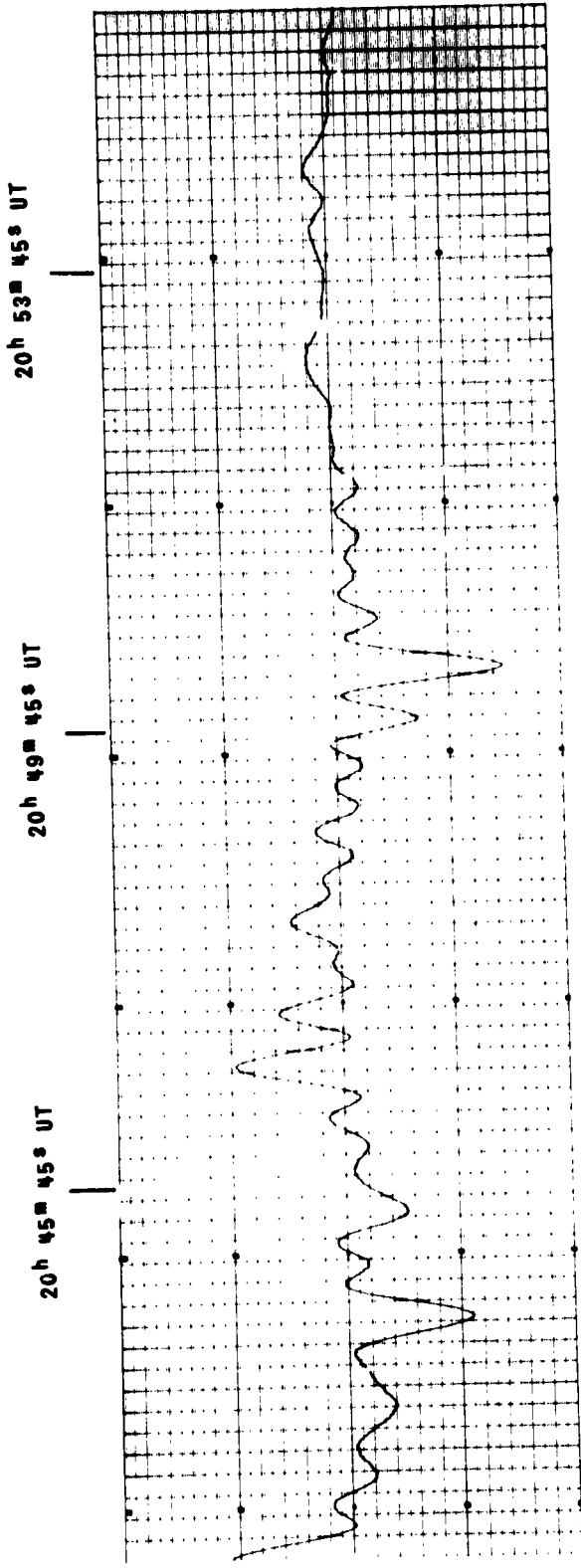


FIG. 6.15 SAMPLE SOLAR RECORD SHOWING PENCIL-BEAM SCANS.

6 JANUARY 1960

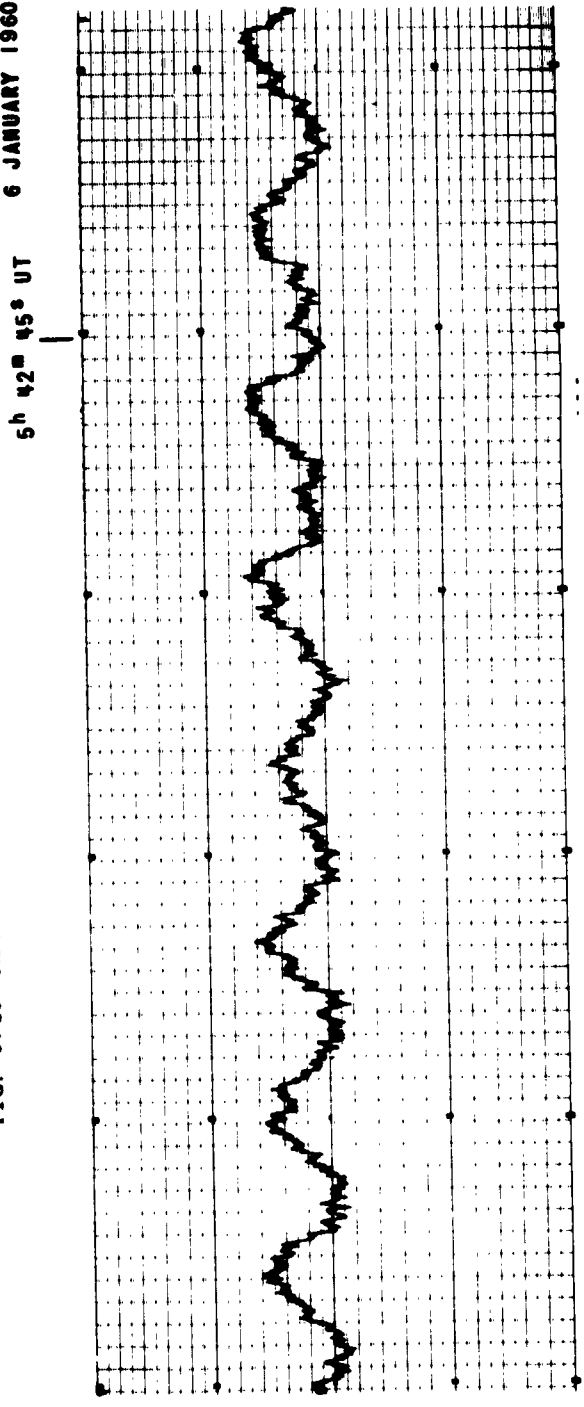


FIG. 6.16 SAMPLE RECORD SHOWING FAN-BEAM SCANS OF THE MOON AS AN EXAMPLE OF A WEAK-SOURCE OBSERVATION.

## VII. CONCLUSIONS

### A. SUMMARY

For all the types of stabilized receivers discussed, the attempts to gain freedom from instability problems result in greater minimum detectable signals. Other methods of improving signal to noise ratios such as repeated measurements or simultaneous observations are demanding with respect to time or equipment and furthermore depend upon the randomness of the noise from measurement to measurement in order that a  $1/\sqrt{N_0}$  of measurements improvement factor can be achieved. When a maximum  $\tau$  and  $\Delta f$  is reached, instabilities are controlled and the system noise temperature is a minimum without yielding a small enough  $\Delta T$ , these multi-measurement techniques can be applied.

The properties of several receivers relative to a total power receiver are shown in Table 7.1. Although this tabulation is an aid in determining the choice of a type of receiver, still, the estimation of the cost and effort required to achieve a certain stability with a receiver in a given application must remain as part of the design problem in which experience is most helpful.

Various receivers have been considered in relation to the effect of instabilities on their calibration curves. From this viewpoint we see that constant zero signal output in the presence of instabilities is achieved by most stabilized receivers including the d-c comparison, correlation, Dicke, and Ryle and Vonberg types. The modulated pilot AGC receiver achieves this for gain changes but not for  $T_{e_s}$  changes. The calibration curve behavior for large signals in the presence of instabilities as shown in Table 7.1 for the Ryle and Vonberg receiver is independent of gain and  $T_{e_s}$  changes and the slope of the calibration curve is maintained constant. For the modulated pilot AGC receiver this is true except that  $T_{e_s}$  changes shift the zero signal output level.

The M value of  $\sqrt{2}$  for the d-c comparison and correlation receivers is low but it is achieved at the expense of dual channels. The correlation receiver with circulators and cooled terminations holds the promise of being a good wide-band receiver.

For modulated signal receivers the M value of 2 remains quite theoretical since in practice a video filter is usually used with the resulting M factor of  $\pi/\sqrt{2}$  or 2.22 for the optimum square-wave modulation.

TABLE 7.1 RELATIVE MERITS OF SEVERAL RECEIVERS WITH EQUAL  $U_L$ 's.

Receiver	M	Normalizer for $\Delta f$	$\zeta$	$T_{es}$	Remarks	Stabilization			
						Zero	$\delta T_{es}$	$\delta$ Gain	Slope
Total Power	1	1	1	$T + T_{er}$		No	No	No	No
Selove DC Comparison	$\sqrt{2}$	2	$\frac{T T_{ref}}{T + T_{er}}$	$T + T_{er}$	T and $T_{ref}$ must be equal for zero stabilization	Yes (See remarks)	Yes	No	No
Correlation	$\sqrt{2}$	2	$\frac{T - (T_C/4)}{2(T + T_{er})}$	$T_{er} + \frac{T + (T_C/4)}{2}$	Requires special handling of circulator-load temperature	Yes (See remarks)	Yes	No	No
Dicke Modulated Signal	2*	2*	$\frac{T T_{ref}}{T + T_{er}}$	$T_{er} + \frac{T + T_{ref}}{2}$	T and $T_{ref}$ must be equal for zero stabilization	Yes (See remarks)	Yes	No	No
AGC Modulated Pilot Signal	2*	2*	$\frac{1}{I}$	$T + T_{er}$	Zero-point stabilized for gain changes but not for $T_{es}$ changes	No (See remarks)	No	Yes	Yes
Ryle and Vonberg Null-Balancing	2*	2*	0	$T + T_{er}$	Insensitive to gain changes with supplemental filter	Yes	Yes	Yes (See remarks)	Yes

\* These values are for square-wave modulation and demodulation only

$$U_L = M T_{es} U_L \sqrt{1 + \left(\frac{I_K}{I_L}\right)^2} \quad U_L = \frac{1}{\sqrt{\tau} \Delta f} \quad I = \text{rms instability noise} \quad I = \text{Reference Receiver Input Temperature}$$

$T$  = Signal Temperature  
 $T_{ref}$  = Reference Load Temperature  
 $T_{er}$  = Reference Receiver Input Temperature  
 $T_C$  = Circulator Load Temperature

All AGC systems deteriorate the M factor of a receiver. The modulated pilot signal AGC receiver can achieve values approaching 2 for M without undue integrating times in the AGC loop with pilot signals about one tenth the system noise temperature. Loop stability places a limitation on this receiver's capabilities.

The null-balancing receiver has a  $\Delta T$  depending upon the  $\Delta T$  for the comparison receiver used. The relationship is one to one except for the integrating time which is reduced by the loop feedback action. This receiver's freedom from instabilities although considerable is not complete since integrating time is a function of loop gain. Integration time is related to the impulse response of the receiver and its effect on signals is to smooth and delay them. When accurate source position measurements are being made, the delay introduced by the integrating filter is important. The fractional change in this delay for a fractional change in gain is independent of the system transfer function of the receiver.

## B. COMPARATIVE RESULTS

An attempt to compare results from the literature will disclose a variety of terminologies and usages. Consequently, the explicit definitions of parameters and consistent treatment used herein are useful in any comparison.

Dicke [Ref. 1] reported the following equation for a linear detector (to which he erroneously attributed an advantage of two over a square-law detector)

$$\Delta T = (T \pi^{3/2} N/8)(a/\Delta\omega)^{1/2}.$$

This equation was subsequently presented in correct form by Bunimovich [Ref. 27] and Selove [Ref. 9], as

$$\Delta T = (T\pi^{3/2} N/4)(a/\Delta\omega)^{1/2}$$

Applying the equations derived and presented in previous chapters, we find the same expression as shown below. Starting with

$$\Delta T = T_{es} M U_L,$$

where

$$U = \sqrt{1/\tau\Delta f} = \sqrt{a\pi/2\Delta\omega} ,$$

when

$$\tau = 4/a \quad \text{and} \quad \Delta f = \Delta\omega/2\pi.$$

Also,

$$M = \pi/\sqrt{2}$$

for square-wave modulation and a video filter. Letting  $T = 290 \text{ }^\circ\text{K}$ ,

$$\begin{aligned} T_{es} &= T_{er} + T \\ &= T[(\bar{F}/2) - 1] + T \end{aligned}$$

so that

$$T_{es} = TN/2$$

in Dicke's symbols. Thus,

$$\begin{aligned} \Delta T &= (TN/2) (\pi/\sqrt{2}) \sqrt{a/2\Delta\omega} \\ &= (TN \pi^{3/2}/4) \sqrt{a/\Delta\omega} \end{aligned}$$

which is identical with the corrected Dicke expression.

Goldstein [Refs. 10,11] gives a value of

$$\Delta T = 4 T_{es} \sqrt{\gamma/a}$$

for a receiver with sine-wave modulation with a video filter. The value  $T_{es}$  is explicit,  $M$  for this case is  $2\sqrt{2}$  (Table 4.2). The integrating time  $\tau = 1/2\gamma$ , since  $\gamma$  is the ideal low-pass-filter cut-off frequency, which is equivalent to  $f_0/2$  in Table 2.1. The reception filter considered is rectangular so that  $a = \Delta f$ . Thus

$$\begin{aligned}\Delta T &= T_{e_s} (2/\sqrt{2}) \sqrt{2\gamma/\Delta f} \\ &= T_{e_s} 4\sqrt{\gamma/a}\end{aligned}$$

which was given.

For the case of square-wave modulation and a video filter we can compare Golstein's [Refs. 10,11]

$$\Delta T = T_{e_s} \pi\sqrt{\gamma/a}$$

using  $M = \pi/\sqrt{2}$ , with

$$\begin{aligned}\Delta T &= T_{e_s} (\pi/\sqrt{2}) \sqrt{2\gamma/a} \\ &= T_{e_s} \pi\sqrt{\gamma/a}\end{aligned}$$

from the above results.

Blum [Ref. 19] uses the value of  $B_c(0)$ , the continuous portion of the PSD of the detector output evaluated at zero frequency as his comparative measure of performance for a variety of radiotelescopes. [His  $A(0) = 2B_c(0)$ ]. By multiplying this with the equivalent width of the smoothing filter we can obtain the total noise power at the receiver output for unity signal-to noise ratio. Blum normalizes  $B_c(0)$  such that the output-signal increment is unity for  $\Delta T = 1^\circ\text{K}$ . Thus, for a total-power receiver he gives  $A(0) = 2T_{e_s}^2/\Delta f$ , and we can write

$$\begin{aligned}\Delta T &= \sqrt{B_c(0) w_H} = \sqrt{A(0) w_H/2} \\ &= \sqrt{2T_{e_s}^2/2\tau\Delta f} = T_{e_s} \sqrt{1/\tau\Delta f}\end{aligned}$$

For the modulated-signal case with square-wave modulation, no filter, and square-wave demodulation, Blum gives the value

$$A(0) = 8 T_{e_s}^2/\Delta f$$

so that

$$\Delta T = \sqrt{\Lambda(0)/2\tau} = 2 T_{es} \sqrt{1/\tau\Delta f}$$

as was given above. For the correlation receiver

$$\Lambda(0) = 4 T_{es}^2 / \Delta f$$

which converts into

$$\Delta T = \sqrt{2} T_{es} \sqrt{1/\tau\Delta f}$$

as was also given above.

When Strum's [Ref. 4] expression for  $\Delta T$  is simplified, it can be written

$$\Delta T = T_{es} \mu \phi \sqrt{1/B \cdot RC} .$$

For a rectangular reception filter,  $B$  and  $\Delta f$  are equal, and for the single-section RC filter  $\tau = 2RC$ . From Strum's corrected table [Ref. 28] for square-wave modulation with a video filter,

$$\begin{aligned} \mu \phi &= \mu \phi' \phi'' \\ &= (\pi/\sqrt{2})(1/\sqrt{2}) \end{aligned}$$

which when inserted into his expression yields

$$\Delta T = T_{es} \pi/2 \sqrt{1/B RC}$$

We find for the same conditions the same result.

These comparisons show the harmony present in the literature when results are reduced to a common form in a consistent manner using clearly defined parameters.

### C. SUGGESTED FURTHER STUDY

The phrase "minimum detectable signal" is widely used, although it is without an accepted standard definition. Of course the difficulty lies in the definition of signal, which probably means something different in every

context. In this study we have restricted the signal for defining  $\Delta T$  to a very simple case, namely, a change in level from one fixed value to another without considering the portion of record during the change. Sufficiently general criteria for signal detectability need to be developed so that a measure of efficacy can be applied to the combination of a given signal and the radiotelescope used for the observation.

A technique that should be developed is a way of optimizing the signal-to-noise ratios for repeated observations. With present-day large radiotelescopes, the cost of observing time is an important factor and measures to improve the utilization of the instruments must be employed.

When the first in a series of observations is complete, there is *a priori* information available in the data that could be used to guide the next measurement. A process of adaptation of receiver parameters toward some optimum for the particular measurement would augment the improvement normally expected just from repetition. The use of "on-line" computers for data handling would provide a means of utilizing filtering techniques of this nature.

## APPENDIX A. USEFUL RELATIONSHIPS

Given  $r(t)$  a sample function from a stationary random process, its time-autocorrelation function  $\rho_r(t)$  is defined as

$$\rho_r(t) = \lim_{T \rightarrow \infty} \frac{1}{2T} \int_{-T}^T r(t) r(t-t) dt. \quad (\text{A.1})$$

The Fourier transform of  $\rho_r(t)$  defines the power spectral density  $D(f)$  of the random process as

$$F[\rho_r(t)] = D(f) = \int_{-\infty}^{\infty} \rho_r(t) \exp(-j2\pi ft) dt \quad (\text{A.2})$$

and

$$\rho_r(t) = \int_{-\infty}^{\infty} D(f) \exp(j2\pi ft) df. \quad (\text{A.3})$$

The central-value theorem states that the integral over infinite limits of a function is equal to the central ordinate of its Fourier transform, e.g.,

$$\int_{-\infty}^{\infty} D(f) df = \rho_r(t) \Big|_0 = \rho_r(0). \quad (\text{A.4})$$

Another useful theorem is the convolution theorem. The Fourier transform of the product of two functions is equal to the convolution of their transforms.

$$\int_{-\infty}^{\infty} D_1(f-f') D_2(f') df' = D_1 * D_2 = \int_{-\infty}^{\infty} \rho_1 \rho_2 \exp(-j2\pi ft) dt \quad (\text{A.5})$$

The following definition for the equivalent width  $w_\rho$ , of a function  $\rho(t)$ , and the equivalent width of its transform  $D(f)$  will be used

$$w_\rho = \int_{-\infty}^{\infty} \rho(t) dt / \rho(0) = D(0) / \int_{-\infty}^{\infty} D(f) df = 1/W_D \quad (\text{A.6})$$

This relationship between the autocorrelation functions for the input and output of a square-law detector has been given by Rice [Ref. 29],

$$\rho_{\text{out}}(t) = 2\rho_{\text{in}}^2(t) + \rho_{\text{in}}^2(0), \quad (\text{A.7})$$

from which we can write

$$B(f) = 2 \int_{-\infty}^{\infty} \rho_{\text{in}} \rho_{\text{in}} \exp(-j2\pi ft) dt + \rho_{\text{in}}^2(0) \delta(f) \quad (\text{A.8})$$

where  $\delta(f)$  is the unit impulse function.

## APPENDIX B ANALYSIS OF A CORRELATION RECEIVER

The receiver analysed below is the one shown in Fig. 4.3, and the assumptions used are as follows

1. All random voltages arise from stationary gaussian processes and have zero mean values
2. All noise contributions of a receiver channel are lumped into equivalent thermal sources at the channel input.
3. Calibration procedures result in a one degree increment of input temperature yielding a unit deflection increment at the output.
4. The smoothing filter bandwidth  $H(f)$  is much narrower than the reception filter bandwidth  $G(f)$ .

At the multiplier, the two input voltages are

$$x_1(t) = n_1(t) + (s/\sqrt{2})(t) \cdot (v_1/4)(t) + (v_2/4)(t) \quad (\text{B } 1)$$

and

$$x_2(t) = n_2(t) + (s/\sqrt{2})(t) \cdot (v_1/4)(t) - (v_2/4)(t) \quad (\text{B } 2)$$

The output of the multiplier

$$\begin{aligned} y(t) = x_1 x_2(t) &= (n_1 n_2 + n_2 s/\sqrt{2}) - (n_2 v_1/4) + (n_2 v_2/4) \\ &+ (n_1 s/\sqrt{2}) + (s^2/2) - (n_1 v_1/4) - (n_1 v_2/4) \\ &+ (v_1^2/16) + (v_1 v_2/8) - (v_2^2/16) \end{aligned} \quad (\text{B } 3)$$

The power spectrum of the receiver output is related by the Fourier transform to the autocorrelation function of  $y(t)$  which is

$$\rho_y(\tau) = \langle y(t) y(t + \tau) \rangle \quad (\text{B } 4)$$

Only the non-zero terms are contained in the expansion below, where we write

$$\begin{aligned}
\rho_y(\tau) = & \langle n_1 n_2(t) n_1 n_2(t+\tau) \rangle + \langle (n_1 s / \sqrt{2})(t) (n_1 s / \sqrt{2})(t+\tau) \rangle \\
& + \langle (n_2 s / \sqrt{2})(t) (n_2 s / \sqrt{2})(t+\tau) \rangle + \langle (n_1 v_1 / 4)(t) (n_1 v_1 / 4)(t+\tau) \rangle \\
& + \langle (n_1 v_2 / 4)(t) (n_1 v_2 / 4)(t+\tau) \rangle + \langle (n_2 v_1 / 4)(t) (n_2 v_1 / 4)(t+\tau) \rangle \\
& + \langle (n_2 v_2 / 4)(t) (n_2 v_2 / 4)(t+\tau) \rangle + \langle (s^2 / 2)(t) (s^2 / 2)(t+\tau) \rangle \\
& - \langle (s^2 / 2)(t) (v_1^2 / 16)(t+\tau) \rangle - \langle (s^2 / 2)(t) (v_2^2 / 16)(t+\tau) \rangle \\
& + \langle (v_1 v_2 / 8)(t) (v_1 v_2 / 8)(t+\tau) \rangle + \langle (v_2^2 / 16)(t) (v_2^2 / 16)(t+\tau) \rangle \\
& + \langle (v_2^2 / 16)(t) (v_1^2 / 16)(t+\tau) \rangle - \langle (v_2^2 / 16)(t) (s^2 / 2)(t+\tau) \rangle \\
& + \langle (v_1^2 / 16)(t) (v_1^2 / 16)(t+\tau) \rangle + \langle (v_1^2 / 16)(t) (v_2^2 / 16)(t+\tau) \rangle \\
& - \langle (v_1^2 / 16)(t) (s^2 / 2)(t+\tau) \rangle
\end{aligned} \tag{B.5}$$

The relationship discussed on p. 45 permits the above expression to be written

$$\begin{aligned}
\rho_y(\tau) = & \rho_{n_1}(\tau) \rho_{n_2}(\tau) + (\rho_{n_1} / 2)(\tau) \rho_s(\tau) + (\rho_{n_2} / 2)(\tau) \rho_s(\tau) \\
& + (\rho_{n_1} / 16)(\tau) \rho_{v_1}(\tau) + (\rho_{n_1} / 16)(\tau) \rho_{v_2}(\tau) + (\rho_{n_2} / 16)(\tau) \rho_{v_1}(\tau) \\
& + (\rho_{n_2} / 16)(\tau) \rho_{v_2}(\tau) + (\rho_s^2 / 2)(\tau) + (\rho_s^2 / 4)(0) - \langle s^2 \rangle / 32 \langle v_1^2 \rangle \\
& - \langle s^2 \rangle / 32 \langle v_2^2 \rangle + (\rho_{v_1} / 64)(\tau) \rho_{v_2}(\tau) + (\rho_{v_2}^2 / 128)(\tau) + (\rho_{v_2}^2 / 256)(0) \\
& + \langle v_1^2 \rangle / 256 \langle v_2^2 \rangle - \langle s^2 \rangle / 32 \langle v_2^2 \rangle + (\rho_{v_1} / 128)(\tau) + (\rho_{v_1}^2 / 256)(0) \\
& + \langle v_1^2 \rangle / 256 \langle v_2^2 \rangle - \langle s^2 \rangle / 32 \langle v_1^2 \rangle
\end{aligned} \tag{B.6}$$

The Fourier transform of this is

$$\begin{aligned}
B(f) = & k^2 G \cdot G \{ T_{er1} T_{er2} + (T/2)(T_{er1} + T_{er2}) + [T_{er1} T_{C1} + T_{er1} T_{C2}]/16 \} \\
& + [(T_{er2} T_{C1} + T_{er2} T_{C2})/16] + (T^2/2) + (T_{C1} T_{C2}/64) + [(T_{C1}^2 + T_{C2}^2)/128] \} \\
& + k^2 \left[ \int_{-\infty}^{\infty} G(f) df \right]^2 \{ (T^2/4) + (T_{C1} T_{C2}/128) - (T/16)(T_{C1} + T_{C2}) \\
& + [T_{C1}^2 + T_{C2}^2]/256 \} \tag{B.7}
\end{aligned}$$

At the receiver output the power spectral density is

$$C(f) = B(f) H(f) \tag{B.8}$$

Using  $C(f)$  the mean meter deflection  $\langle y \rangle$ , the signal power  $S$  and the noise power  $N$  can be found. Thus

$$\langle y \rangle = k [H(0)]^{1/2} \int_{-\infty}^{\infty} G(f) df [(T/2) - (T_{C1}/16) - (T_{C2}/16)] \tag{B.9}$$

$$S = k [H(0)]^{1/2} \int_{-\infty}^{\infty} G(f) df \Delta T/2 \tag{B.10}$$

and

$$N = k \left[ \int_{-\infty}^{\infty} H(f) df \right]^{1/2} [G \cdot G|_0]^{1/2} T_{es} \tag{B.11}$$

With a unity signal to noise ratio

$$\begin{aligned}
S/N = 1 = & \left\{ \frac{\left[ \int_{-\infty}^{\infty} G(f) df \right]^2 H(0) \frac{\Delta T}{2T_{es}}}{G \cdot G|_0 \int_{-\infty}^{\infty} H(f) df} \right\} \\
= & \sqrt{2\Delta f_7} \Delta T/T_{es}. \tag{B.12}
\end{aligned}$$

From which we get

$$\Delta T = (\sqrt{2} / \sqrt{\Delta f \tau}) T_{es}. \quad (\text{B. 13})$$

The system effective noise temperature

$$\begin{aligned} T_{es} = & (T_{er1} T_{er2} + (T/2)(T_{er1} + T_{er2}) + [(T_{er1} T_{C1} + T_{er1} T_{C2})/16] \\ & + [T_{er2} T_{C1} + T_{er2} T_{C2}]/16) + (T^2/2) + (T_{C1} T_{C2}/64) \\ & + [(T_{C1}^2 + T_{C2}^2)/128] \}^{1/2} \end{aligned} \quad (\text{B. 14})$$

For identical channels, when

$$T_{er1} = T_{er2} = T_{er}$$

and

$$T_{C1} = T_{C2} = T_C$$

Equation (B.14) simplifies to

$$T_{es} = [T_{er}^2 + T_{er} T + (T_{er} T_C/4) + (T^2/2) + (T_C^2/32)]^{1/2} \quad (\text{B. 15})$$

so that when  $T/T_{er}$  and  $T_C/T_{er}$  are less than 1,

$$\begin{aligned} T_{es} & \approx T_{er} \{1 + (1/2T_{er}) [T + (T_C/4)]\} \\ & = T_{er} + (T/2) + (T_C/8) \end{aligned} \quad (\text{B. 16})$$

Using this expression for  $T_{es}$  we find

$$\Delta T = \sqrt{2} / \sqrt{\Delta f \tau} [T_{er} + (T/2) + (T_C/8)] \quad (\text{B. 17})$$

## APPENDIX C. DETAILED ANALYSIS OF THE MODULATED RECEIVER

The modulated receiver is shown in block diagram form in Fig. 3.1. This illustration includes all the components of the elemental receiver plus additional components to perform the modulation and demodulation. A function generator, a modulator, and a coherent demodulator are necessary. The video-frequency filter is not essential but is usually present in practice.

The procedure followed will be to calculate the power spectral density at the output of the receiver and from this determine the signal-to-noise ratio. The minimum-detectable input-temperature increment produces a unity signal-to-noise ratio.

The equivalent source temperature for the reception-filter input will be

$$T_{er} + T_{\eta}(t)$$

where

$$\begin{aligned} T_{\eta}(t) &= \eta(t) (T - T_{ref}) + T_{ref} \\ &= [(T - T_{ref})/2][1 - \mu(t)] + T_{ref} \end{aligned} \quad (C.1)$$

The waveform  $\mu(t)$  determines the form of the power modulation.

At the detector output the voltage  $y(t)$  is a measure of the instantaneous power. When averaged over times long compared with  $w_{\rho_y}$  [an equivalent width of the autocorrelation function for  $y(t)$ ], but short compared with the modulation period, we describe this function approximately as a varying time-average

$$\langle y \rangle(t) = \langle x^2 \rangle(t) + k \int_{-\infty}^{\infty} G(f) df \{T_{er} + T_{ref} + [(T - T_{ref})/2][1 - \mu(t)]\} \quad (C.2)$$

If we form an expression for  $x(t)$  as the sum of two voltages derived from the modulated source and the effective receiver input noise temperature  $T_{er} + T_{ref}$ , we have

$$x(t) = m(t) \nu(t) + n(t) \quad (C.3)$$

and

$$\langle x^2 \rangle(t) = \langle m^2(t) \rangle \nu^2(t) + \langle n^2(t) \rangle \quad (\text{C. 4})$$

where

$$\langle n^2(t) \rangle = k \int_{-\infty}^{\infty} G(f) df (T_{er} + T_{ref})$$

$$\langle m^2(t) \rangle = k \int_{-\infty}^{\infty} G(f) df (T - T_{ref}) \quad (\text{C. 5})$$

and

$$\nu^2(t) = [1 - \mu(t)]/2 = \eta(t)$$

Since  $\mu(t)$  is descriptive of the form of modulation,  $\nu(t)$  is seldom specified.

First we consider the case for  $J(f) = 1$ . Then

$$y_2(t) = y(t) \xi(t) = x^2(t) \xi(t). \quad (\text{C. 6})$$

The autocorrelation function

$$\begin{aligned} \rho_{y_2}(\tau) &= \lim_{T \rightarrow \infty} \frac{1}{2T} \int_{-T}^T x(t) x(t+\tau) x(t) x(t+\tau) \xi(t) \xi(t+\tau) dt \\ &= \langle x(t) x(t+\tau) x(t) x(t+\tau) \xi(t) \xi(t+\tau) \rangle \\ &= \langle [m^2(t) \eta(t) + 2m(t) n(t) \nu(t) + n^2(t)] \\ &\quad \cdot [m^2(t+\tau) \eta(t+\tau) + 2m(t+\tau) n(t+\tau) \nu(t+\tau) + n^2(t+\tau)] \cdot \\ &\quad [\xi(t) \xi(t+\tau)] \rangle \quad (\text{C. 7}) \end{aligned}$$

From this expression the following terms have non-zero values:

$$\begin{aligned} &\langle m^2(t) m^2(t+\tau) \eta(t) \eta(t+\tau) \xi(t) \xi(t+\tau) \rangle \\ &\langle 4m(t) m(t+\tau) n(t) n(t+\tau) \nu(t) \nu(t+\tau) \xi(t) \xi(t+\tau) \rangle \\ &\langle n^2(t) n^2(t+\tau) \xi(t) \xi(t+\tau) \rangle. \end{aligned}$$

After evaluating the random portions of these expressions we have

$$\begin{aligned} & [\langle m^2(t) \rangle^2 + 2\rho_m^2(\tau)] \langle \eta(t) \eta(t+\tau) \xi(t) \xi(t+\tau) \rangle \\ & 4\rho_n(\tau) \rho_m(\tau) \langle \nu(t) \nu(t+\tau) \xi(t) \xi(t+\tau) \rangle \\ & 2\rho_n^2(\tau) \langle \xi(t) \xi(t+\tau) \rangle + \langle n^2(t) \rangle^2 \langle \xi(t) \xi(t+\tau) \rangle \end{aligned}$$

The periodic portion of the first term can be written

$$\begin{aligned} & \langle \{ [1 - \mu(t)]/4 \} [1 - \mu(t+\tau)] \xi(t) \xi(t+\tau) \rangle \\ & \langle 1/4 [1 - \mu(t) - \mu(t+\tau) + \mu(t) \mu(t+\tau)] \xi(t) \xi(t+\tau) \rangle \end{aligned}$$

The only d-c component (which must be signal) is determined by the mean value of the term

$$1/4 \langle \mu(t) \mu(t+\tau) \xi(t) \xi(t+\tau) \rangle \cdot \langle m^2(t) \rangle^2$$

Now, since we are interested in determining the signal-to-noise ratio at zero signal, the noise-power spectrum is that which is the Fourier transform of

$$2\rho_n^2(\tau) \langle \xi(t) \xi(t+\tau) \rangle$$

The mean value or d-c component of an autocorrelation function for a periodic function is equal to the square of the average value of the function over a period  $T$ . Thus

$$\begin{aligned} S &= H(0) \frac{1}{4} \left[ \frac{1}{T} \int_0^T \mu(t) \xi(t) dt \right]^2 \langle m^2(t) \rangle^2 \\ &= H(0) \frac{1}{4} k (T - T_{ref})^2 \left[ \int_{-\infty}^{\infty} G(f) df \right]^2 \left[ \frac{1}{T} \int_0^T \mu(t) \xi(t) dt \right]^2. \quad (C.8) \end{aligned}$$

When  $\xi(t)$  is written in Fourier series form,

$$\xi(t) = \sum_{n=-\infty}^{\infty} K_{\xi_n} \exp(nj2\pi f_m t) \exp(nj\theta). \quad (C.9)$$

Then

$$\langle \xi(t) \xi(t+\tau) \rangle = \sum_{n=-\infty}^{\infty} |K_{\xi_n}|^2 \exp(nj2\pi f_n \tau) \quad (C.10)$$

The noise-power spectrum at the output of the receiver is

$$C_c(f) = \{2k^2(T_{er} + T_{ref})\}^2 [G * G] * \sum_{n=-\infty}^{\infty} |K_{\xi_n}|^2 \delta(f - nf_n) \} H(f) \quad (C.11)$$

This spectrum is very wide compared with the spectrum of  $\xi(t)$ ; therefore, to a close approximation, we can write for the noise-power output

$$N = 2k^2(T_{er} + T_{ref})^2 [G * G] \Big|_0 \sum_{n=-\infty}^{\infty} |K_{\xi_n}|^2 \int_{-\infty}^{\infty} H(f) df. \quad (C.12)$$

Now, making use of the definitions for  $\tau$  and  $\Delta f$  we form the signal-to-noise power ratio and set it equal to unity, thus

$$\begin{aligned} \frac{S^2}{N^2} = 1 &= \frac{H(0) \frac{1}{4} \left[ \frac{1}{T} \int_0^T \mu(t) \xi(t) dt \right]^2 k^2 \Delta T^2 \left[ \int_{-\infty}^{\infty} G(f) df \right]^2}{2k^2(T_{er} + T_{ref})^2 [G * G] \Big|_0 \sum_{n=-\infty}^{\infty} |K_{\xi_n}|^2 \int_{-\infty}^{\infty} H(f) df} \\ &= \frac{\frac{1}{4} \Delta T \tau \Delta f \left[ \frac{1}{T} \int_0^T \mu(t) \xi(t) dt \right]^2}{(T_{er} + T_{ref})^2 \sum_{n=-\infty}^{\infty} |K_{\xi_n}|^2} \end{aligned} \quad (C.13)$$

From this we find the minimum detectable input temperature increment

$$\Delta T = M (T_{er} + T_{ref}) \sqrt{1/\tau \Delta f}, \quad (C.14)$$

where

$$M = 2 \sqrt{\frac{\sum_{n=-\infty}^{\infty} |K_{\xi_n}|^2}{\left[ (1/T) \int_0^T \mu(t) \xi(t) dt \right]^2}} = 2 \sqrt{\frac{\langle \xi(t)^2 \rangle}{\left[ (1/T) \int_0^T \mu(t) \xi(t) dt \right]^2}} \quad (C.15)$$

Interest centers on minimum values for M, given explicit waveforms. The phase of  $\xi(t)$  must be set for the maximum value of the denominator in the above expression in order to achieve the minimum M. Table 4.1 contains values of M for various combinations of  $\mu(t)$  and  $\xi(t)$ .

In order to include a video filter in the analysis we need the detector output spectrum. Knowing this the effect of the video filter can be considered and the spectrum at the input to the coherent demodulator can be determined.

The autocorrelation function for the detector output is

$$\rho_y(\tau) = \langle x(t) x(t+\tau) x(t) x(t+\tau) \rangle \quad (C.16)$$

The non-zero terms in this expression are

$$\begin{aligned} &\langle m^2(t) \rangle^2 \langle \eta(t) \eta(t+\tau) \rangle + 2\rho_m^2(\tau) \langle \eta(t) \eta(t+\tau) \rangle \\ &4\rho_m(\tau) \rho_n(\tau) \langle v(t) v(t+\tau) \rangle \\ &\langle n^2(t) \rangle^2 + 2\rho_n^2(\tau) \end{aligned}$$

For zero signal conditions the noise power is derived from the term

$$2\rho_n^2(\tau)$$

and the signal-power information is in the term

$$\langle m^2(t) \rangle^2 \cdot \langle \eta(t) \eta(t+\tau) \rangle.$$

The Fourier transforms of these terms times the power-transfer characteristic of the video filter are the noise and signal components of the power spectrum given below

$$B_{y_1}(f) = 2k^2 (T_{er} + T_{ref})^2 G * G J(f) + k^2 (T - T_{ref})^2 \left[ \int_{-\infty}^{\infty} G(f) df \right]^2 F[\langle \eta(t) \eta(t+\tau) \rangle] J(f). \quad (C.17)$$

Two forms for  $J(f)$  of interest are: (1) a response that excludes frequencies in the band around twice the reception filter mid-frequency, as is common for envelope detectors, and (2) a narrow band including only the fundamental of the modulation frequency. For the first case, since  $f_m$  must be small compared to  $\Delta f$ , all the harmonics of  $\mu(t)$  will pass and contribute to the signal-power output. The noise power output will be the same as with no filter and hence the factor  $M$  is not affected.

In the second case, let  $J(f) = 1$  for all significant values of  $H(f - f_m)$  and  $H(f + f_m)$ ; i.e., the smoothing filter is much narrower than the pass band of the filter  $J(f)$ . Then, for the noise component of the output spectrum we can write

$$2k^2(T_{er} + T_{ref})^2 G * G|_0 \cdot 2 |K_{\xi_1}|^2 H(f)$$

since only the fundamental component of the demodulating signal gives rise to power within the smoothing-filter passband. The signal component of the power spectral density at the output of  $J(f)$  is

$$(k^2/4)(T - T_{ref})^2 \left[ \int_{-\infty}^{\infty} G(f) df \right]^2 F[\langle \mu(t) \mu(t+\tau) \rangle] J(f)$$

or

$$(k^2/4)(T - T_{ref})^2 \left[ \int_{-\infty}^{\infty} G(f) df \right]^2 [ |K_{\mu_1}|^2 \delta(f+f_m) + |K_{\mu_1}|^2 \delta(f - f_m) ].$$

when  $\mu(f) = \sum_{n=-\infty}^{\infty} K_{\mu_n} \exp(jn2\pi f_m t)$ . This can be associated with a voltage  $y_1(t)$ , where

$$y_1(t) = (k/2)(T - T_{ref}) \left[ \int_{-\infty}^{\infty} G(f) df \right] 2 |K_{\mu_1}| \cos 2\pi f_m t \quad (C.18)$$

Now at the output of the coherent demodulator

$$y_2(t) = y_1(t) \xi(t)$$

and

$$\rho_{y_2}(\tau) = (T - T_{\text{ref}})^2 \left[ \int_{-\infty}^{\infty} G(f) df \right]^2 |K_{\mu_1}|^2 \langle \cos 2\pi f_m t \cos 2\pi f(t+\tau) \cdot \xi(t) \xi(t+\tau) \rangle, \quad (\text{C. 19})$$

from which as in Eq. (C.8) we can write for the signal-power output

$$S^2 = H(0)k^2(T - T_{\text{ref}})^2 \left[ \int_{-\infty}^{\infty} G(f) df \right]^2 |K_{\mu_1}|^2 \left[ (1/T) \int_0^T \xi(t) \cos 2\pi f_m t dt \right]^2 \quad (\text{C. 20})$$

Determining the signal to-noise power ratio as before

$$S^2/N^2 = 1 = \frac{\Delta T^2 \tau \Delta f \left[ (1/T) \int_0^T \xi(t) \cos 2\pi f_m t dt \right]^2 |K_{\mu_1}|^2}{(T_{\text{er}} + T_{\text{ref}})^2 2 |K_{\xi_1}|^2} \quad (\text{C. 21})$$

So we find

$$\Delta T = M (T_{\text{er}} + T_{\text{ref}}) \sqrt{1/\tau \Delta f}$$

where

$$M = \frac{\sqrt{2} |K_{\xi_1}|}{|K_{\mu_1}| \left[ (1/T) \int_0^T \xi(t) \cos 2\pi f_m t dt \right]} \quad (\text{C. 22})$$

For the case when the relative phase of  $\mu(t)$  and  $\xi(t)$  is zero i.e.,  $\theta = 0$ ,

$$|K_{\mu_1}| = (1/T) \int_0^T \xi(t) \cos 2\pi f_m t dt,$$

since this is just one-half times the expression for the fundamental coefficient in a cosine Fourier series ( $K_{\xi_1}$  is the positive frequency fundamental coefficient in the exponential form of the Fourier series). This substitution results in the simplified expression

$$M = \sqrt{2}/|K_{\mu_1}| \quad (C. 23)$$

In Table 4.2 values for M with three different waveforms for  $\mu(t)$  have been calculated.

When a phase angle  $\theta$  exists between the fundamental components of  $\mu(t)$  and  $\xi(t)$ ,

$$(1/T) \int_0^T \xi(t) \cos 2\pi f_m t \, dt = |K_{\xi_1}| \cos \theta \quad (C. 24)$$

and

$$M = \sqrt{2}/|K_{\mu_1}| \cos \theta \quad (C. 25)$$

APPENDIX D. PROOF OF THEOREM ON TIME DISPLACEMENTS DUE TO SMOOTHING

**THEOREM:** The centroid of the signal waveform  $\bar{t}_s$  will be located  $\bar{t}_h$  sec in time before the centroid of the recorded waveform  $\bar{t}_r$ , where  $\bar{t}_h$  is the time coordinate of the centroid of the impulse response in relation to its origin or time of impulse.

**GIVEN:** A signal  $s(t)$ , a smoothing filter with an impulse response  $h(t)$ , and the output signal  $r(t)$ . We define the time coordinate of the centroid of the waveform as  $\bar{t}$ , which, for  $r(t)$ , is expressed

$$\bar{t}_r = \frac{\int_{-\infty}^{\infty} t r(t) dt}{\int_{-\infty}^{\infty} r(t) dt}$$

**TO PROVE:**

$$\bar{t}_s = \bar{t}_r - \bar{t}_h$$

**PROOF:** We use the relationships

$$R'(0)/-j2\pi = \int_{-\infty}^{\infty} t r(t) dt$$

and

$$R(0) = \int_{-\infty}^{\infty} r(t) dt$$

so that

$$\bar{t}_r = R'(0)/j2\pi R(0)$$

and similarly for the other functions, where  $R(f)$ , the Fourier transform of  $r(t)$ , can be written terms of the transforms of  $s(t)$  and  $h(t)$  as

$$R(f) = S(f) H(f).$$

The derivative of this expression is

$$R'(f) = S(f) H'(f) + S'(f) H(f).$$

Now we can write

$$\begin{aligned} \bar{t}_s &= \frac{1}{-j2\pi} \left[ \frac{S(f) H'(f)}{S(0) H(0)} \Bigg|_0 + \frac{S'(f) H(f)}{S(0) H(0)} \Bigg|_0 \right] - \bar{t}_h \\ &= S'(0) / -j2\pi S(0) \\ &= \bar{t}_s \end{aligned}$$

Q. E. D.

The impulse response may have its centroid located at the origin when it has a zero first moment and has a positive area. In this case the recorded waveform centroid will not be shifted relative to the signal waveform but serious distortion of shape will occur.

The tendency exists for the evaluation of the centroid of a waveform by eye to be made on the basis of the area under the absolute value of the waveform. For applications such as those involving smoothing, this must be avoided. In general, smoothing filters with oscillatory responses which may have zero first moments are not used, but in servo type receivers the possibility exists.

## APPENDIX E. DETAILS OF THE VARACTOR-DIODE SHORTING SECTION

The varactor diode is mounted in the center of the broad face of the guide, grounded to one wall and with a switching-signal connection fed through a by-passing mount to a BNC connector. With the diode so mounted and electrically connected to the switching voltage of reversible polarity, a measurement of the minimum SWR present was made for any position of the short behind the diode. This minimum SWR is indicative of the losses present and hence expected loss in the device when used as a variable short. For the two states of the diode the predominant change is in the susceptance. A given susceptance change yields the greatest phase-length change when the two values are equal but of opposite sign. This condition for the susceptance can be met since the adjustment of the short position moves the admittances along nearly constant-G circles on the Smith chart.

When adjusted in that manner, the maximum phase-length change observed for the WE 427A diodes was 88 percent of the required quarter-wave. A full quarter-wave shift could be obtained if these admittances were transformed to unity per unit magnitude. A quarter-wave transformer section made with a dielectric slab accomplished this transformation and the required phase-length change was observed. An alternative procedure that is presently being used is to taper the waveguide so that the diode is mounted in the proper guide admittance.

As well as having the quarter-wave shift, one of the sections must have a total path length longer than the other by a quarter-wave. Consequently, one of the diode sections was made that much longer so that, after separate adjustment of the quarter wave change had been made, the complete assembly could be finally adjusted with shim-like sections of waveguide and small polystyrene blocks in the guide.

## REFERENCES

1. R. H. Dicke, "The Measurement of Thermal Radiation at Microwave Frequencies," *Rev. Sci. Instr.*, 17, 7, pp. 268-275, July, 1946
2. A. E. Siegman, "Thermal Noise in Microwave Systems," *Microwave J*, 4, 3-5, pp., 81-90, 66-73, and 93-104, March, April and May, 1961.
3. "IRE Standards on Methods of Measuring Noise in Linear Two-Ports. 1959", *Proc. IRE*, 48, 1, pp. 60-68, January 1960.
4. P. D. Strum, "Considerations in High-Sensitivity Microwave Radiometry," *Proc IRE*, 46, pp. 43-53, January, 1958.
5. D. G. Lampard, "The Minimum Detectable Change in the Mean Noise-Input Power to a Radio Receiver," *Proc. IEE*, 101, Part IV, pp. 118-128, February, 1954.
6. E. J. Kelly, D. H. Lyons, and W. L. Root, "The Theory of the Radiometer," MIT, Lincoln Lab. Group 312, Group Report 47.16, 2 May 1958.
7. J. L. Steinberg, "Receivers for Radio Frequency Noise. I. Measurement of Temperature by Means of Thermionics Radiation Using very High Radio Frequencies," *Onde elect.* 32, pp. 445-54, November 1952. II. Gain Fluctuations in Measuring Apparatus. Use of Modulation," *Onde elect.* 32, pp. 519-26, December 1952.
8. R. N. Bracewell, "Radio Astronomy Techniques," *Handbuch der Physik*, 54, S. Flügge, Ed., Springer, Berlin (in press)
9. W. Selove, "A d-c Comparison Radiometer," *Rev. Sci. Instr.*, 25, pp. 120-122, February, 1954.
10. S. J. Goldstein, Jr., "A Comparison of Two Radiometer Circuits," *Proc. IRE*, 43, pp. 1663-1666, November, 1955.
11. D. G. Tucker, M. H. Graham, and S. J. Goldstein, Jr., "A Comparison of Two Radiometer Circuits," *Proc. IRE*, 45, pp. 365-366, March, 1957.
12. C. L. Seeger, F. L. H. M. Stumpers, and N. van Hurck, "A 75 cm Receiver for Radio Astronomy and Some Observational Results," *Philips Tech Rev.*, 18, pp. 141-144, 1956/1957.
13. R. M. Sloanaker, J. H. Nichols, "Measurements of the Positions, Fluxes, and Sizes of Celestial Radio Sources at 10.2 cm," NRL Report No. 5485, U. S. Naval Research Laboratory, Washington, D. C., July 13, 1960.
14. C. L. Seeger, "A Tentative Measure of the Flux Density of Cassiopeia A at 400 Mc/s," *B.A.N.*, 13, 472, pp. 100-104, November 1956
15. R. Adgie and F. G. Smith, "The Radio Emission Spectra of Four Discrete Sources and of the Background Radiation," *Obs*, 76, 894, pp. 181-187, 1956.
16. N. W. Broten and W. J. Medd, "Absolute Flux Measurements of Cassiopeia A, Taurus A, and Cygnus A, at 3200 Mc/s," *Astrophys Jour.* 132, 2, September 1960.

## REFERENCES (Cont'd)

17. M. Ryle and D. D. Vonberg, "An Investigation of Radio-Frequency Radiation from the Sun," *Proc. Roy. Soc., A*, 193, pp. 98-119, 1948.
18. D. Middleton, *An Introduction To Statistical Communication Theory*, McGraw-Hill Book Co., Inc., New York, p. 343, 1960.
19. E. J. Blum, "Sensibilité des Radiotélescopes and Récepteurs a Corrélation," *Annales d'Astrophysique*, 22, 2, pp. 140-163, March-April, 1959
20. L. D. Strom, "The Theoretical Sensitivity of the Dicke Radiometer," *Proc. IRE*, 45, pp. 1291-1292, September, 1957.
21. B. M. Oliver, "Automatic Volume Control as a Feedback Problem," *Proc. IRE*, 36, pp. 466-473, April, 1948.
22. K. E. Machin, M. Ryle, and D. D. Vonberg, "The Design of an Equipment for Measuring Small Radio-Frequency Noise Powers," *Proc. IEE*, pt. III, 99, pp. 127-134, May, 1952.
23. J. G. Truxal, *Automatic Feedback Control System Synthesis*, McGraw-Hill Book Co., Inc., New York, pp. 80-87, 1955.
24. R. N. Bracewell and G. Swarup, "The Stanford Microwave Spectroheliograph Antenna, a Microsteradian Pencil-Beam Antenna," *IRE Trans. on Ant and Prop.*, AP-9, 1, pp. 22-30, January 1961.
25. G. Swarup, "Studies of Solar Microwave Emission Using a Highly Directional Antenna," SR No. 13 [AF18(603)-53], AFSOR No. 265, Stanford Electronics Laboratories, Stanford University, Stanford, California, p. 31, February 6, 1961.
26. G. Swarup, "Stanford Microwave Spectroheliograms for 1960 April, May, and June;" Scientific Reports No. 8, 10, and 11. [AF18(603)-53], Stanford Electronics Laboratories, Stanford University, Stanford, California, December 15, 1960, January 15, 1961, and April 28, 1961.
27. V. I. Bunimovich, "Radiometer Sensitivity," *Zhurnal Tekhnicheskoi Fiziki*, 20, 8, pp. 944-953, 1950 (In Russian).
28. P. D. Strum, "Correction to 'Considerations in High-Sensitivity Microwave Radiometry'," *Proc. IRE*, 47, 12, p. 2105, December 1959.
29. S. O. Rice, "Mathematical Analysis of Random Noise; Part IV, Noise Through Non-Linear Devices," *Bell System Tech. Jour.* 24, pp. 115-156, 1945 (In particular p. 149.)

DISTRIBUTION LIST - AF18(603)-53  
November 1961

3 Commander  
AF Office of Scientific Res.  
Washington 25, D.C.  
Attn: SRYF

2 Commander  
AF Research Division  
Washington 25, D.C.  
Attn: KURTL

4 Commander  
Wright Air Development Division  
Wright-Patterson AFB, Ohio  
Attn: ASAFKD-DIST

1 Commander  
AF Cambridge Res. Laboratories  
L.G. Hanscom Field  
Bedford, Massachusetts  
Attn: CRREL

1 Commander  
Rome Air Development Center  
Griffiss Air Force Base  
Rome, New York  
Attn: RCOYL-2

2 Commander  
Detachment 1  
HQ AF Research Division  
The Shell Building  
Brussels, Belgium

1 P.O. Box AA  
Wright-Patterson Air Force Base  
Ohio

1 Aeronautical Research Labs.  
Wright-Patterson AFB, Ohio  
Attn: Tech Lib., Bldg. 450

10 ASTIA  
Arlington Hall Station  
Arlington 12, Virginia  
Attn: TIPCR

1 Director of Res. and Dev't  
Headquarters, USAF  
Washington 25, D.C.  
Attn: AFDRD

1 Office of Naval Research  
Washington 25, D.C.  
Department of the Navy  
Attn: Code 420

1 Director, Naval Res. Lab.  
Washington 25, D.C.  
Attn: Tech. Info. Officer

1 Director, Army Res. Office  
Dept. of the Army  
Washington 25, D.C.  
Attn: Scientific Info. Br.

1 Chief, Physics Br.  
Division of Research  
U.S. Atomic Energy Commission  
Washington 25, D.C.

1 U.S. Atomic Energy Commission  
Tech. Info. Extension  
P.O. Box 62  
Oak Ridge, Tennessee

1 National Bureau of Standards  
Library, Rm. 203, NW Building  
Washington 25, D.C.

1 Physics Program  
National Science Foundation  
Washington 25, D.C.

1 Director, Office of Ord. Res.  
Box CM, Duke Station  
Durham, North Carolina

1 Director, Dept. of Commerce  
Office of Tech. Services  
Washington 25, D.C.

1 ARO, Inc.  
Arnold Air Force Station  
Tullahoma, Tennessee  
Attn: AMDC Library

1 Commander  
AF Flight Test Center  
Edwards Air Force Base, Calif.  
Attn: FTOTL

1 Commander  
AF Special Weapons Ctr.  
Kirtland Air Force Base, N.M.  
Attn: SWOI

1 Commander  
AF Missile Dev't Ctr.  
Holloman AFB, New Mexico  
Attn: HDOJ

1 Commander  
Army Rocket & Guided Missile  
Agency  
Redstone Arsenal, Ala  
Attn: ORDXR-OTL

1 Commandant  
AF Institute of Tech. (AU Lib)  
NCLI-LIB, Bldg., 125, Area B  
Wright-Patterson AFB, Ohio

1 Commander  
Air Research & Dev't Command  
Andrews Air Force Base  
Washington 25, D.C.  
Attn: RDR 2 cys  
RDB 1 cy  
RDC 1 cy  
RDRS 1 cy

1 Commanding General  
U.S. Army Signal Corps Res.  
and Dev't Lab.  
Ft. Monmouth, New Jersey  
Attn: SIGPW/EL-RPO

6 National Aeronautics & Space  
Administration  
Washington 25, D.C.

1 Advanced Research Projs. Agcy  
Washington 25, D.C.

1 Rand Corporation  
1700 Main Street  
Santa Monica, California

1 Chairman, Canadian Joint Staff  
2450 Massachusetts Ave., N.W.  
Washington 25, D.C.  
For DRB/DSIS